NASA CR-54422
AGC 8800-5

DESIGN STUDY OF MODIFICATION OF M-1 LIQUID HYDROGEN TURBOPUMP FOR USE IN NUCLEAR REACTOR TEST FACILITY

By

W. H. Knuth, J. Farquhar, and B. Lindley

Prepared for

NATIONAL AERONAUTICS AND SPACE ADMINISTRATION

Contract NAS3-2555
Amendment No. 14

AEROJET-GENERAL CORPORATION

SACRAMENTO, CALIFORNIA

NOTICE

This report was prepared as an account of Government sponsored work. Neither the United States, nor the National Aeronautics and Space Administration (NASA), nor any person acting on behalf of NASA:

A.) Makes any warranty or representation, expressed or implied, with respect to the accuracy, completeness, or usefulness of the information contained in this report, or that the use of any information, apparatus, method, or process disclosed in this report may not infringe privately owned rights; or

B.) Assumes any liabilities with respect to the use of, or for damages resulting from the use of any information, apparatus, method or process disclosed in this report.

As used above, "person acting on behalf of NASA" includes any employee or contractor of NASA, or employee of such contractor, to the extent that such employee or contractor of NASA, or employee of such contractor prepares, disseminates, or provides access to, any information pursuant to his employment or contract with NASA, or his employment with such contractor.

Requests for copies of this report should be referred to

National Aeronautics and Space Administration
Office of Scientific and Technical Information
Attention: AFSS-A
Washington, D.C. 20546

NASA CR-54422
AGC 8800-5

TECHNOLOGY REPORT

DESIGN STUDY OF MODIFICATION OF M-1 LIQUID HYDROGEN TURBOPUMP FOR USE IN NUCLEAR REACTOR TEST FACILITY

Prepared For

NATIONAL AERONAUTICS AND SPACE ADMINISTRATION

May 15, 1965

CONTRACT NAS3-2555

AMENDMENT NO. 14

Prepared by
AEROJET-GENERAL CORPORATION
LIQUID ROCKET OPERATIONS
SACRAMENTO, CALIFORNIA

AUTHORS: W. H. Knuth
J. Farquahr
B. Lindley

APPROVED: C. H. Lee
Manager
M-1 Turbopump Project

Technical Management
NASA LEWIS RESEARCH CENTER
CLEVELAND, OHIO

TECHNICAL MANAGER: W. W. Wilcox

APPROVED: W. F. Dankhoff
M-1 Program Manager

ABSTRACT

27692

A design study was conducted to determine the capability of adapting the M-1 fuel turbopump to satisfy the requirements of the PHOEBUS II Reactor Liquid Hydrogen Feed System.

Appropriate design and performance analyses as well as mechanical design effort were performed to the extent needed to permit rapid transition into a development program.

A 20% stall margin is predicted for the resulting pump hydraulic geometry at the nominal PHOEBUS operating point. A nominal speed of 11,500 rpm will be required to produce a 1400 psi pressure rise at a hydrogen weight flow of 350 lb/sec. The predicted nominal turbine weight flow is approximately 55 lb/sec.

Author

TABLE OF CONTENTS

TABLE LIST

FIGURE LIST

FIGURE LIST (Continued)

I. INTRODUCTION

PHOEBUS is the designation for a ground test nuclear reactor experiment to be conducted by the Los Alamos Scientific Laboratory (LASL) of the University of California under the joint auspices of the National Aeronautics and Space Administration and the Atomic Energy Commission. The experiment will be conducted at the Nuclear Rocket Development Station (NRDS), Jackass Flats, Nevada.

In operation, the PHOEBUS reactor is cooled and partially-moderated by pump-fed liquid hydrogen. The heated hydrogen is then expelled through a nozzle to produce thrust.

To accommodate various reactor operating modes and power settings, including start-up and shutdown transients, a versatile turbopump having wide operating range capability is required. Also, this turbopump should be both rugged and reliable because a turbopump failure could jeopardize the reactor. Other prerequisites include an extended mean operating time between overhauls (to minimize facility down time for pump replacement) as well as a reasonable uprating capability inherent in the design because future reactor and/or nozzle requirements may increase demands upon pump performance.

A program of detailed analysis and design work was completed by the Aerojet-General Corporation to adapt the M-1 fuel turbopump to the reactor liquid hydrogen feed system requirements in accordance with the specific performance requirements and parameters provided by NASA/LeRC. They are referenced as appropriate in the ensuing technical discussions. Appendix A is the list of symbols used in the figures, as appropriate, throughout this text.

The work performed was comprised of a final analysis and design to provide a detailed performance prediction, analysis of the modified turbopump and its sub-components, and to prepare all of the major designs and drawings needed to initiate hardware fabrication. Also, detailed procurement and fabrication planning was accomplished to permit rapid activation of a research and development program.

All of the study goals have been achieved. Individual areas of effort are summarized herein and the technical approach as well as results in each area are presented.

Based upon the results of this detailed study, it is concluded that the appropriately modified M-1 fuel turbopump design currently will meet all of the PHOEBUS reactor system requirements with a high margin of safety for all components. Also, the turbopump design provides an extensive up-rating capability. The turbopump can be fabricated, performance and demonstration tests conducted, and delivery accomplished within the required PHOEBUS schedule.

The information provided herein is the same as that originally submitted as the Final Report, Phase I, M-1 Fuel Turbopump Modification Program (Contract NAS 3-2555, Amendment No. 14).

II. SUMMARY

There are 13 major categories of endeavor comprising the M-1 Fuel Turbopump Modification Study. Each category is briefly summarized in this section and further amplified in the technical discussion.

A. DESIGN REQUIREMENTS

The design specification sheet for the PHOEBUS turbopump is provided as Table 1 and the required head-capacity operating envelope is shown as Figure 1. The PHOEBUS turbopump was designed to produce a nominal 1400-psi pressure rise at 350 lb/sec of liquid hydrogen with a 20% stall margin. Net positive suction pressure was assumed to be 25 psi. The turbine will be driven by hydrogen gas at ambient temperature bootstrapped from the pump discharge through a heat exchanger.

As a design goal, the turbopump is to have a two-hour life span between overhauls and the capability for single operating durations of 30 minutes. Mechanically-sound operation up to 14,500 rpm is required.

It is also necessary that the turbopump be able to follow commanded speed variations at frequencies up to 4 cps and with an amplitude of ± 5% of nominal operating speed desired.

B. DESIGN MODIFICATIONS

The special requirements for the PHOEBUS application necessitated some design modifications of the M-1 fuel turbopump.

The M-1 fuel turbopump was designed for a liquid hydrogen flow rate of approximately 600 lb/sec; therefore, it does not have an adequate stall margin for the PHOEBUS flow of 350 lb/sec (See Figure 2).

The M-1 turbine was designed for low pressure ratio operation using hot gas and would exhibit excessive tip leakage at the PHOEBUS higher pressure ratios using hydrogen gas at ambient temperature as planned for the PHOEBUS application.

Essentially, the M-1 fuel turbopump operates at a single speed and head-capacity point while PHOEBUS must accommodate an extensive range of speed as well as wide flow range excursions. The attendant shifts in axial thrust require that an axial thrust control system be incorporated into the PHOEBUS turbopump.

The thrust bearings used for M-1 are designed for relatively constant load with an expected life-span of one-hour while a two-hour life-span is required for PHOEBUS as well as the capability to accept load variations.

TABLE 1

DESIGN POINT SPECIFICATIONS, PHOEBUS TURBOPUMP

PUMP

Parameters	Specified Value
Propellant	Liquid Hydrogen
Propellant Temperature (inlet)	42°R
Propellant Density (inlet)	4.20 lb/ft^3
Shaft Speed	11,500 rpm
Total Discharge Pressure	1460 psia
Total Suction Pressure	60 psia
Total Pressure Rise	1400 psi
Total Head Rise (Cavitating) (based upon inlet density)	48,000 ft
Weight Flow	350 lb/sec
Capacity (based upon inlet density)	34,400 gpm
Specific Speed (based on cavitating head)	675
Efficiency	77.5%
Fluid Horsepower	30,900 fhp
Shaft Horsepower	37,200 bhp
Net Positive Suction Pressure	25 psi
Suction Specific Speed	14,400

TURBINE

Gas	Gaseous Hydrogen
Shaft Power	37,200 hp
Gas Weight Flow	54.5 lb/sec
Gas Inlet Total Temperature	60°F
Pressure Ratio	7.35
Static Back Pressure	60 psia
Shaft Speed	11,500 rpm
Efficiency	62%
Gas Inlet Total Pressure	444 psia
Nozzle Area	20.25 in.^{2}
Specific Heat	3.475 Btu/lb-°R
Specific Heat Ratio	1.399
Gas Constant	771.5 $\frac{\text{ft-lbf}}{\text{lbm-°R}}$

PHOEBUS PUMP
REQUIRED OPERATING ENVELOPE

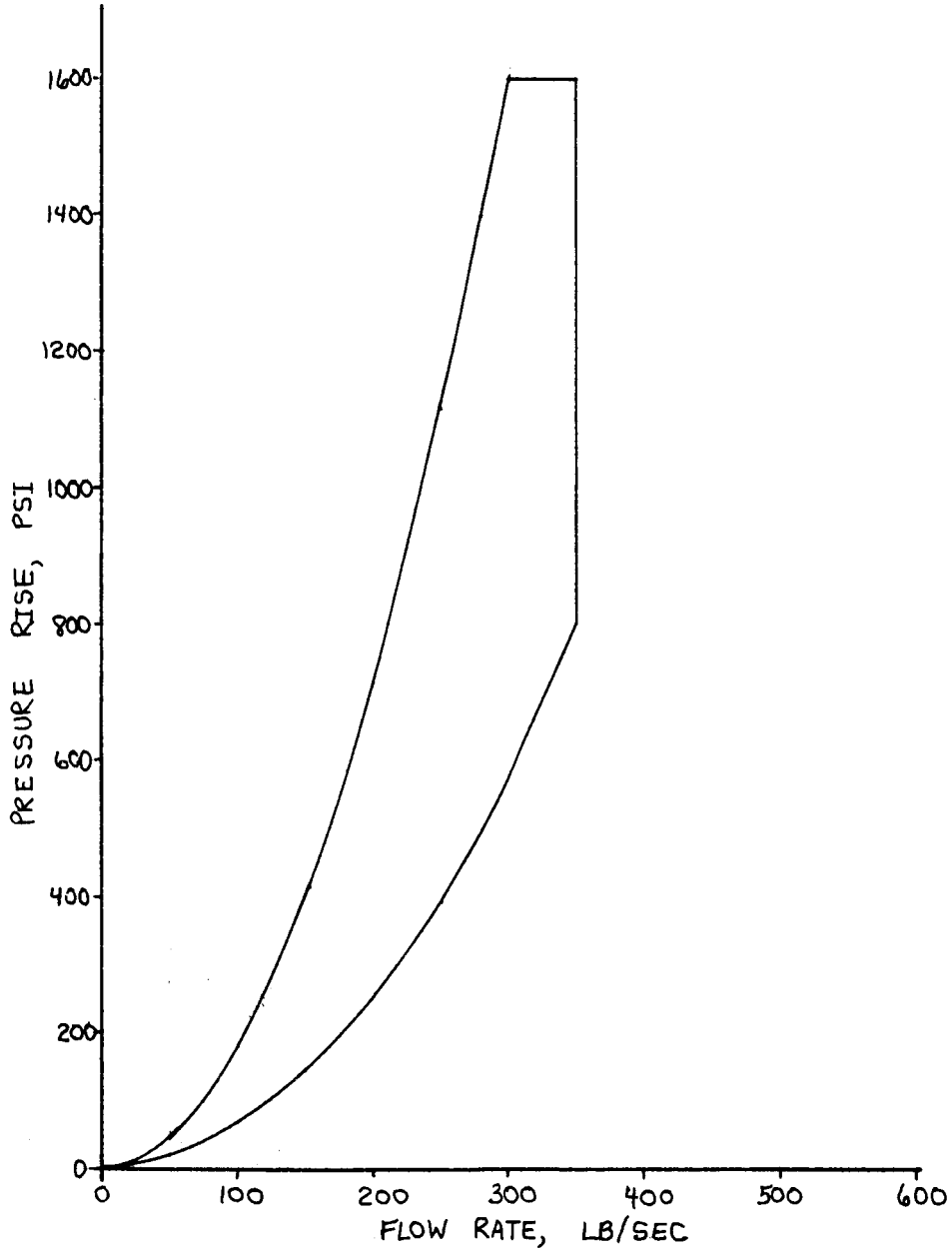

Figure 1

The PHOEBUS application requires that the turbopump dwell for extended periods within a range of speeds up to a nominal of 11,500 rpm. Therefore, the blading must be free from harmful natural frequencies excited to resonance at the lower speeds.

1. Inducer

The inducer was redesigned to maintain approximately the same flow coefficient as the M-1. This redesigned inducer has a reduced inlet tip diameter and a larger hub throughout. Also, the exit vane angle has been increased to accommodate a wider range of flow coefficient without cavitation of the stator.

2. Inducer Stator

The M-1 inducer stator vane contours were retained but the shroud dimensions were changed to match the new inducer and faired smoothly into the transition stage.

3. Transition Stage

The transition stage was redesigned to match the new velocity profile leaving the inducer stator, and to provide a nearly-uniform head and velocity distribution to the remaining stages.

4. Main Stages

The main stage rotor blades were reduced in height only by trimming the blade tips. The existing rotor blade tooling does not require modifications. However, modified stator Eloxing electrodes will be required.

5. Turbine

Honeycomb seals were added at the periphery of the turbine wheels to prevent excessive tip leakage. A simplified turbine exhaust manifold, which includes larger exhaust ports to minimize turbine back-pressure, is also planned.

6. Thrust Bearings

The M-1 thrust bearings were altered to incorporate a single curvature outer race instead of the "Gothic Arch" to eliminate the possibility of three-point contact under high-speed, light-load conditions. The roller bearings as well as the bearing coolant system are unchanged.

7. Axial Thrust Control

Valves were provided in the PHOEBUS balance piston bleed lines to control net axial thrust. The first valve is triggered closed by a pressure switch as pump speed rises, while the second (and possibly a third valve) is triggered closed by a speed signal. These valves are triggered to open in reverse order as speed decays.

8. Special Features

Special features in the form of rotor dynamic position sensors and a rotor lock were provided in the PHOEBUS design. Also, the design provides for the incorporation of a slip-ring assembly for backup torque measurements and to allow strain gage instrumentation of the rotor blading.

C. PERFORMANCE ANALYSIS AND AXIAL THRUST PREDICTION

Design and off-design head-capacity as well as stall line predictions were made using analysis techniques identical to those used for M-1. The method has been checked with data from 3/8-scale model M-1 fuel pump tests using water as the test fluid. These empirical results indicate that the actual head-capacity curve will have less slope than the predicted curve. The stall line prediction was within 2% of the measured value.

Axial thrust has been analyzed in detail for steady-state conditions over the entire operating map. Although the complexity of this analysis leaves some degree of uncertainty as to the results, it was found that the thrust control system has an extensive over-capacity which would provide for correction of any possible substantial variations from the predicted thrust values. It is estimated that a maximum net thrust of 20,000 lb is permissible for a two-hour thrust bearing life.

D. STRESS AND VIBRATION ANALYSES

Comprehensive stress and vibration analyses of all turbopump blading were performed. In some cases, it was possible to verify the analysis methods by using empirical results from the M-1 blade vibration tests. The steady-state stress levels of all blading was found to be satisfactory, but the vibration analysis disclosed several operating speeds which, it is predicted will produce blade resonances. The significance of these findings is detailed in the appropriate technical discussion. Detailed stress calculations were also made for other modified parts or existing parts running at new conditions. All parts were found to have positive margins of safety.

All running clearances and spline fits were reviewed. The PHOEBUS spline fits are either the same as for the M-1 or slightly tighter because the lower speed reduces centrifugal growth. Running clearances are either the same or slightly greater than used for M-1 except at the inducer, where the tip clearances was intentionally reduced to 0.090-in. from the 0.150-in. used for M-1.

E. BEARING COOLANT FLOW ANALYSIS

Bearings for the PHOEBUS application will be run at lower speeds and loads than in the M-1. However, the bearing coolant system was unaltered, thereby assuring more than adequate coolant flow.

F. COMPUTER MODEL OF PHOEBUS TURBOPUMP

Work was initiated to adapt the M-1 digital computer model to the PHOEBUS turbopump. When completed, this model will permit dynamic studies to be made of the turbopump operation in the E-Area test stand (Aerojet-General) as well as in the reactor facility (NRDS). Also, transient axial thrust conditions can be predicted as well as the analytical response of the turbopump to 4-cps speed commands. The basic computer program has been completed.

G. BASIC MECHANICAL DESIGN TASKS

Each modification of the M-1 fuel turbopump was fully supported by appropriate mechanical design effort to incorporate the change into the PHOEBUS turbopump. This effort included complete definition of the modifications by means of a Basic Parts List.

H. PLUMBING

Detailed analysis and design of plumbing for the reactor facility installation has been completed. Also, a portion of the detailed drawings were completed. It is planned that pump inlet and discharge lines as well as turbine inlet and exhaust lines would be supplied by Aerojet-General.

I. SHIPPING CONTAINER AND FACILITY MOUNT

Design of the shipping container and the NRDS reactor facility turbopump mount were completed.

J. DRAFTING

All major drafting effort in connection with the M-1 fuel turbopump design modifications was completed and the drawings are on file. The remaining work which will be accomplished during Phase II, consists of minor short lead-time hardware items and commercial item callouts.

K. PERT

A significant effort was directed toward evolving a comprehensive PERT network for the M-1 Fuel Turbopump Modification Program. The relatively tight Phase II schedule required that close control of all aspects of the procurement and assembly schedules be maintained. The PHOEBUS PERT network prepared is comparable to that for the M-1 fuel turbopump.

L. QUALITY CONTROL

Quality Control planning for the M-1 Fuel Turbopump Modification Program is based upon MPC 200-2. This quality control program has been streamlined to minimize costs without detracting from its effectiveness and is detailed in the appropriate technical discussion.

M. DESIGN PRODUCIBILITY STUDIES

To assure that no delays would be encountered in fabricating the modified guidevane housing (inducer stator) casting as well as the new inducer, design producibility studies were conducted in both cases. A casting pattern was fabricated for the guidevane housing and a computer programing system for Omnimil generation of the inducer blading was demonstrated by cutting a prototype PHOEBUS inducer.

III. CONCLUSIONS AND RECOMMENDATIONS

A. CONCLUSIONS

As a result of the M-1 Fuel Turbopump Modification Study, the following conclusions are presented.

1. There are no major design or fabrication problems involved in adapting the M-1 fuel turbopump to the PHOEBUS feed system requirements.

2. The modified M-1 fuel turbopump will have adequate stall margin and a broad range of operating capability.

3. The modified M-1 fuel turbopump can be plumbed directly into existing reactor facility plumbing.

4. The PHOEBUS hydraulic performance requirements are significantly less than the M-1 requirements. As a result, the PHOEBUS turbopump has a substantial mechanical over-design along with an attendant potential for long-life and extended operating range.

5. An axial thrust control system will be required to maintain bearing loads within the predicted necessary levels for a two-hour operating life. More than adequate control can be achieved by the use of off-on valves in the thrust piston return lines.

6. The M-1 bearing coolant supply system is more than adequate for the PHOEBUS application.

7. Analyses of blading vibration modes and frequencies have shown that:

   a. Sufficient internal damping is available to eliminate many frequencies from consideration.

   b. The stator shroud design could be modified to allow for attaching two or more blades together, thereby eliminating an additional group of frequencies.

   c. Consideration should be given to limiting operating time at particular speed levels where undesirable frequencies cannot otherwise be avoided.

8. Areas in which potential fabrication problems could be encountered because of the uniqueness of PHOEBUS hardware have been resolved by completing a guidevane housing casting pattern and generating a prototype PHOEBUS inducer.

9. The turbine has significant excessive power capability to assure satisfying the requirement for 4-cps speed response capability.

10. The three-stage turbine, specifically designed for this application, could reduce the required turbine weight flow of gaseous hydrogen by approximately 20% to 25%.

B. RECOMMENDATIONS

1. The modified M-1 fuel turbopump described herein is recommended for the PHOEBUS application. The wide operating range along with the uprating capability of this turbopump provide ready-adaptability to existing reactor requirements as well as permitting accommodation of a substantial increase in reactor operating levels in the future.

2. To conserve hydrogen, thereby increasing run duration capability and reducing cost, a "workhorse" three-stage turbine should be considered for this application.

3. To accommodate turbine gas flow rates ranging upward from 50 lb/sec, the reactor facility parallel turbine exhaust line sizes should be increased to approximately 15-in. (inside diameter).

IV. TECHNICAL DISCUSSION

A. DESIGN REQUIREMENTS

1. Technical Requirements for the Modified Pump

a. The nominal operating point is 300 lb/sec delivered hydrogen flow rate at a pressure rise of 1400 psi, plus approximately 55 lb/sec turbine bootstrap flow.

b. A minimum of 20% margin to the stall line at the nominal point. (For this study, stall margin is defined as weight flow rate margin along a constant 1400 psi pressure differential line with the nominal flow rate defined as the delivered flow rate plus 50 lb/sec, which is an allowance for the turbine requirement.)

c. The required area of operation is shown in Figure 1. The limit line on the minimum flow rate side of the envelope is defined by the stall limits delineated in Item b above.

d. No major efforts are to be made to improve performance outside of the specified area.

e. Turbine gas at a turbine inlet pressure of 440 psi is to be derived by bootstrapping a part of the pump flow through a water-to-liquid hydrogen heat exchanger.

f. Nominal turbine inlet temperature is 520°R.

g. Control systems will not be furnished by the contractor but speed signals and an overspeed safety device are required for the turbopump package.

h. The turbopump must be able to follow a 4-cps sine wave speed command signal at nominal speed.

i. The pump shall be mechanically sound when operated at 14,500 rpm.

j. The maximum available NPSP is assumed to be 25 psi and the pump should require no higher NPSP when operating within the envelope of Figure 1. (For this study, it is also assumed that no values of NPSP less than 25 psi will be supplied.)

k. The pump shall be capable of running continuously for 30 minutes and have as a goal, a two-hour operating life without dissassembly.

1. A feasibility study is to be conducted for installation of a rotor locking device and a proximity measuring device for radial and axial movement of the rotor.

2. Analysis Effort

a. New axial thrust at the nominal and off-design conditions.

b. Stress analysis of all modified parts or existing parts operating at new conditions.

c. Vibration analyses of all blading and rotor discs.

d. Determination of critical speed of the modified rotating assembly.

e. Bearing coolant flow over the entire operating range.

f. Performance of the turbine under the expected nominal and off-design conditions.

g. Running clearance and spline fits for parts operating under conditions different from those for the current M-1 fuel turbopump.

h. Detailed study of necessary modifications to the axial flow blading to meet the design requirements.

i. Study of control and safety requirements to assure safe operation for 30 minutes.

3. Additional Information

a. A requirement was added for a 30-sec run duration at the overspeed condition of 14,500 rpm. Also, one for definition of the pumping system envelope dimensions and allowable flange loads.

b. A capability for a 4-cps speed variation of ± 5% amplitude at the nominal speed condition was added.

B. COMPARISON OF PHOEBUS DESIGN REQUIREMENTS WITH THE UNMODIFIED M-1 FUEL TURBOPUMP

Figure 2 shows the nominal and uprated PHOEBUS operating points on a plot of the M-1 fuel pump pressure rise versus weight flow rate for lines of constant speed. The unmodified M-1 fuel turbopump does not have an adequate stall margin for the reduced flowrates of the PHOEBUS requirements. Design modifications are required in the hydraulic passages and in the pump blading geometry. Figure 3 shows the non-dimensional predicted performance for the modified turbopump.

The M-1 Model II fuel turbine stages were designed essentially as impulse stages. Operation of the turbine using hydrogen gas at ambient temperature at the PHOEBUS speeds and powers results in a relatively large reaction which causes a pressure drop and leakage across the rotors. No provision was made in the M-1 design for sealing on the rotor outer shrouds. It is advantageous that such sealing be provided in the PHOEBUS design. The leakage losses are discussed and a description of the proposed turbine design modifications are presented in the appropriate turbine design discussion.

A "Gothic Arch" thrust bearing outer race configuration was used in the M-1 fuel turbopump, to minimize axial rotor travel. At high speeds and low axial thrust loads, three-point contact of the balls can occur with such geometry. This presents no problem for the M-1 design, which has essentially only a single steady-state operating point; however, it may pose a problem in the PHOEBUS application where the thrust load on the bearing may vary at high speeds because of the action of the thrust control system. Therefore, it is planned to use a conventional single-curvature outer race configuration in the thrust bearings in the PHOEBUS application to extend the low-load operating capability of the bearings at high speeds.

The current M-1 thrust bearings are designed to operate at a thrust load of 35,000 lb and a speed of 13,300 rpm for one hour. To achieve the two-hour operating life for the PHOEBUS application, the thrust balance control system is designed to limit the maximum load to 20,000 lb. At the reduced load, better axial stability of the rotating assembly is obtained if half of the Belleville spring stacks used in the M-1 design are removed. To limit the bearing axial thrust force, control valves must be installed in the thrust balance piston return flow lines. These changes are detailed under the Power Transmission Assembly discussion.

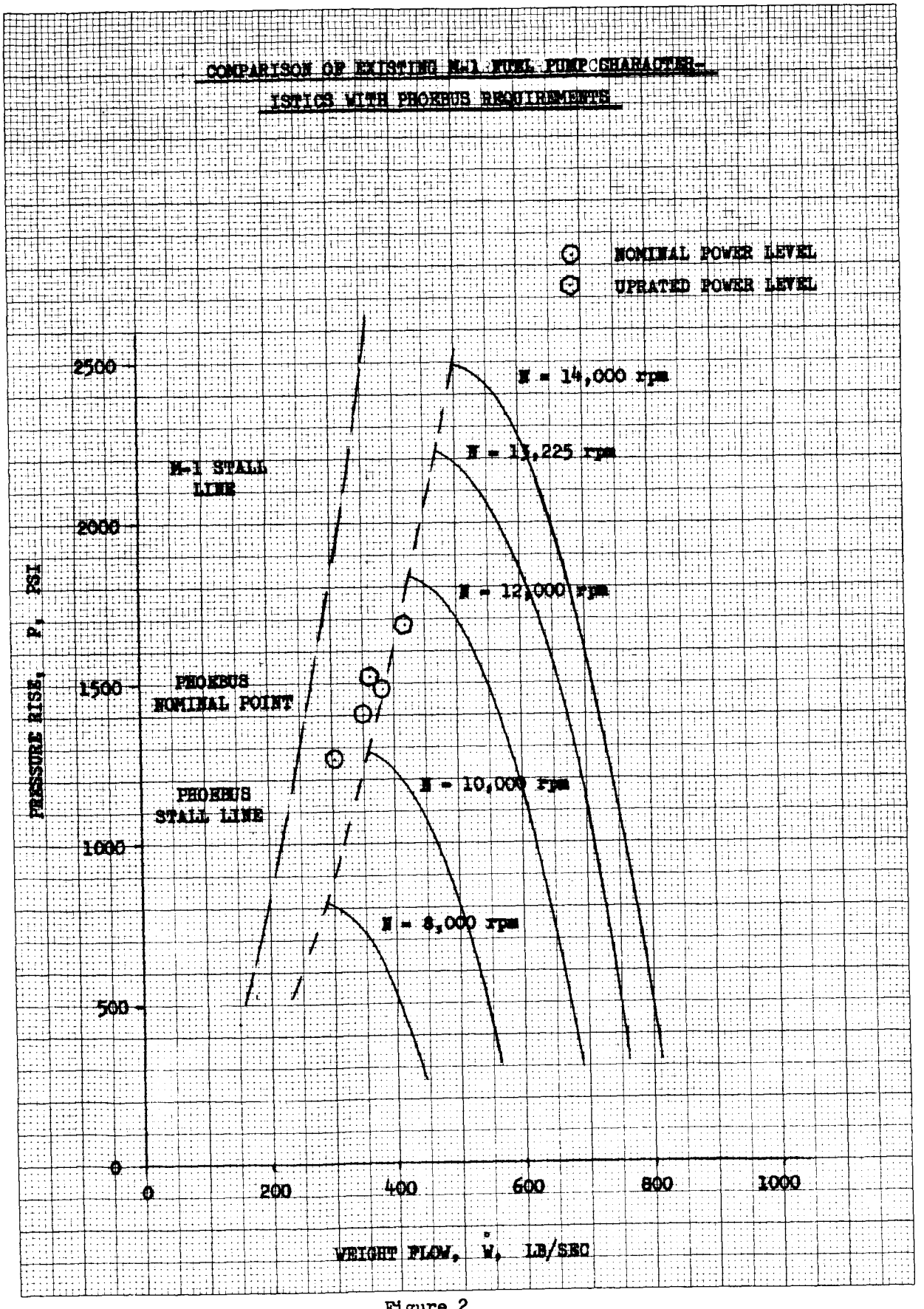

Figure 2
Page 14

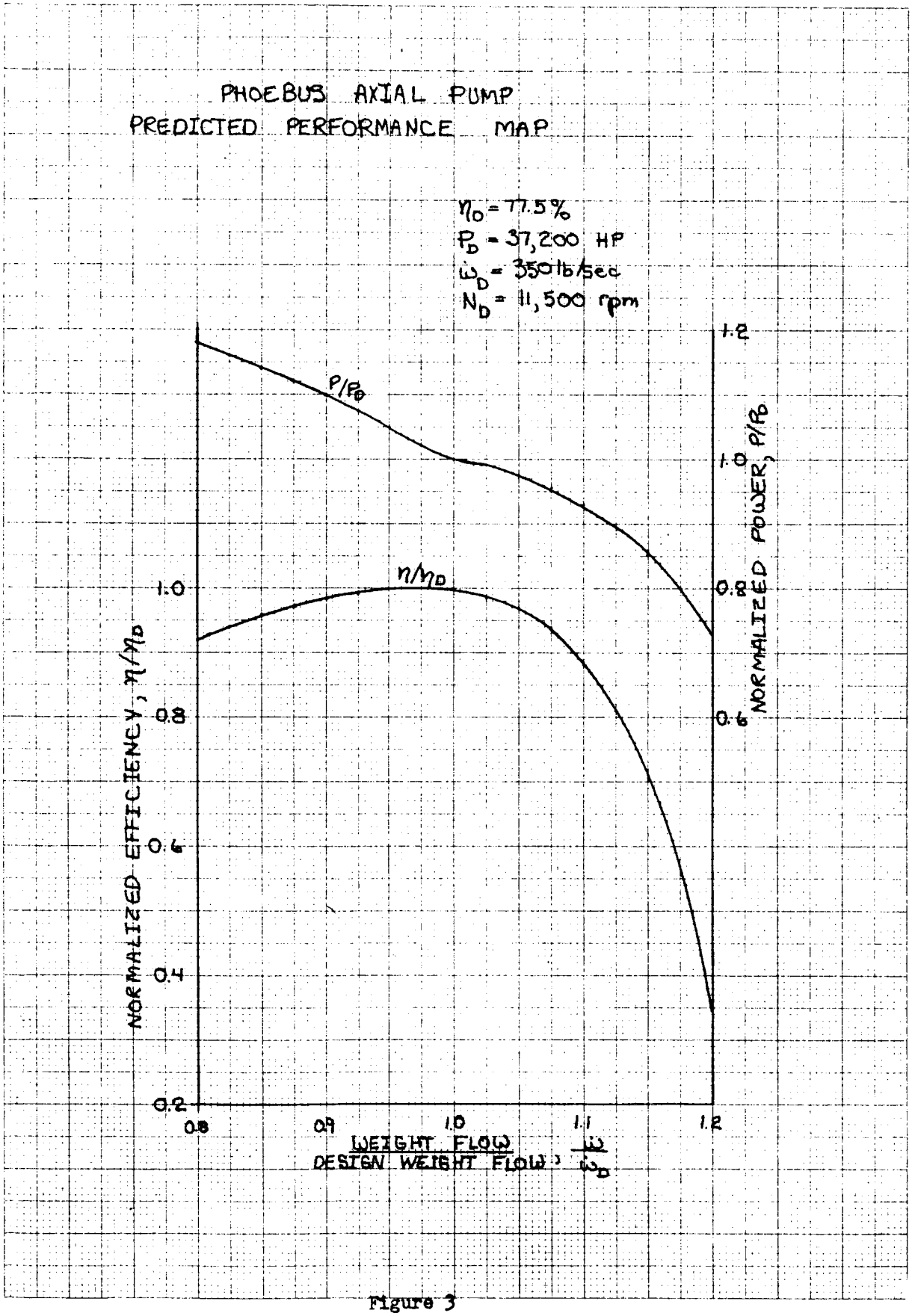

Figure 3
Page 15

The existing M-1 fuel pump design has no provision for locking the rotor, or measuring axial or radial rotor position during operation. Details of proposed modifications to incorporate these features are discussed under Special Features.

In addition to the modifications which stem directly from the special PHOEBUS design requirements, the following are desirable modifications. They are also detailed in the Special Features discussion.

1. A rotor breakaway and running torque measuring device, which will provide a more convenient method of performing this operation in the NRDS installation where clearance between the turbopump and floor level is limited.

2. A strain gauge/slip ring device for measuring operating torque which is intended as an alternative, particularly for low torque levels, where the existing M-1 device may not be accurate.

3. Devices for measuring pump rotor and stator vane strains would be used to check stresses during development testing, particularly those which are dynamic in nature.

C. PUMP HYDRODYNAMIC DESIGN MODIFICATIONS AND PERFORMANCE ANALYSIS

The design objective was to modify the M-1 axial flow fuel pump for the PHOEBUS application with a minimum amount of hardware change. To achieve this objective, a study was conducted to determine the necessary modifications.

The analysis showed that by maintaining the M-1 design flow coefficient, the major modifications would consist of a reduction in hydraulic passage height as well as a redesign of inducer and transition stages. Because of the inducer stator casting complexity, modification to this element was limited to meridional contour profiles, which imposed additional requirements upon both the upstream and downstream elements. The PHOEBUS inducer rotor was designed to meet suction performance requirements while producing a greater percentage of the total head rise. The PHOEBUS transition stage was designed as a lightly-loaded stage which would flatten the head distribution and provide the first main stage rotor with the proper flow conditions.

Figure 4 shows the hydraulic passage dimensions of the modified pump. Table 2 is a listing of the critical dimensions and design parameters for both the M-1 fuel turbopump and the M-1 fuel turbopump as modified for PHOEBUS.

PHOEBUS TURBOPUMP ASSEMBLY

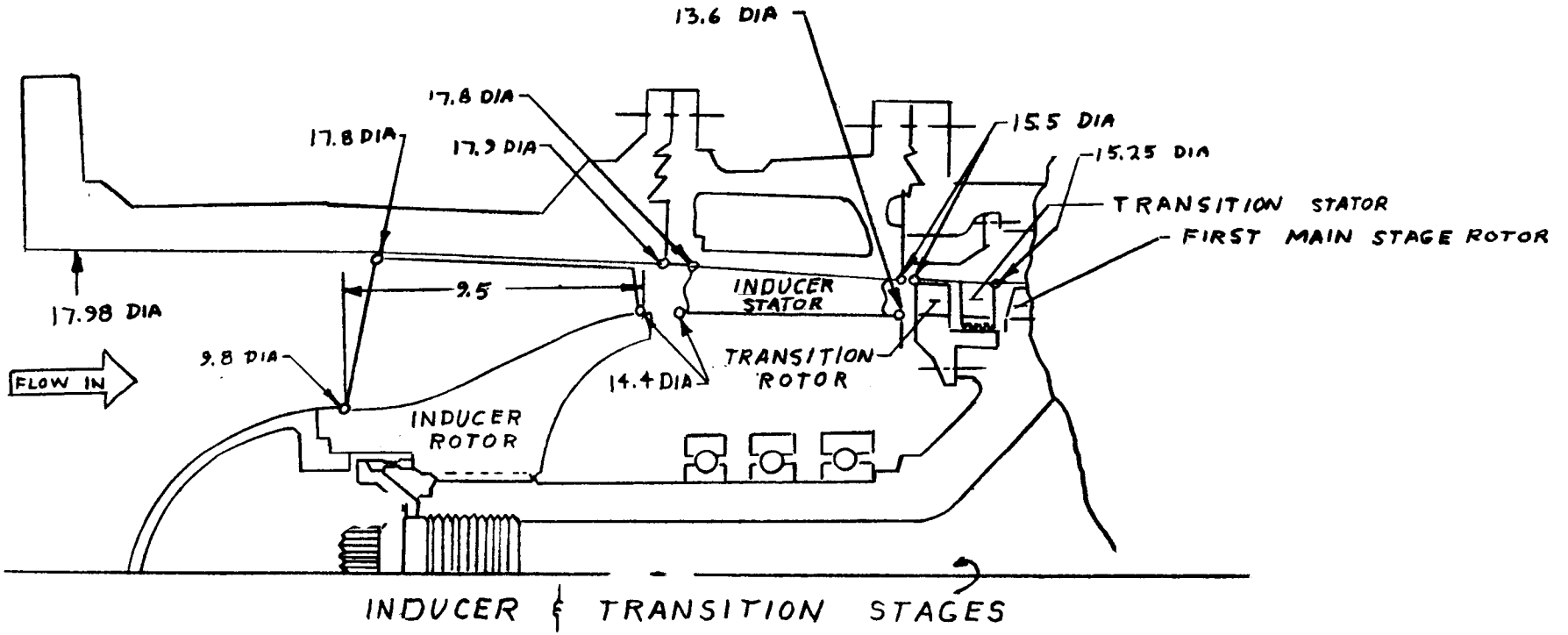

INDUCER & TRANSITION STAGES

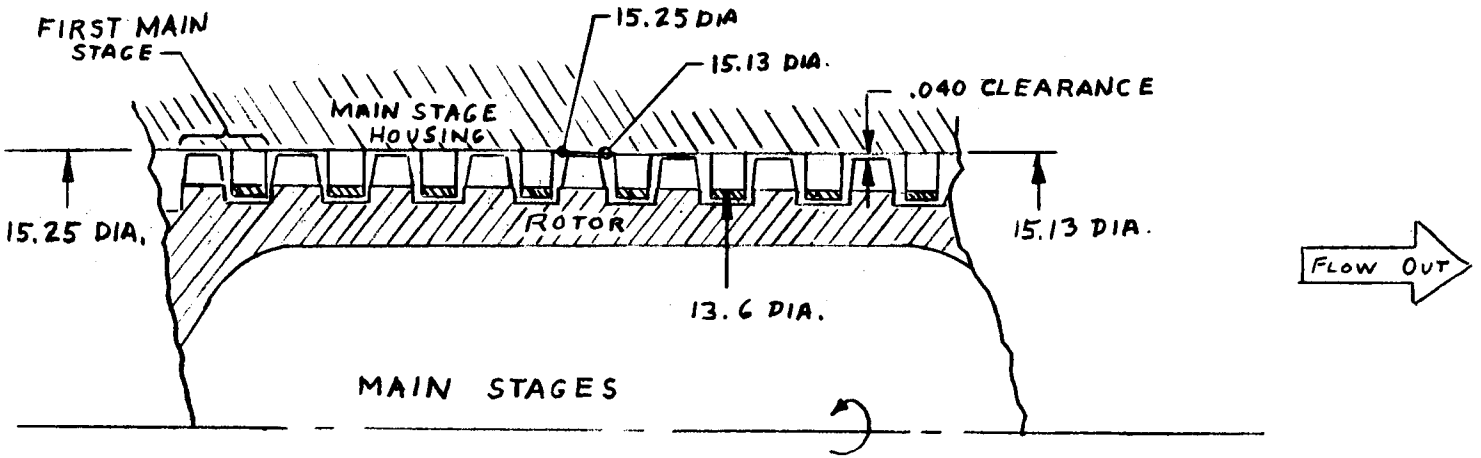

MAIN STAGES

Figure 4
Page 17

TABLE 2

MODIFIED PUMP BLADING

Inducer Stage	M-1	PHOEBUS
Type of Inducer	Cambered	Flat Plate
Number of Rotor Blades	6	6
Inlet Tip Radius (in.)	9.6	8.9
Inlet Radius Ratio	0.45	0.55
Blade Inlet Angle at Tip (Degrees)	5.92	7.65
Max. Hub Thickness to Max. Height Ratio	1.0	0.851
Max. Thickness to Max. Height Ratio	0.189	0.213
Max. Predicted Stress (ksi)	30.8	32.4
Design Suction Specific Speed	20,000	49,700
Nominal Suction Specific Speed	21,400	14,200
ϕ Inlet Nominal No Blockage	0.0779	0.0765
Transition Stage		
Type of Blade	C-4	C-4
Number Rotor Blades	31	31
Number Stator Blades	45	45
T/C Hub Rotor	0.10	0.12
T/C Hub Stator	0.08	0.12
ϕ Discharge Nominal (No Blockage)	0.381	0.374

The actual blade profiles have been omitted from this report because of the extensive description associated with the blade (ten profiles per blade).

Blade coordinates for all elements, except the inducer rotor, were computed using standard C-4 section properties. The inducer rotor blade coordinates for machining and inspection were calculated by an impeller design computer program. This program, which is delineated in the inducer discussion, required blade angle distribution at tip and hub, contour shape, and blade thickness distribution at tip and hub as computer input.

1. Inducer Stage

The inlet geometry was determined using the method described by L. B. Stripling in his paper discussing cavitation in turbopumps(1). The necessary design parameters were speed, flow, tip radius, radius ratio, and inlet incidence angle to blade angle ratio (i/β). A design flow rate of 350 lb/sec was used. The speed was set at 11,500 rpm by the main stage blading (flow coefficient and stall margin). The tip radius selected was the same as the existing inducer stator inlet radius (8.900-in.) to obtain a cylindrical inducer. Blade height was limited to 4.0-in. because of stress and vibrational considerations. The i/β ratio was obtained from existing test data, which show that maximum suction performance occurs at a value of 0.425. With these design parameters, the inducer is expected to be capable of good suction performance while operating at relatively low stress levels. The design suction specific speed is 49,700. Maximum predicted blade stress is 32.4 ksi at the "worst case" operating point.

The inducer rotor discharge geometry was set by the required stage head rise and the necessary hydraulic match with the existing stator blade form. To determine the optimum discharge geometry, a parametric study was conducted with discharge blade angle and discharge hub and tip radii as variables.

If the discharge tip diameter was reduced below 8.9-in., the benefit of the existing large stator inlet angles at the outer shroud would be lost because they would be covered by the shroud. The high stator inlet angles are necessary to maintain reasonable stator incidence because of the high whirl velocities in the fluid leaving the tip of the rotor discharge. Therefore, the rotor discharge radius was set at the maximum (equal to the M-1).

(1) ASME Paper No. 61-WA-98, Volume 84, 1962, L. B. Stripling, Cavitation in Turbopumps, Part 2.

As shown in Figure 5, the stator incidence angle decreases with increasing rotor hub radius, but is only slightly influenced by the inducer rotor discharge vane angle, Figure 6. From these comparisons, which are shown at the design point, a hub radius of 7.2-in. was selected. This provides positive incidence (2 degrees at mean streamline) to the stator at the design point while maintaining the required stall margin.

Predicted inducer rotor head rise at the design point was 9760 feet with discharge blade angles of 19.8 degrees at the tip and 26.0 degrees at the hub. This head rise results in an inducer design specific speed of 2,200 $\frac{\text{rpm gpm}^{1/2}}{\text{ft}^{3/4}}$. The total rotor blade angle distribution at tip and hub are shown in Figure7. Inducer blade wrap angle and thickness distribution are shown in Figures 8 and 9, respectively.

The inducer non-cavitating performance (head rise and discharge velocity distribution) was determined using a two-dimensional axi-symmetric solution where simple radial equilibrium is assumed to exist, $dh/dr = \frac{V_T^2}{gr}$. This assumption appears to be justified for this design because the streamline curvature is small near the discharge as can be seen from the inducer profile, Figure 10. The solution of the radial equilibrium equation is performed inside the blade, where the fluid angle is known, and progresses outside the blade, where the fluid angular momentum is assumed to remain constant. Inducer loss coefficients assumed were the same as those used for the M-1 design. The values assumed were 0.15 at the hub, 0.08 near the mean streamline and 0.30 at the tip. These values were based upon NASA data for a series of inducers (see Figure 11).

The inducer stator serves two functions: it is a hydraulic guide vane; and a structural support (containing coolant supply passages) for the pump bearings. The M-1 stator casting pattern will be used with modification to the shroud contours. At the inlet, the hub radius will be increased from 6.8-in. to 7.2-in. Discharge radii are changed to 6.8-in. at hub and 7.75-in. at tip. Both tip and hub contours will be conical from inlet to discharge. As previously noted, the inlet annulus was placed at the maximum radius to take advantage of the existing high inlet vane angles at the outer shroud streamline.

In M-1 subscale fuel pump testing, it appeared that the inducer stator did not stall at the flows above 80% of nominal. For this reason as well as the difficulty involved in producing new blade forms, no changes were made in the blade shape. Figures 12 through 14 show predicted rotor, stator, and over-all stage performance for the inducer stage.

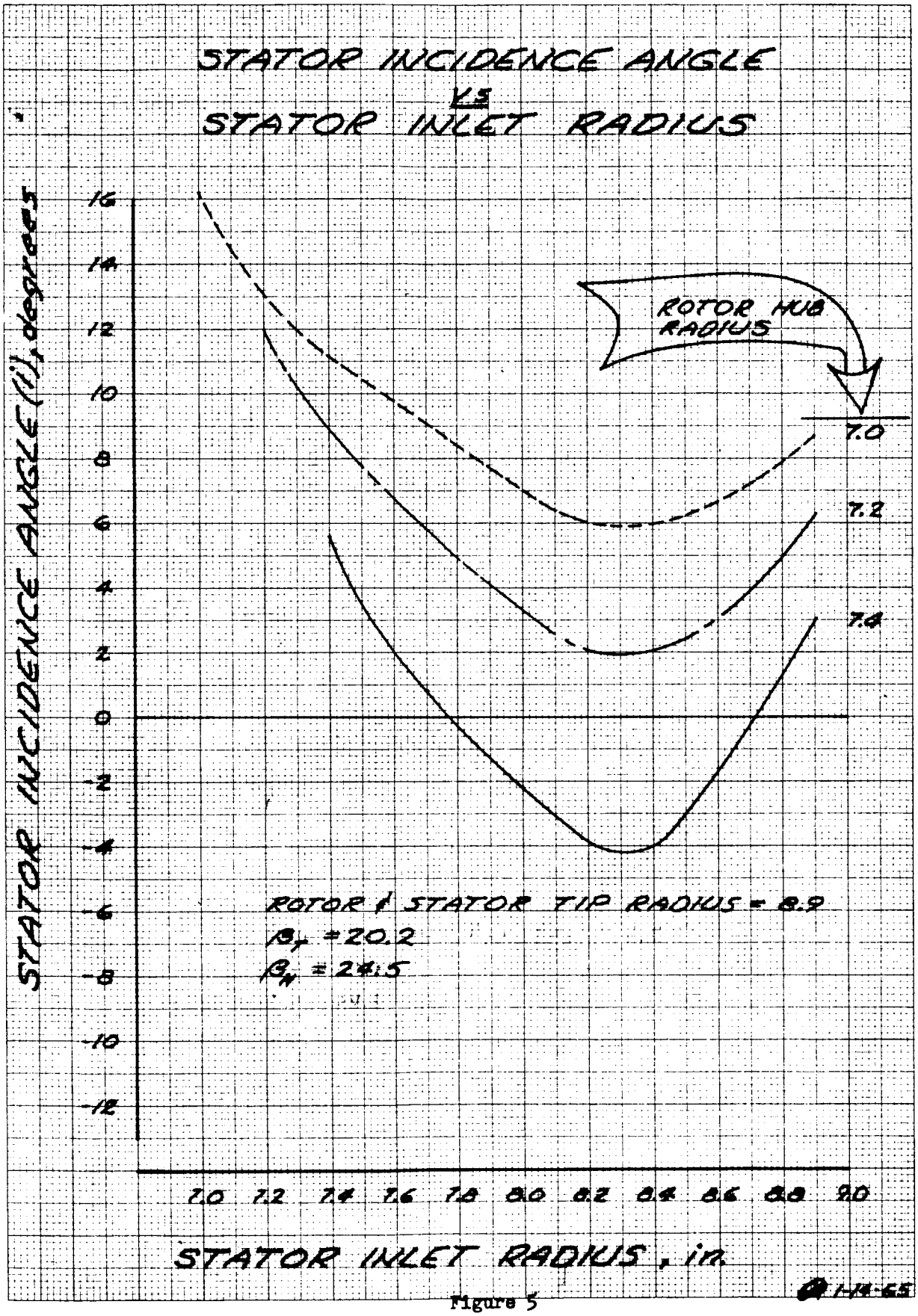
STATOR INCIDENCE ANGLE
VS
STATOR INLET RADIUS
STATOR INCIDENCE ANGLE (i), degrees
16
14
12
10
8
6
4
2
0
-2
-4
-6
-8
-10
-12
ROTOR HUB RADIUS
7.0
7.2
7.4
ROTOR & STATOR TIP RADIUS = 8.9
β_1 = 20.2
β_N = 24.5
7.0 7.2 7.4 7.6 7.8 8.0 8.2 8.4 8.6 8.8 9.0
STATOR INLET RADIUS, in.
1-14-65

Figure 5

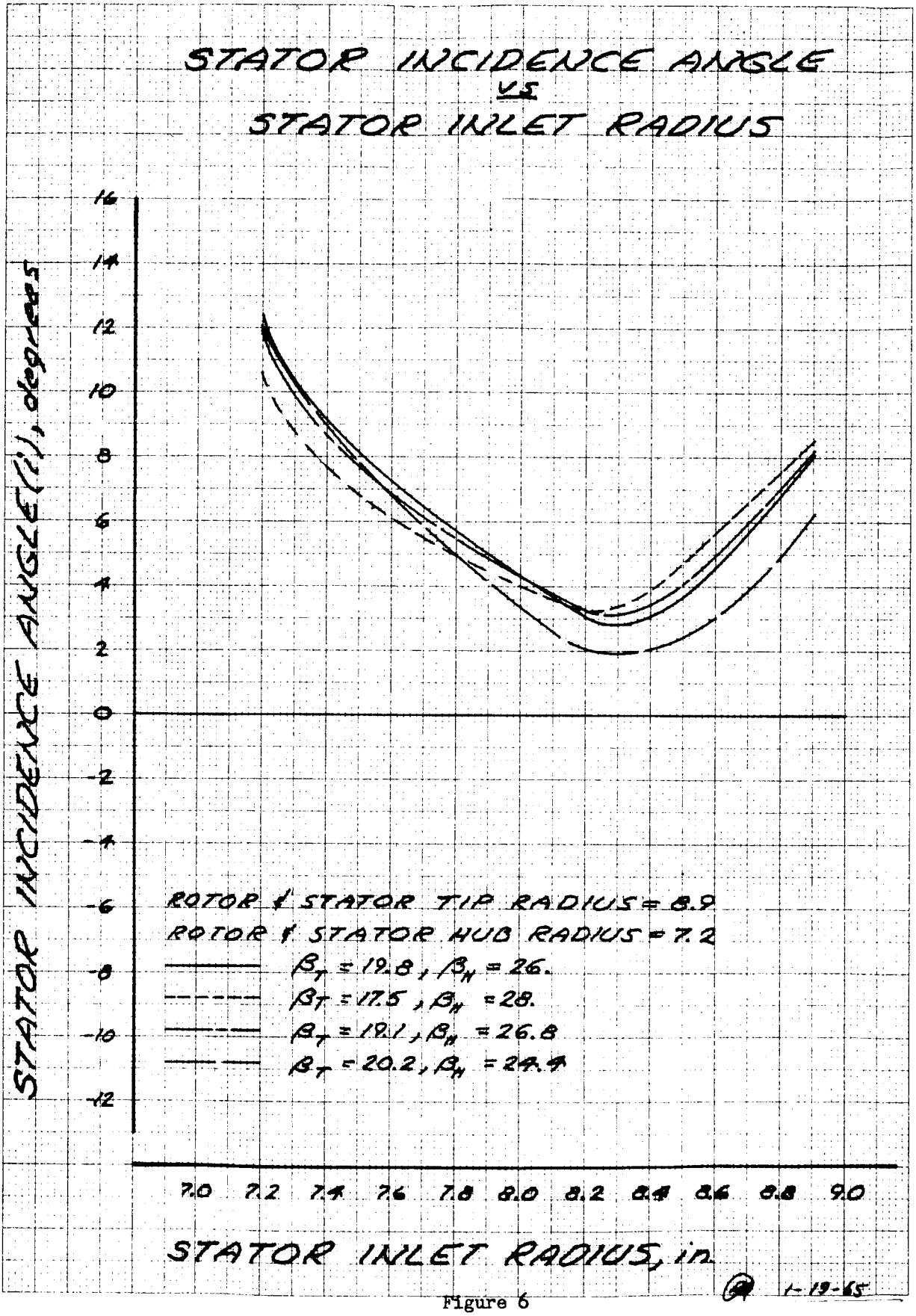

Figure 6
Page 22

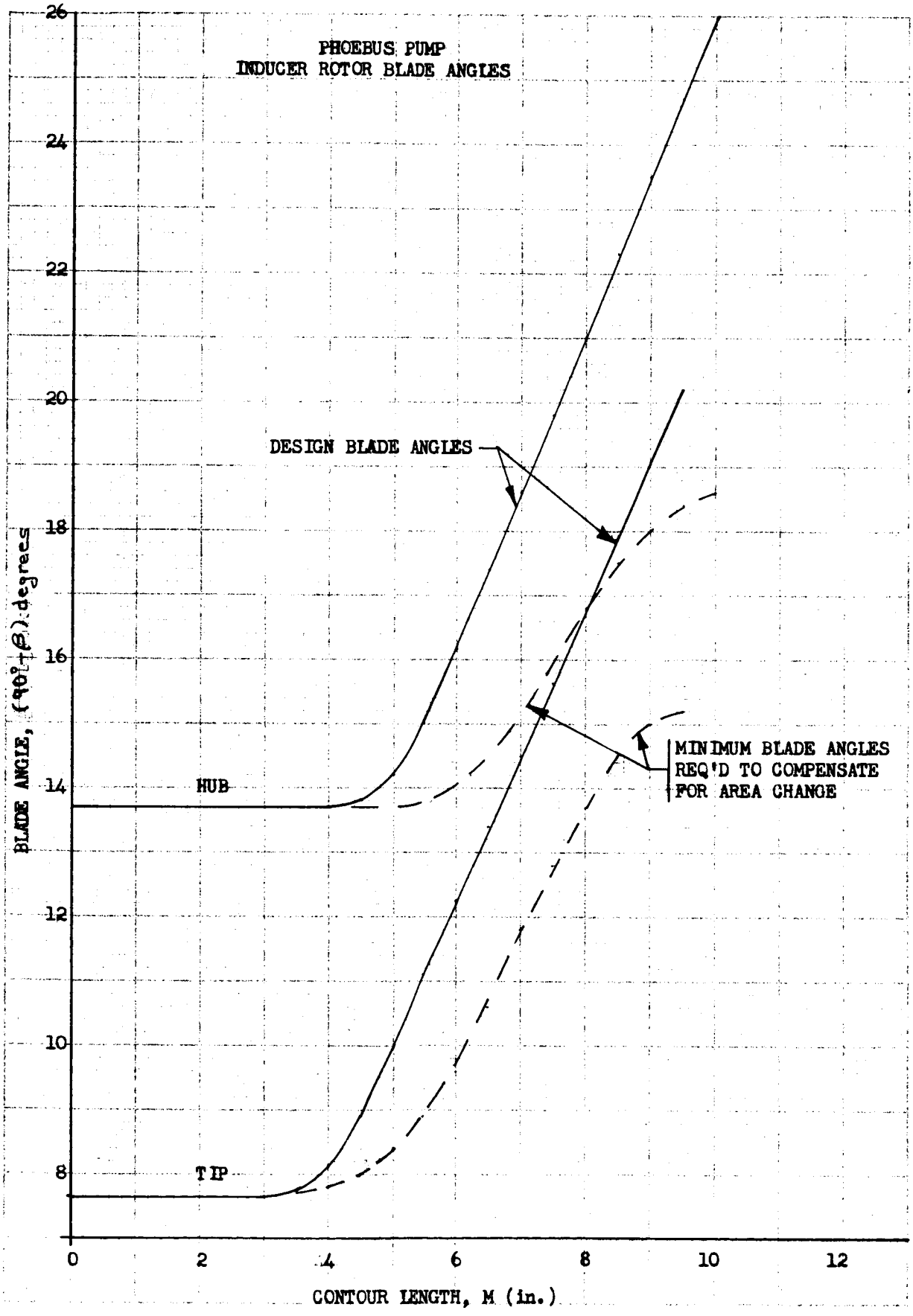

Figure 7
Page 23

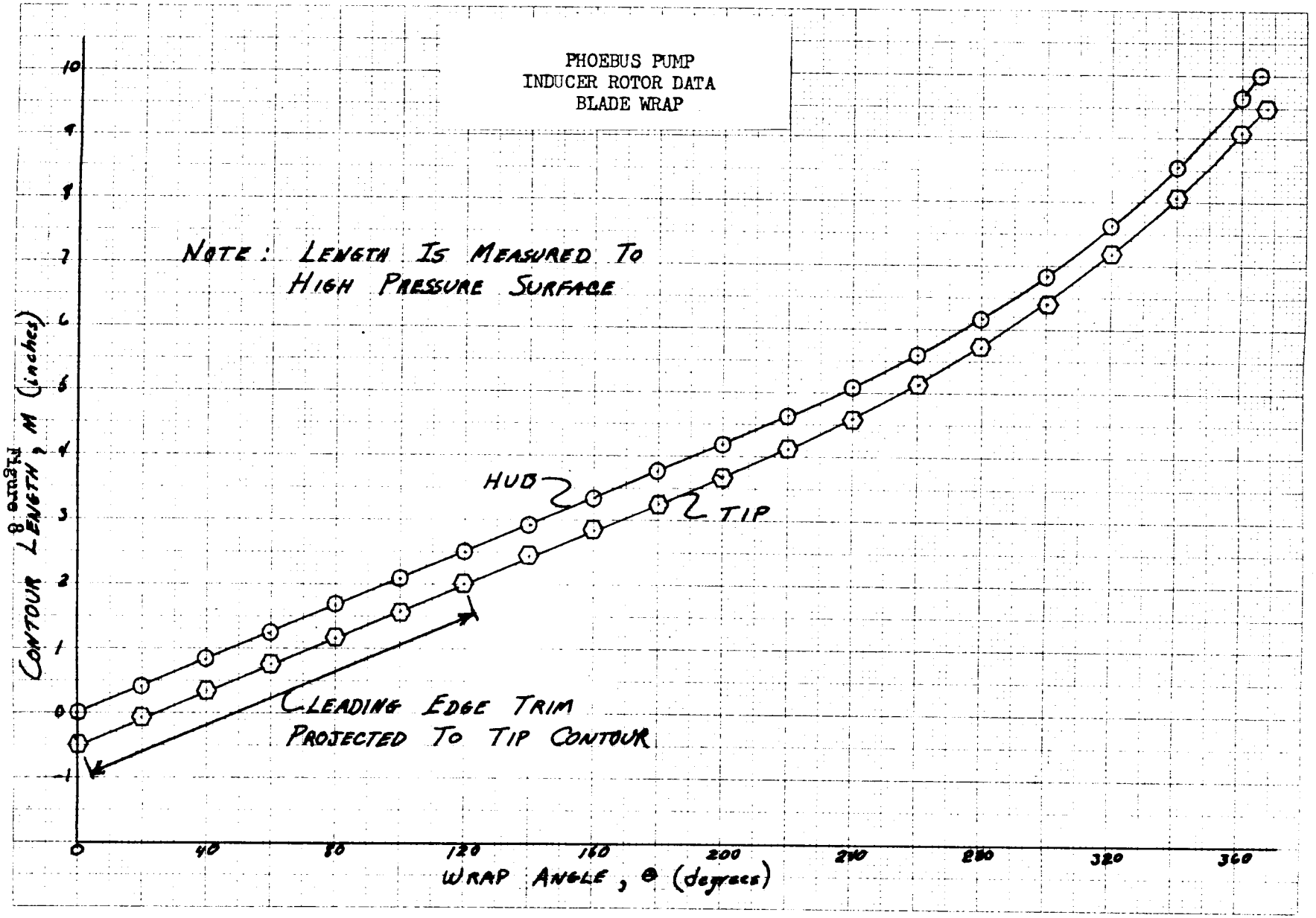
PHOEBUS PUMP
INDUCER ROTOR DATA
BLADE WRAP
NOTE: LENGTH IS MEASURED TO HIGH PRESSURE SURFACE
HUB
TIP
LEADING EDGE TRIM PROJECTED TO TIP CONTOUR
CONTOUR LENGTH, M (inches)
WRAP ANGLE, θ (degrees)
10
9
8
7
6
5
4
3
2
1
0
-1
0
40
80
120
160
200
240
280
320
360

Figure 8

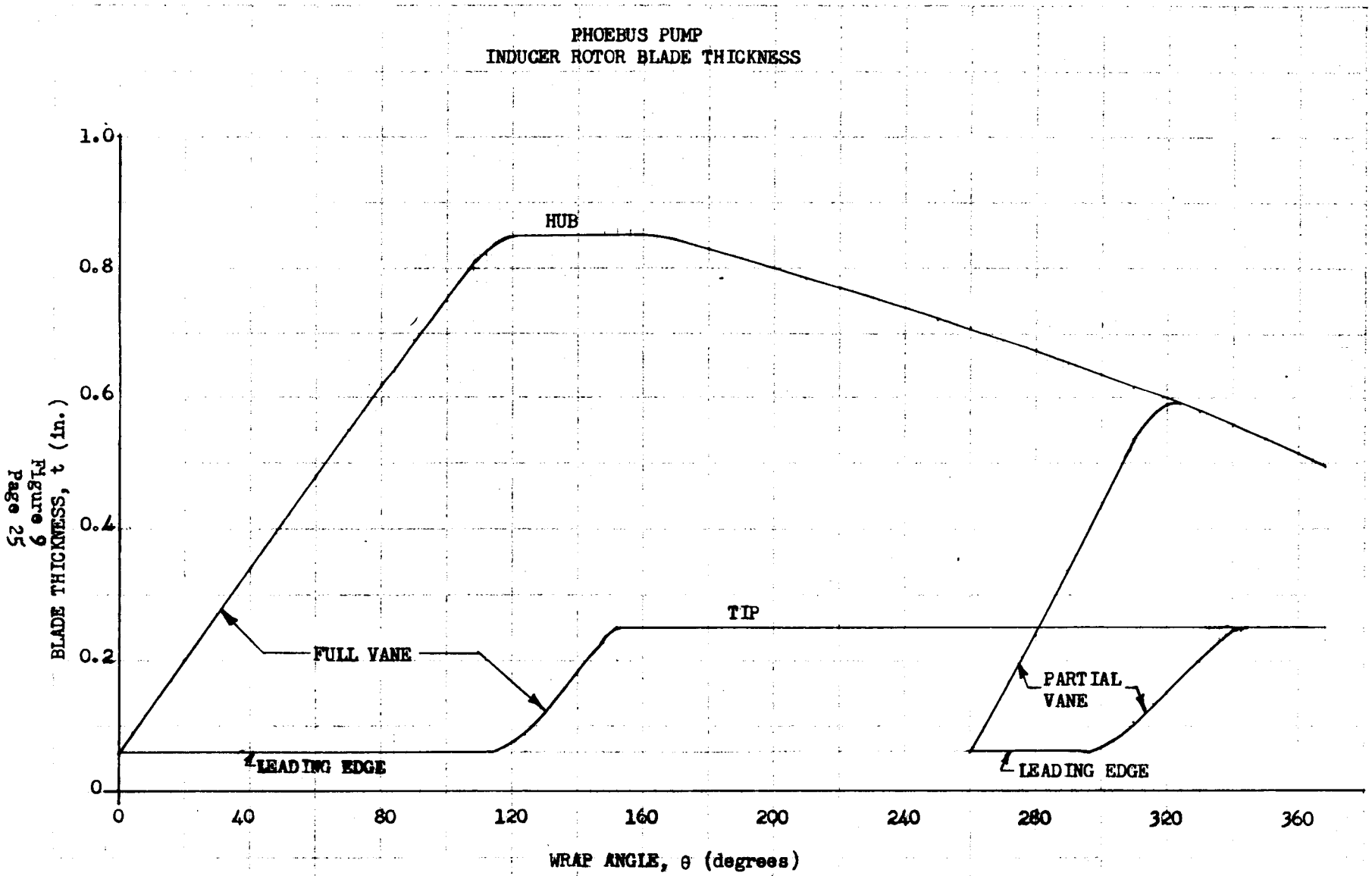

Figure 9
Page 25

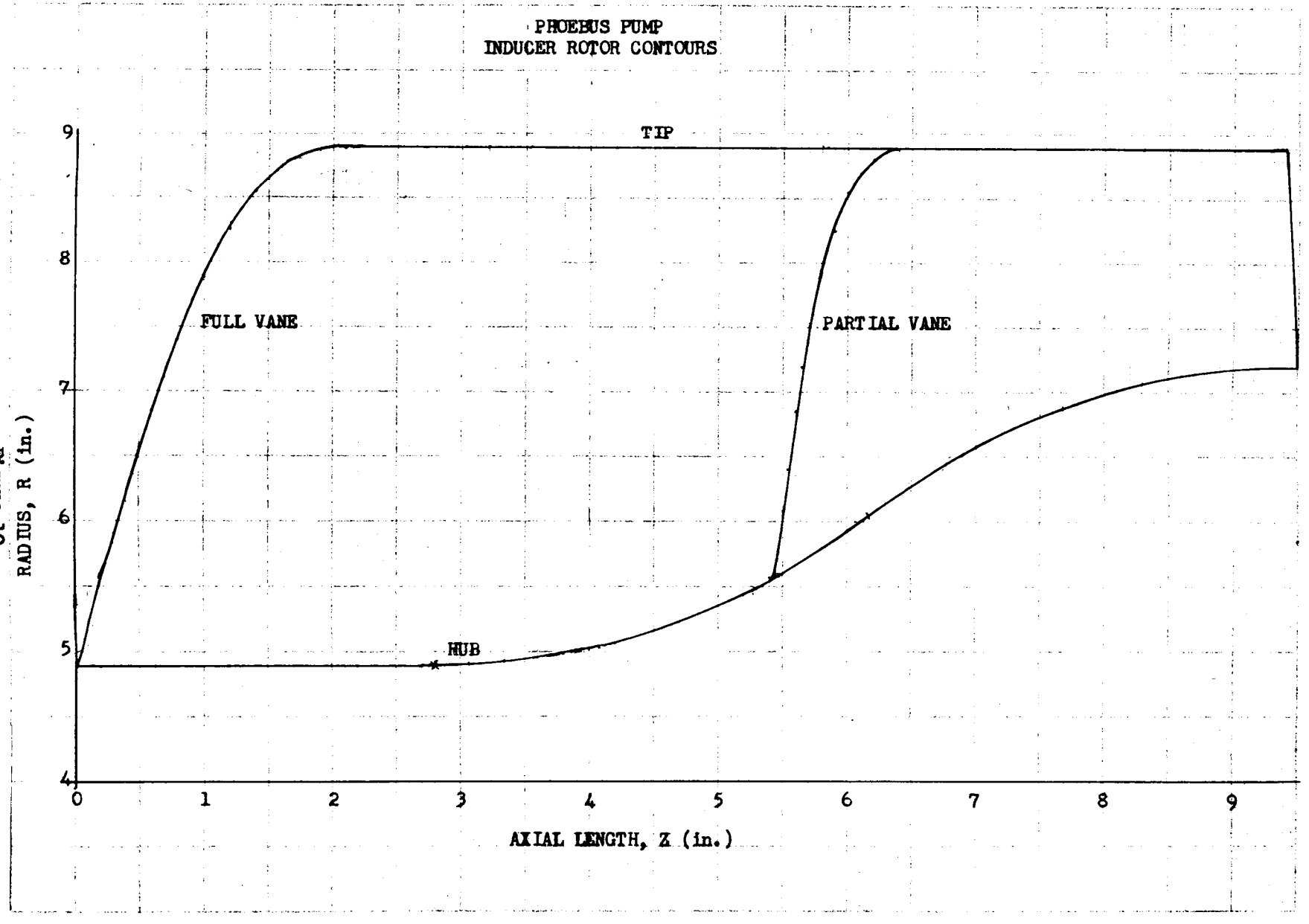

Figure 10
Page 26

Figure 11

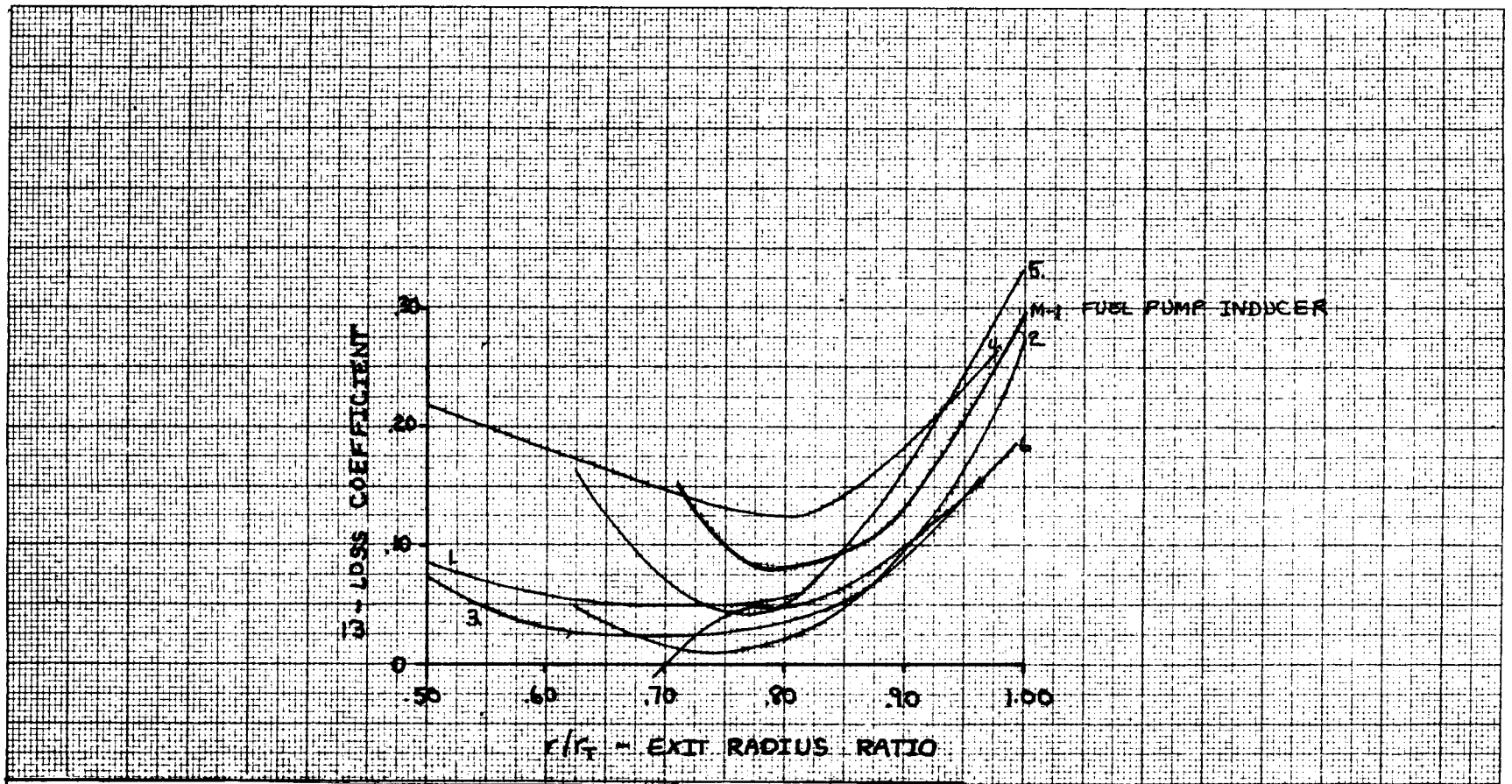

CURVE NO.	ϕ	ψ	S	β_T
1.	.268		6,600	66.5
2.	.110	.172	10,302	78.0
3.	.268		13,800	66.5
4.	.255		16,500	66.5
5.	.110	.085	25,064	78.0
6.	109	.120		57.4

$$\bar{\omega} = \frac{\Delta H_{Loss}}{W_1^2/2g}$$

W_1 = INLET RELATIVE VELOCITY

r_T = RADIUS AT TIP

REF. NASA TN D-1109
NASA TN D-583
NASA THREE STAGE INDUCER DATA

LOSS COEFFICIENT
VS
EXIT RADIUS RATIO

Component NASA INDUCERS

Part No. | Serial No.

Component Mfr. | Plot No.

Fig. No.

Page No.

Forget-General CORPORATION

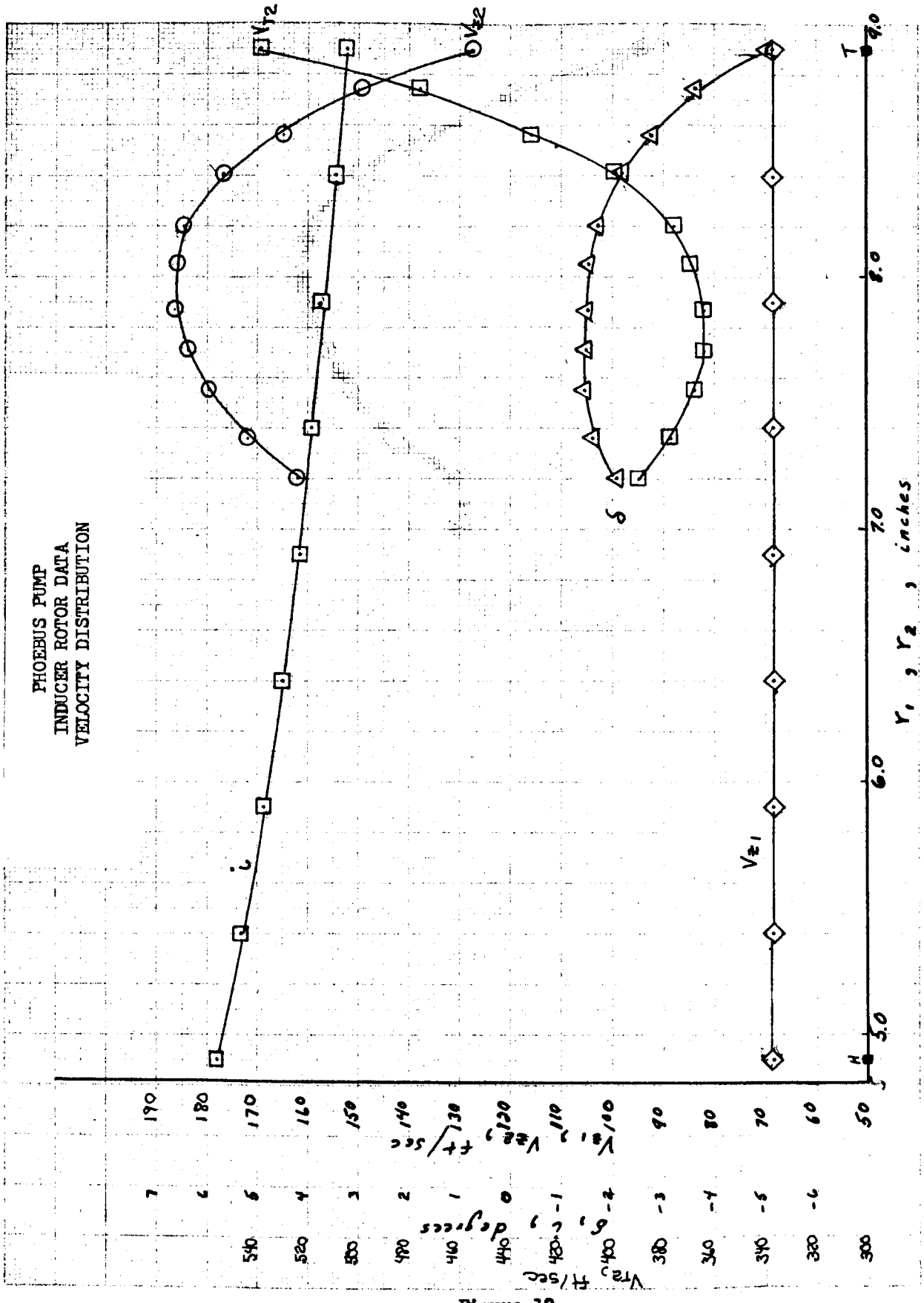

Figure 12
Page 28

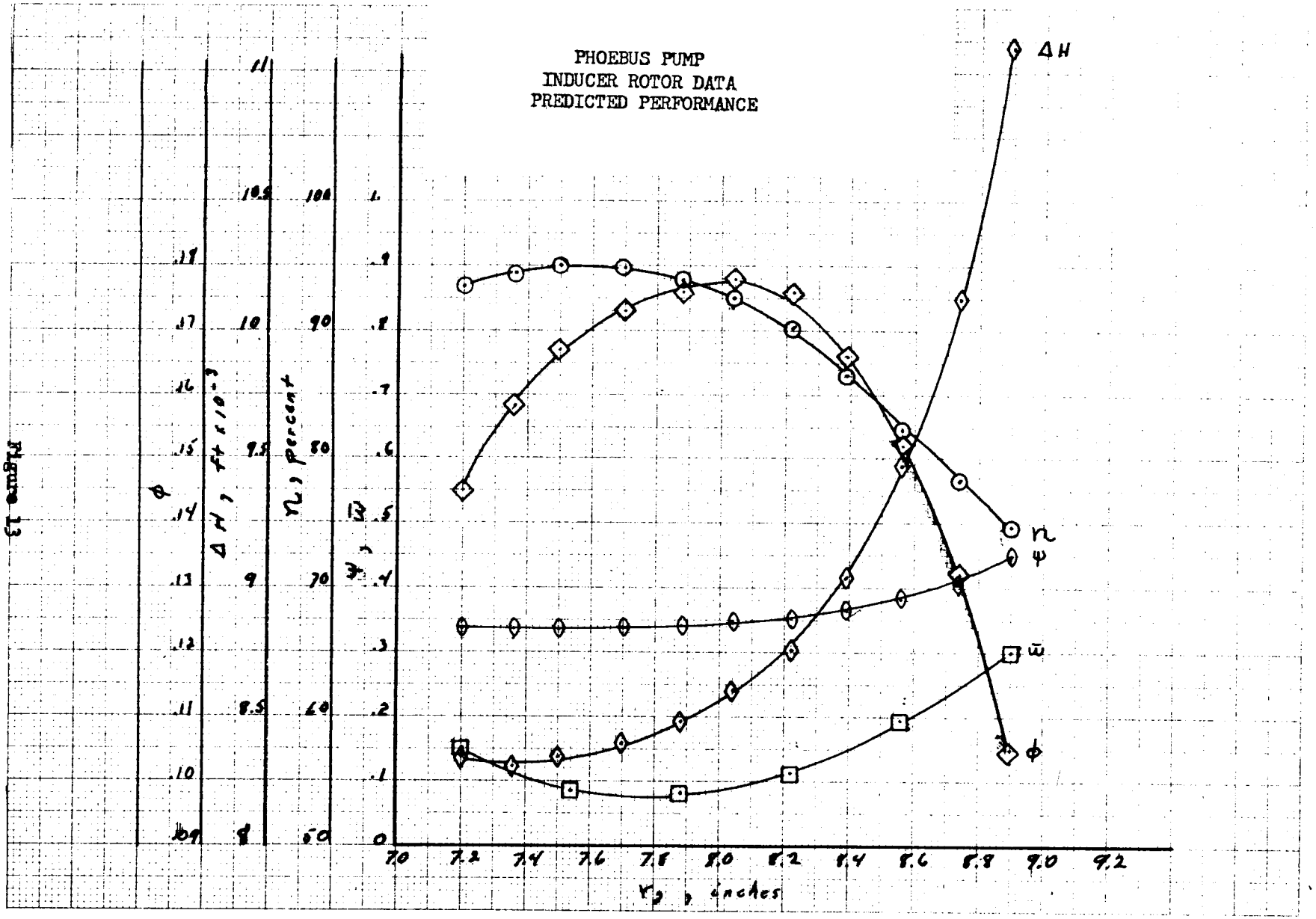

Figure 13
Page 29

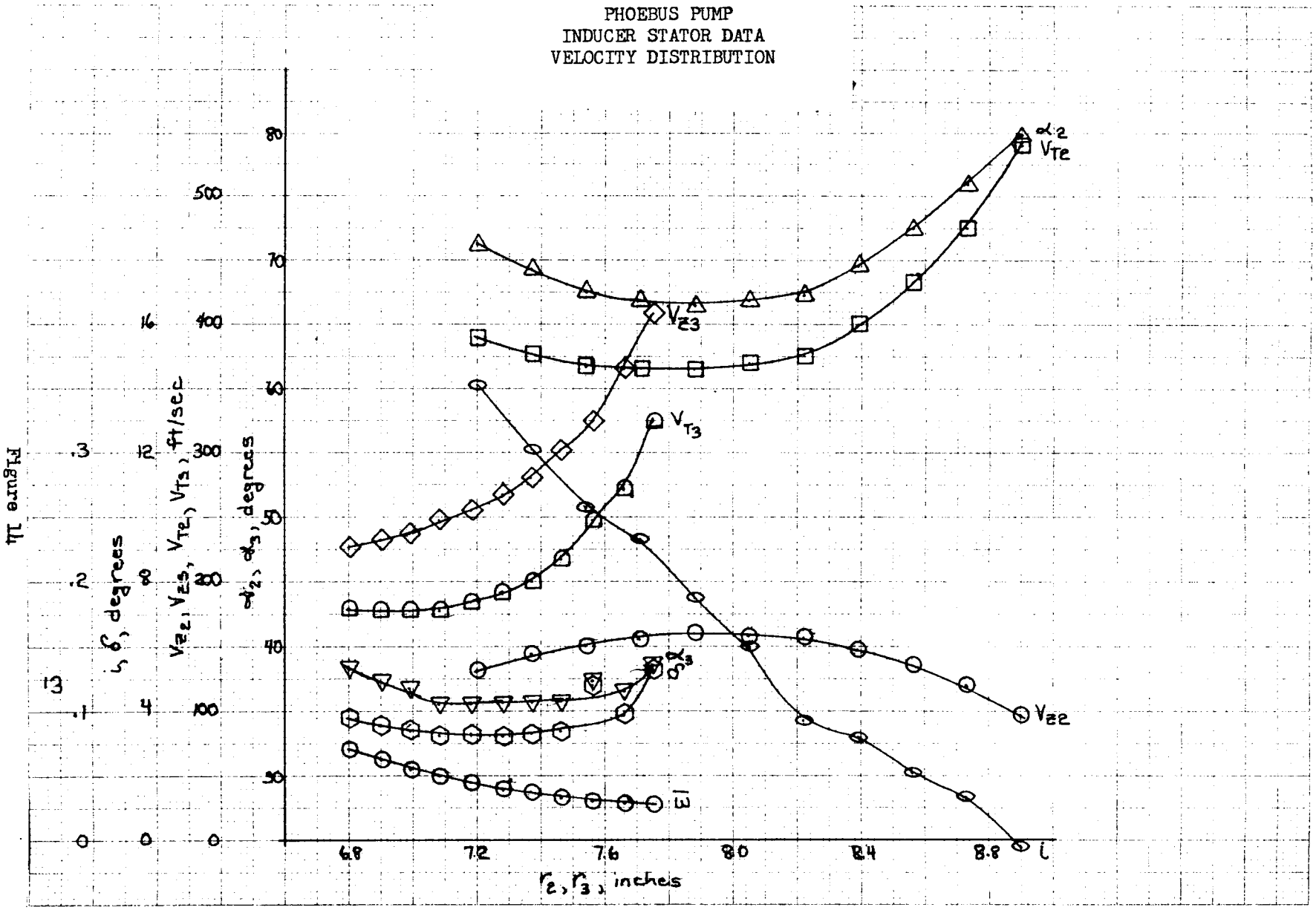

Figure 14
Page 30

2. Transition Stage

The transition stage, which was completely redesigned for the PHOEBUS application, compensates for the non-uniform head generated by the inducer stage. To achieve this compensation, the transition-rotor adds sufficient energy to each streamline to produce a nearly constant outlet head at design conditions. In addition, the design is lightly-loaded at the nominal flow coefficient to ensure a broad operating range, thereby minimizing the effects of any mismatch which may occur with the stage outlet conditions.

The design criteria for establishing incidence angles, deviation angles, and loss coefficients is identical to that used for M-1. Figures 15 through 18 show rotor, stator, and stage performance values.

3. Main Stages

While maintaining the same hub diameter as the M-1, the tip diameter was reduced until the flow coefficient was approximately the same as the M-1. Thus, the PHOEBUS main stage blading is identical to that of the M-1 fuel pump except that the blade height has been reduced. This resulted in a 0.375-in. decrease in blade height. The slight "hook" in the M-1 rotor blade at the tip is removed by this trimming. It was not added to the PHOEBUS blade because it would have required new tooling and it is believed unnecessary for the PHOEBUS blade aspect ratio.

At the fourth stage stator, the tip diameter was decreased from 7.625-in. to 7.565-in. to account for fluid compressibility. The diffusion parameter (D^*) at the mean streamline increases from 1.65 at the first stage to 1.69 at the fourth stage. After the contour step, the diffusion parameter increases from 1.59 at the fifth stage to 1.65 at the last stage. Rotor, stator, and stage performance for the first main stage is shown in Figures 19 through 22. Stage performance for the eighth main stage is shown in Figures 23 through 26.

The composite predicted performance of the inducer, transition, and first main stage over a range of flow coefficients is shown in Figure 27.

4. Discharge Diffuser and Housing

The discharge diffuser and housing configuration remain unchanged from the M-1 design because predicted losses are too small to warrant changing these major parts. The hydraulic flow losses estimated for the PHOEBUS application were based on two considerations: The M-1 sub-scale fuel pump testing; and the flow area change between the last main stage stator discharge and the guidevane housing inlet.

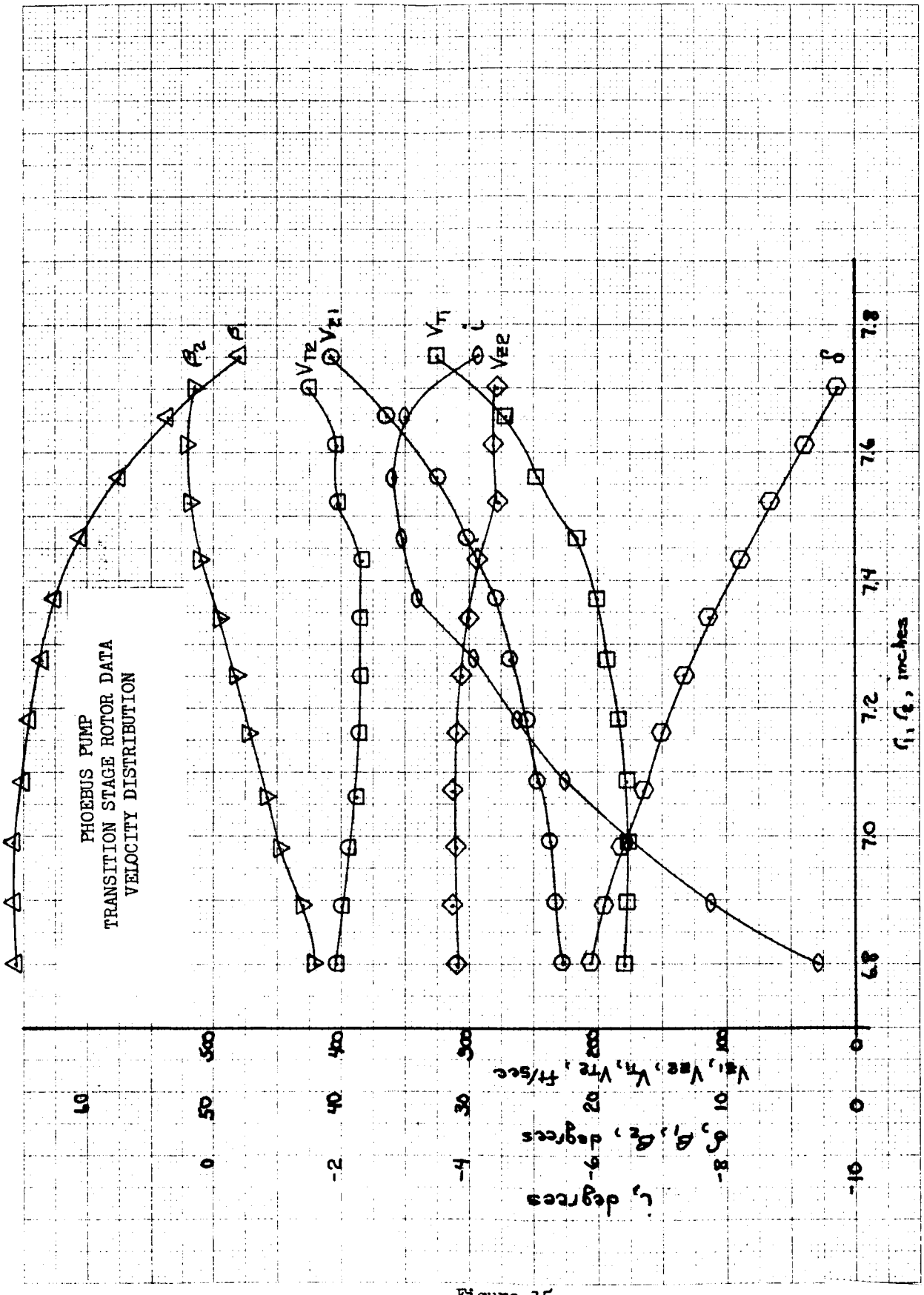

Figure 15
Page 32

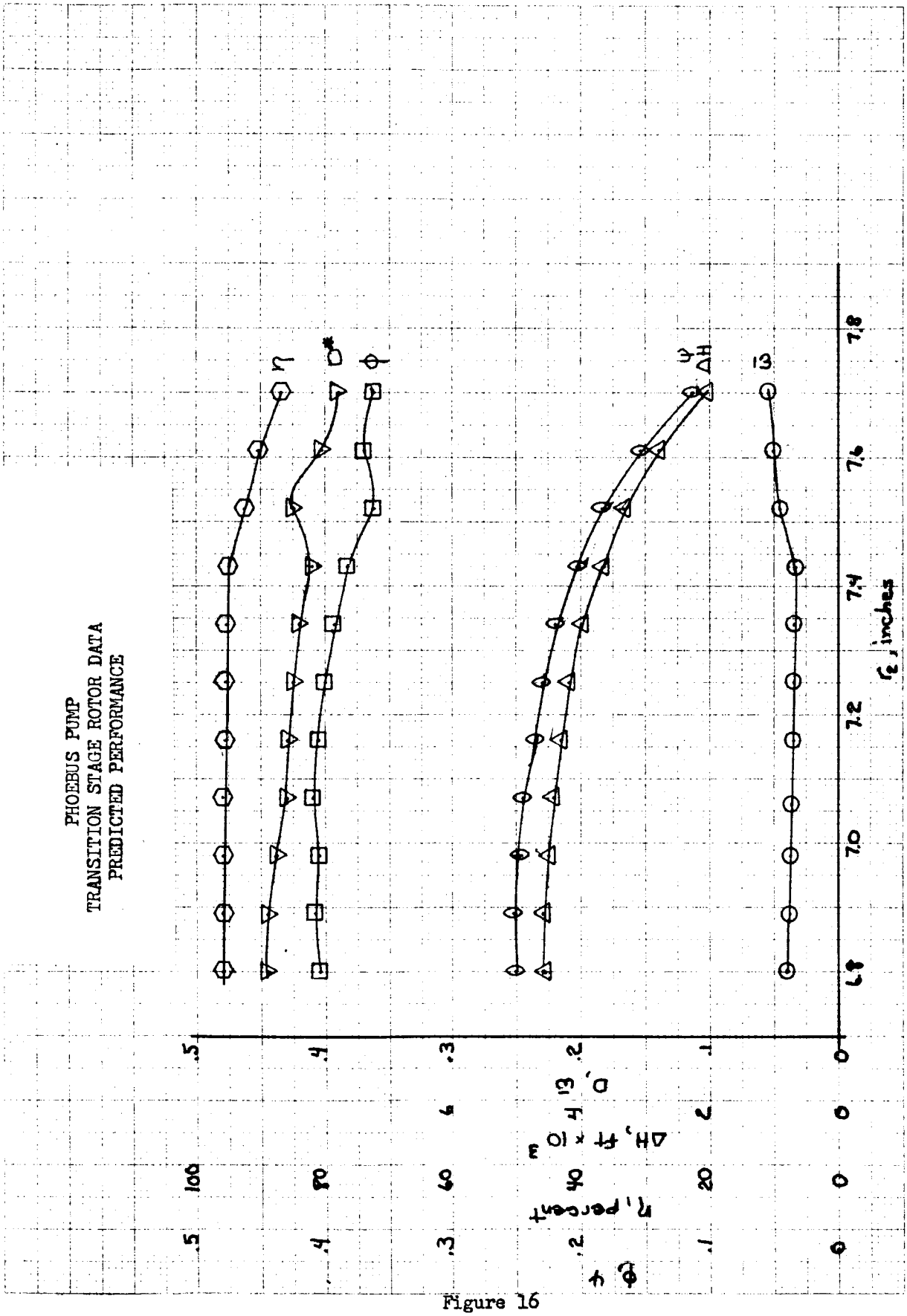

Figure 16
Page 33

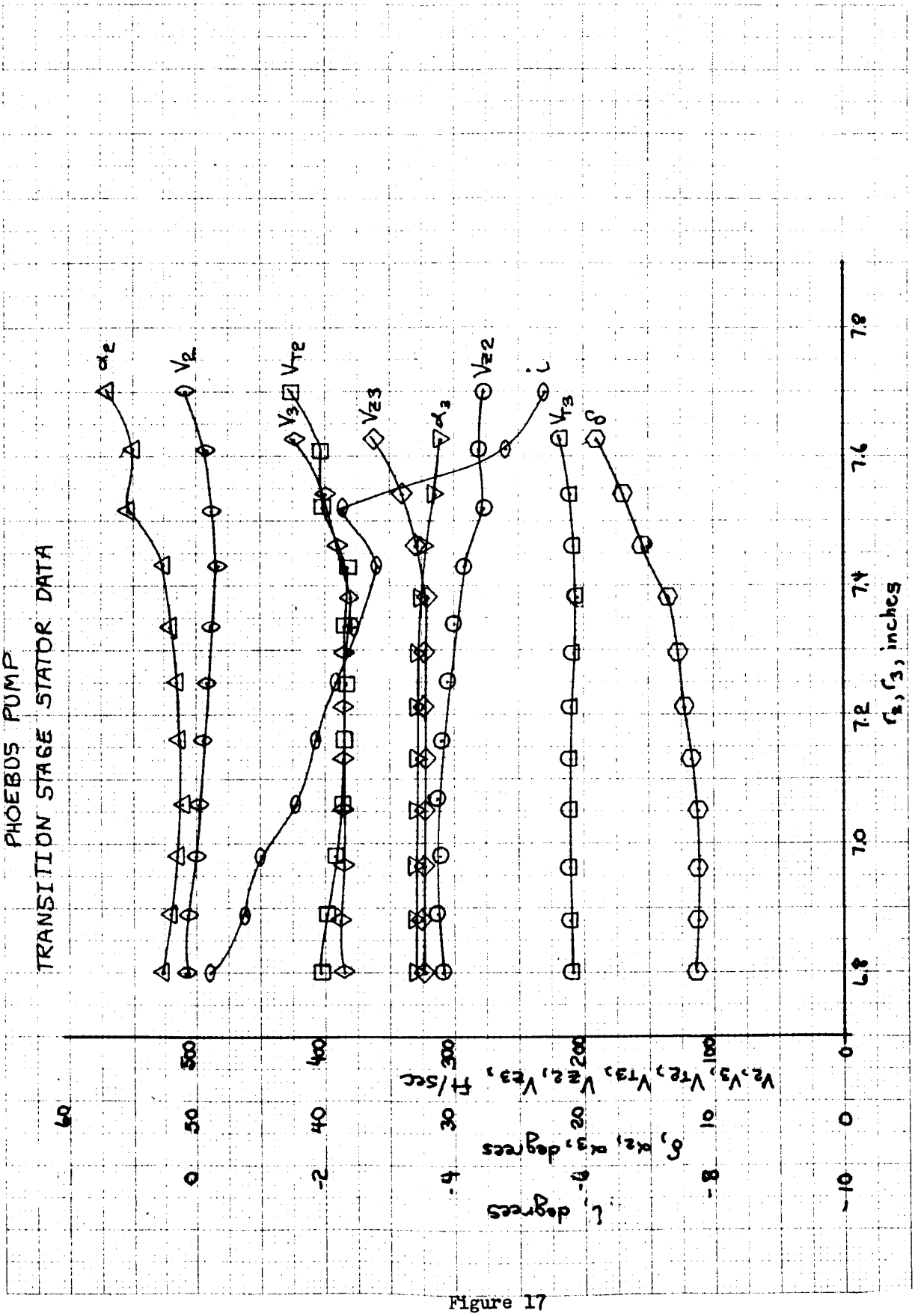

Figure 17

Page 34

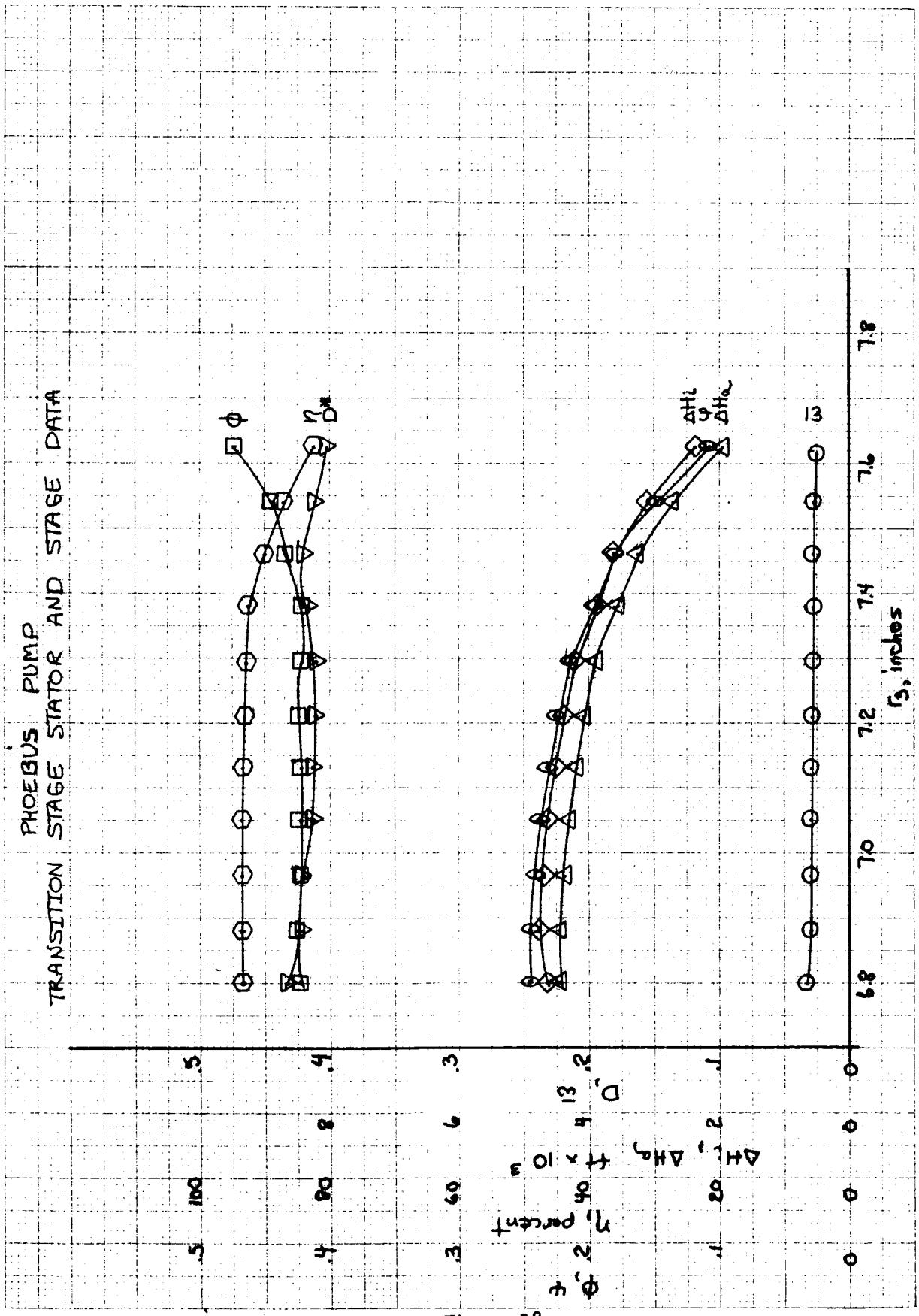
PHOEBUS PUMP
TRANSITION STAGE STATOR AND STAGE DATA
ϕ
ηD*
ΔHi
ΔHo
13
rs, inches
7.8
7.6
7.4
7.2
7.0
6.8
D, 13
ϕ, ψ
ηD*, percent
ΔHi, ΔHo, ft x 10³

Figure 18

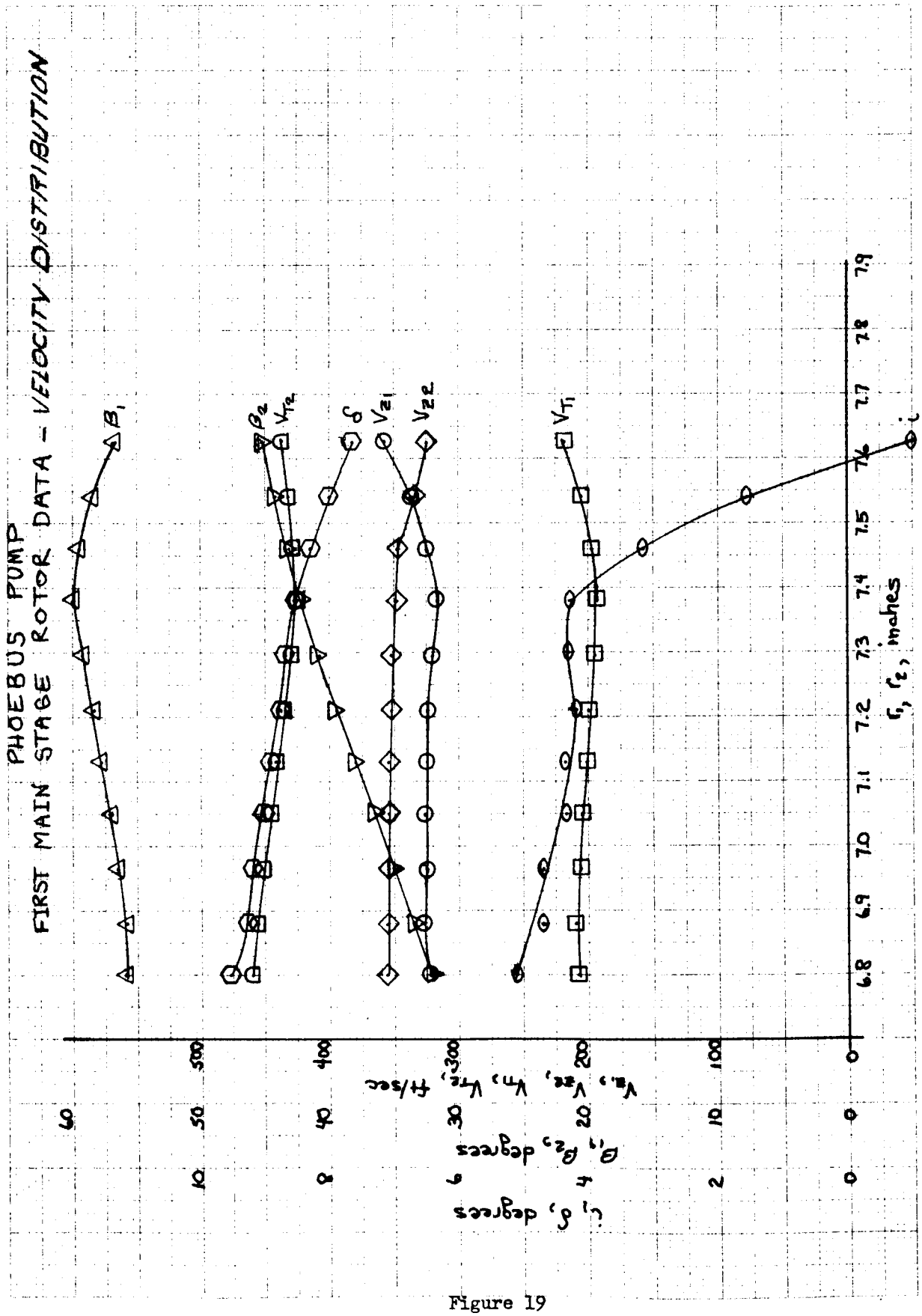
PHOEBUS PUMP
FIRST MAIN STAGE ROTOR DATA - VELOCITY DISTRIBUTION
β_1
β_2
V_{T2}
δ
V_{z1}
V_{z2}
V_{T1}
i
r_1, r_2, inches
V_a, V_{z2}, V_m, V_{T2}, ft/sec
β_1, β_2, degrees
i, δ, degrees

Figure 19

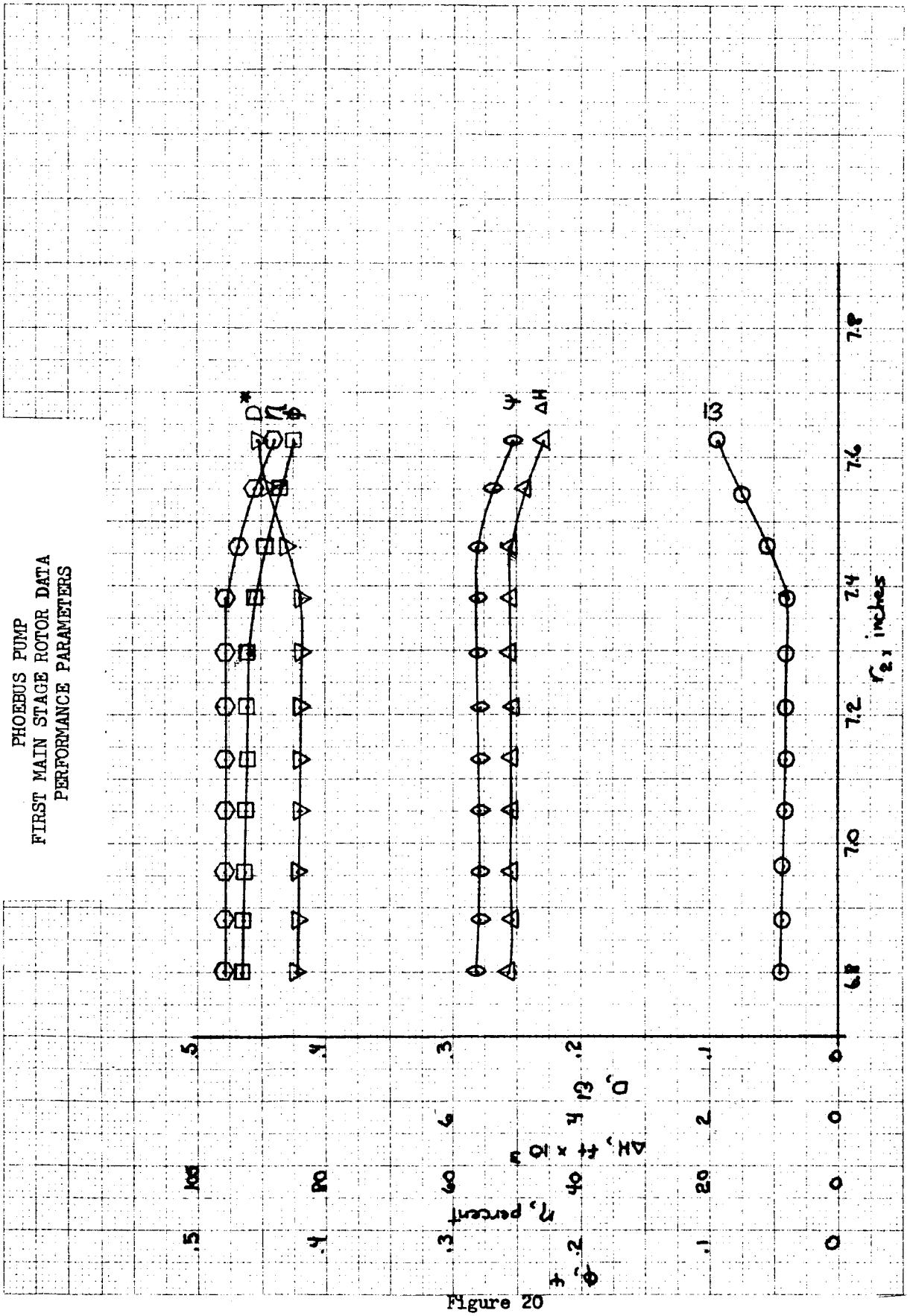

Figure 20
Page 37

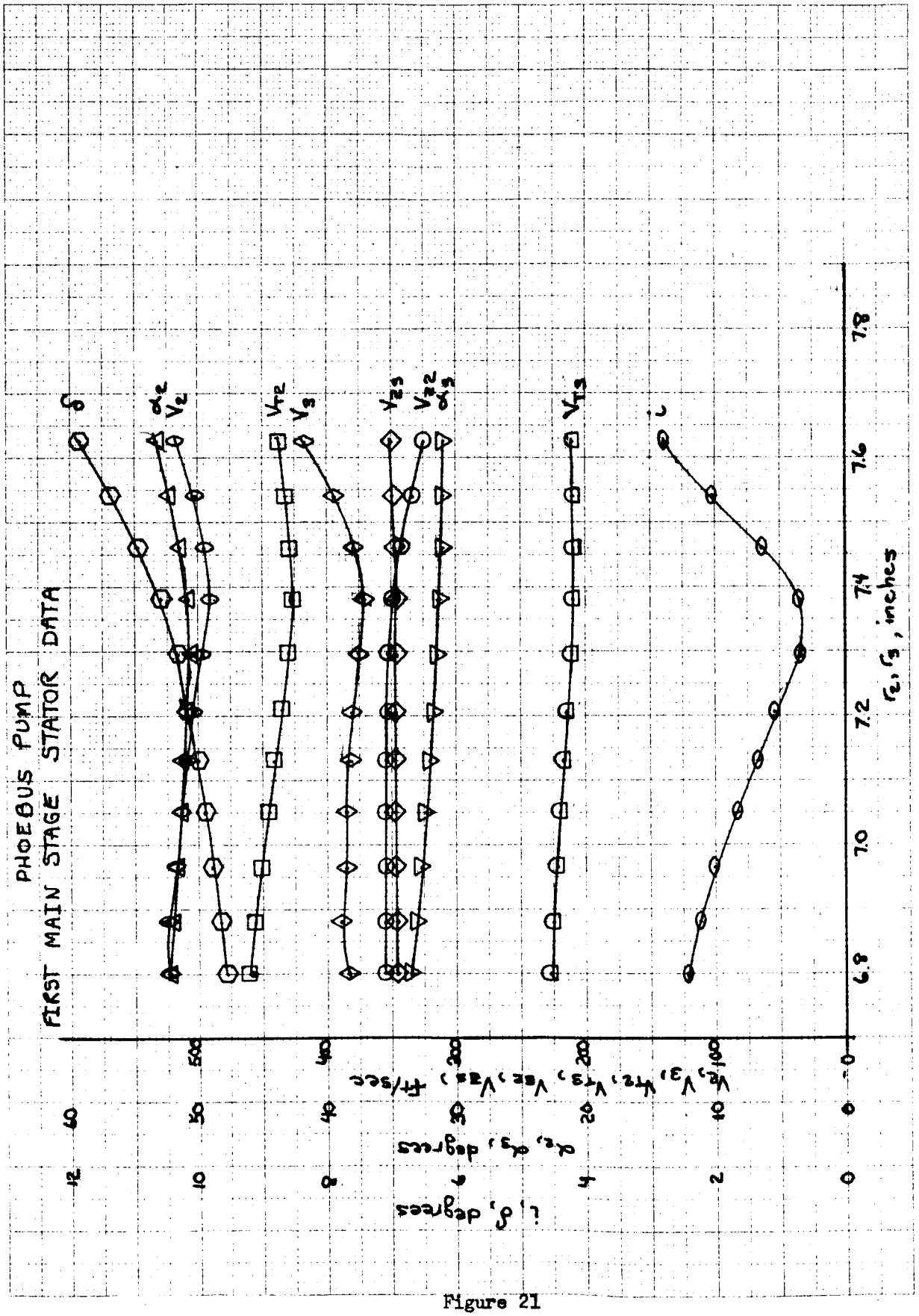
PHOEBUS PUMP
FIRST MAIN STAGE STATOR DATA
i, δ, degrees
α_2, α_3, degrees
V_r, V_3, V_{r2}, V_{r3}, V_{a2}, V_{a3}, ft/sec
r_2, r_3, inches
δ
α_2
V_2
V_{r2}
V_3
V_{z3}
V_{z2}
α_3
V_{r3}
i
6.8
7.0
7.2
7.4
7.6
7.8

Figure 21

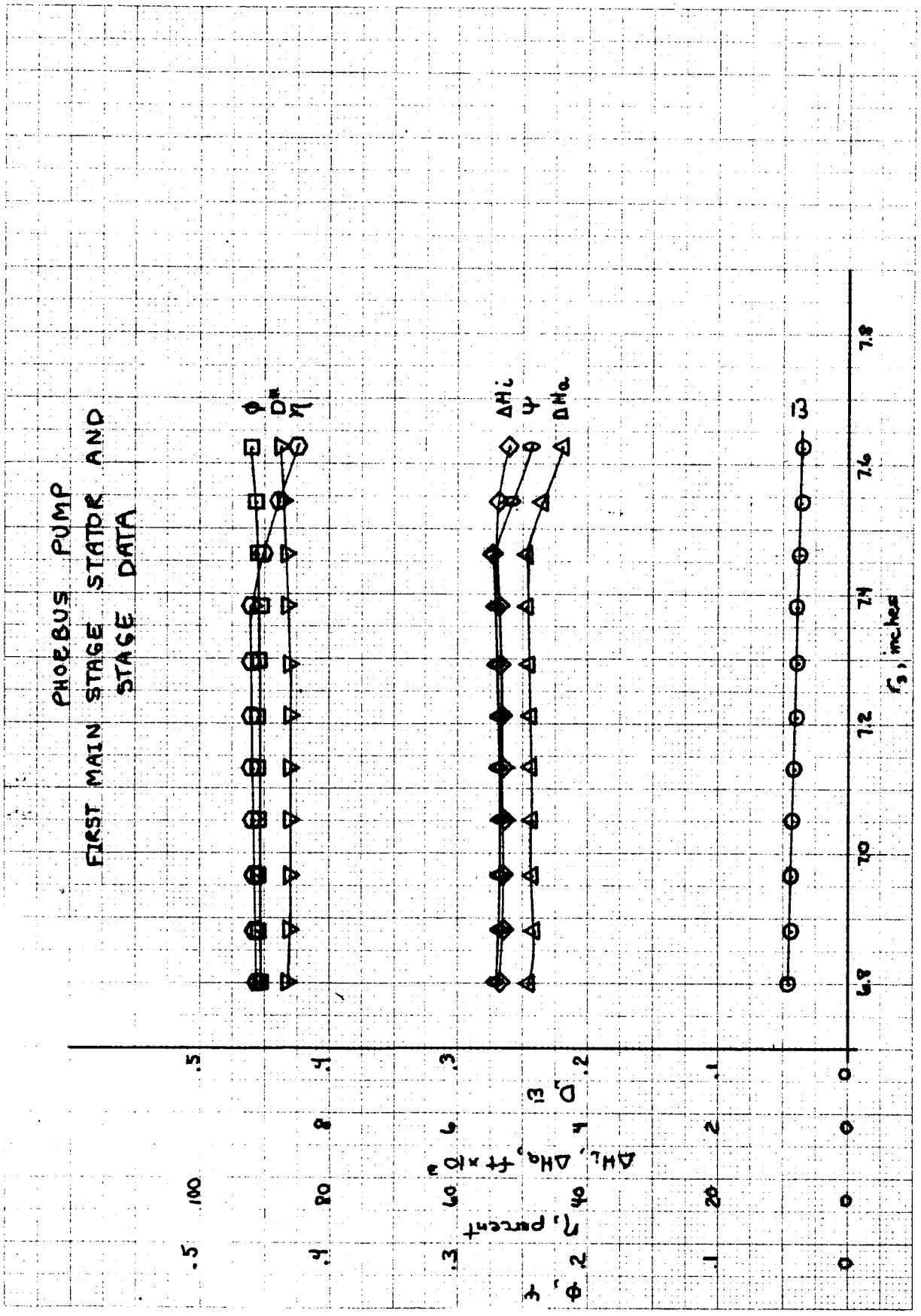

Figure 22
Page 39

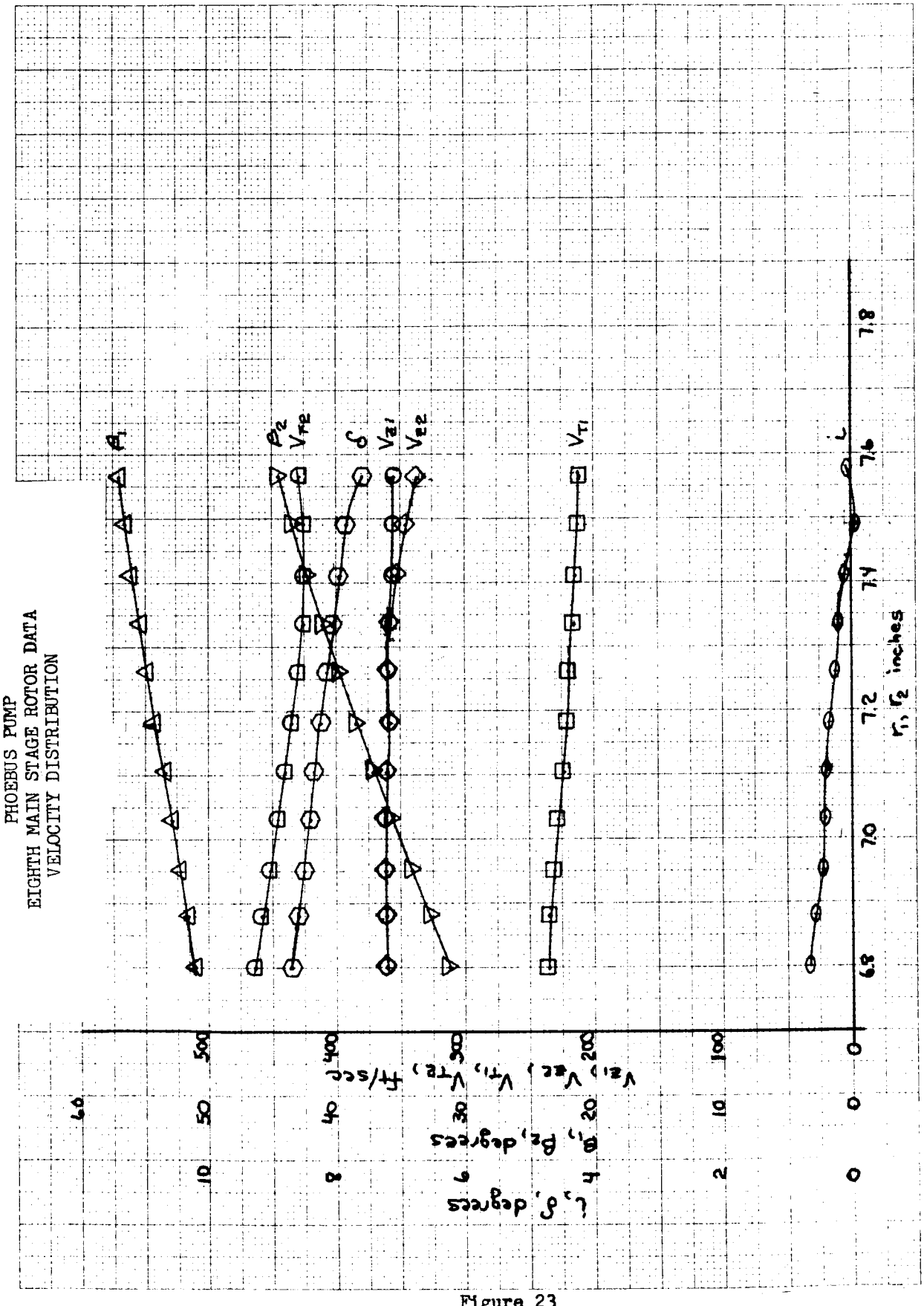

Figure 23
Page 40

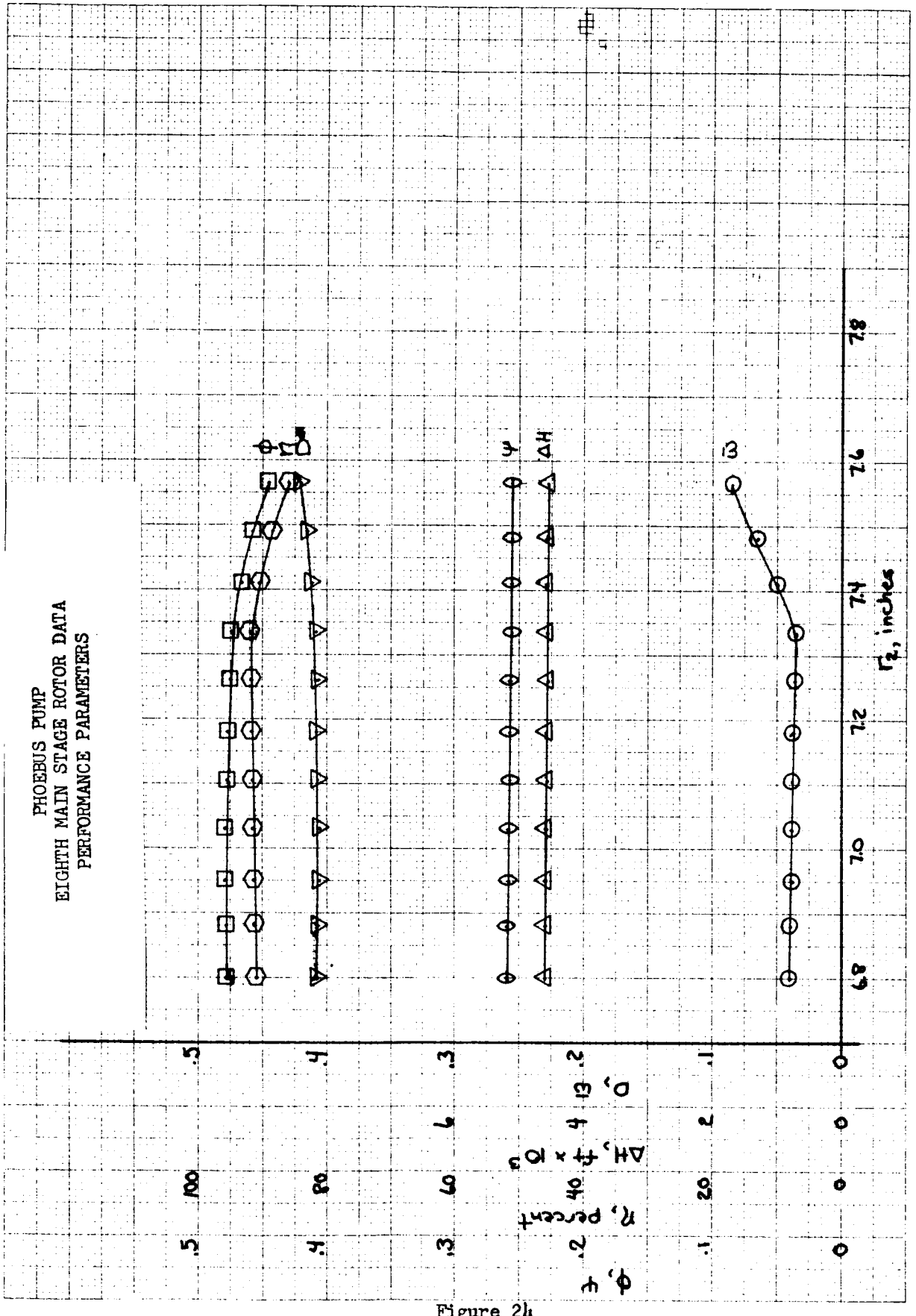

Figure 24
Page 41

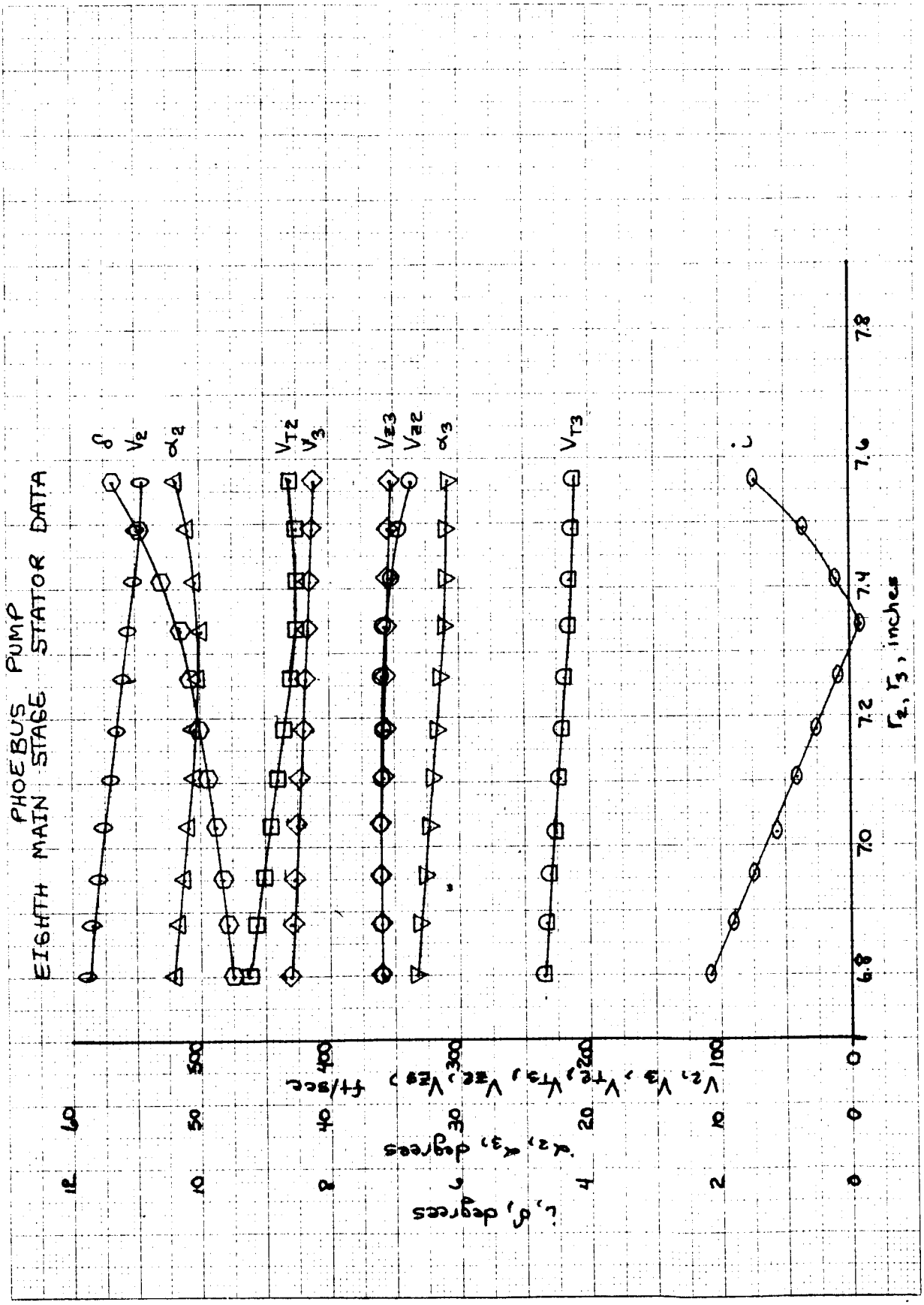

Figure 25
Page 42

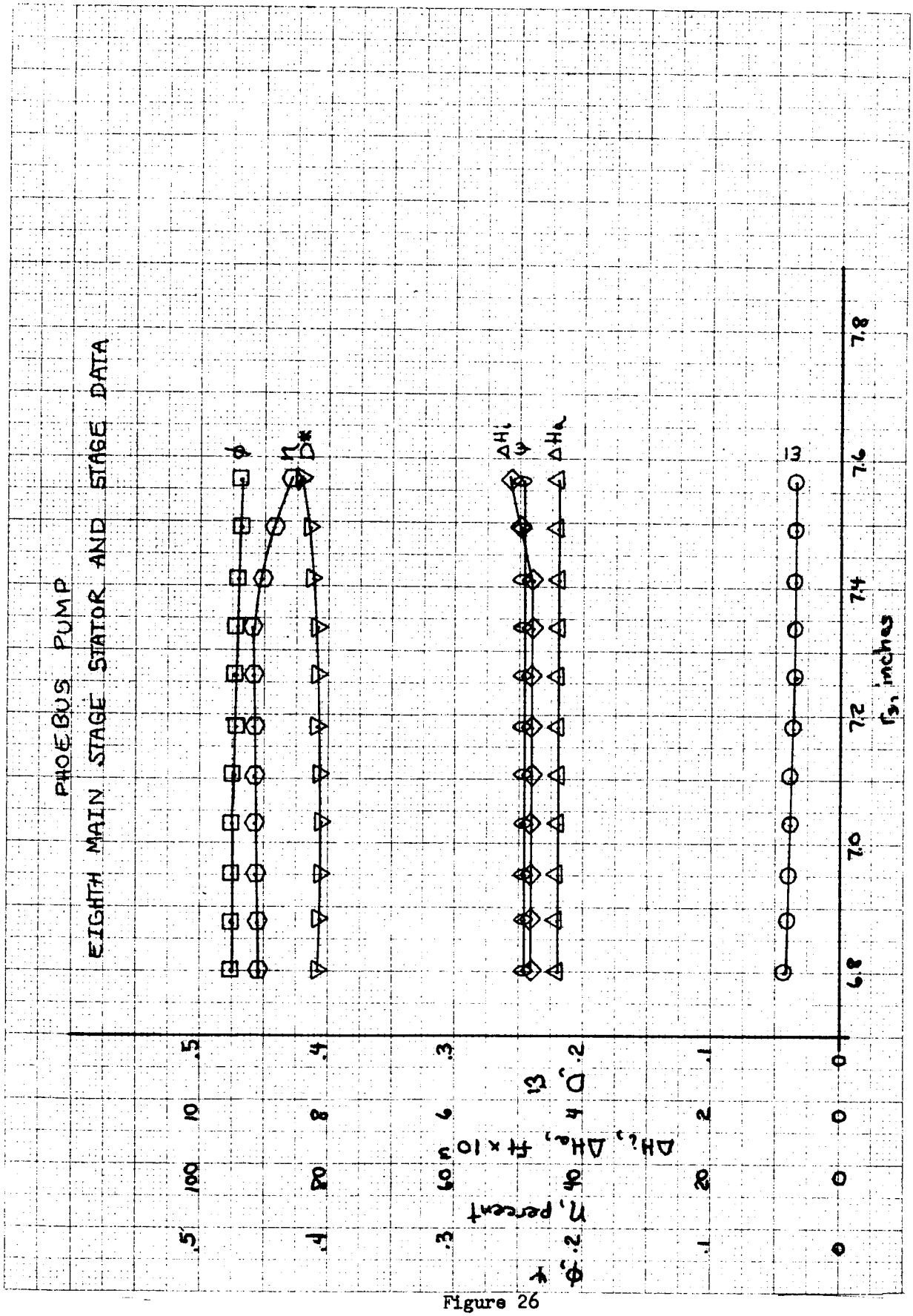

Figure 26
Page 43

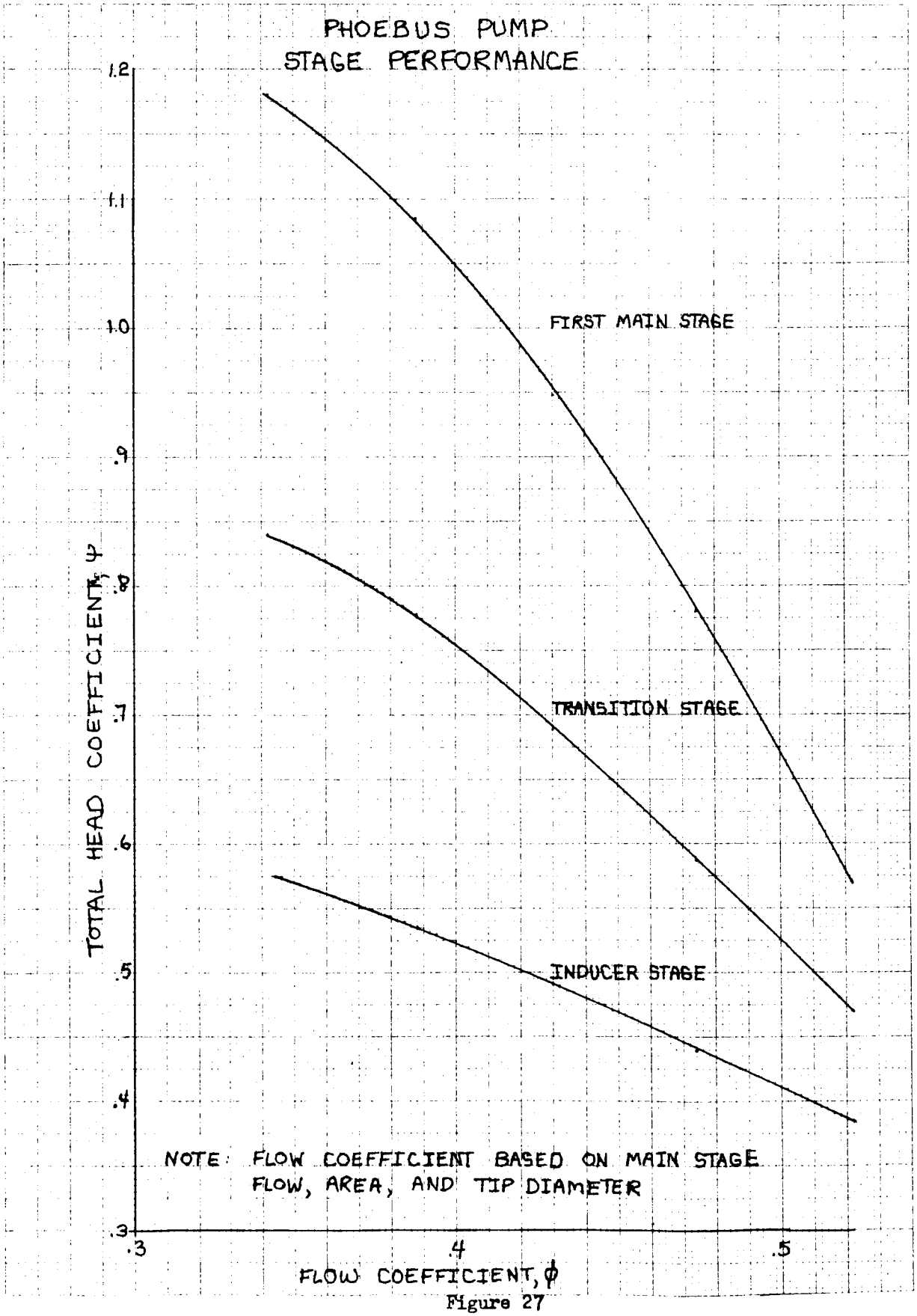
PHOEBUS PUMP
STAGE PERFORMANCE
TOTAL HEAD COEFFICIENT, ψ
1.2
1.1
1.0
.9
.8
.7
.6
.5
.4
.3
FIRST MAIN STAGE
TRANSITION STAGE
INDUCER STAGE
NOTE: FLOW COEFFICIENT BASED ON MAIN STAGE
FLOW, AREA, AND TIP DIAMETER
.3
.4
.5
FLOW COEFFICIENT, ϕ

Figure 27

Data from subscale testing was used to estimate the M-1 housing and guidevane loss. At nominal flow, a loss coefficient was calculated based upon discharge pressure and the third main stage (last stage for subscale) stator discharge pressure. This loss coefficient was then applied to the PHOEBUS design using the appropriate flow, velocities, and pressures. The area change, which results from the reduced blade heights, was taken into account by assuming that the head loss equaled the velocity head change in the axial directions.

The predicted total loss through the PHOEBUS housing will be approximately 80 psi or 5.6% of the total pump head rise of 1425 psi.

5. Off-Design Pump Performance

Off-design performance was predicted using the axial pump computer program. This program is a two-dimensional blade element solution which satisfies radial equilibrium. The deviation angle variation, stall criteria, and loss criteria were determined using S. Lieblein's analytical approach(2).

When the axial pump computer program was used to predict M-1 fuel subscale performance, and correlated with scale pump test data, some performance error existed at the high flow off-design conditions. Because there was limited subscale test data and the error was negative (predicted head was low), no modifications were made when predicting the PHOEBUS off-design performance. As additional M-1 test data becomes available, modifications will be made to deviation angle corrections and loss coefficients to improve prediction accuracy.

Figure 28 shows the predicted pressure rise weight flow map of the M-1 fuel turbopump modified for the PHOEBUS application.

6. Blade Loading

The blade loading used for stress analysis use was taken at the "worst case" condition. This condition occurs at the point where the maximum allowable housing pressure line and the maximum allowable speed line intersect. The operating point for this condition is 14,500 rpm, 1965 psi, and 460 lb/sec.

(2) NACA RME 57A28, Volume 81, 1959, entitled: Analysis of Experimental Low Speed Loss and Stall Characteristics of Two-Dimensional Compressor Blade Cascades

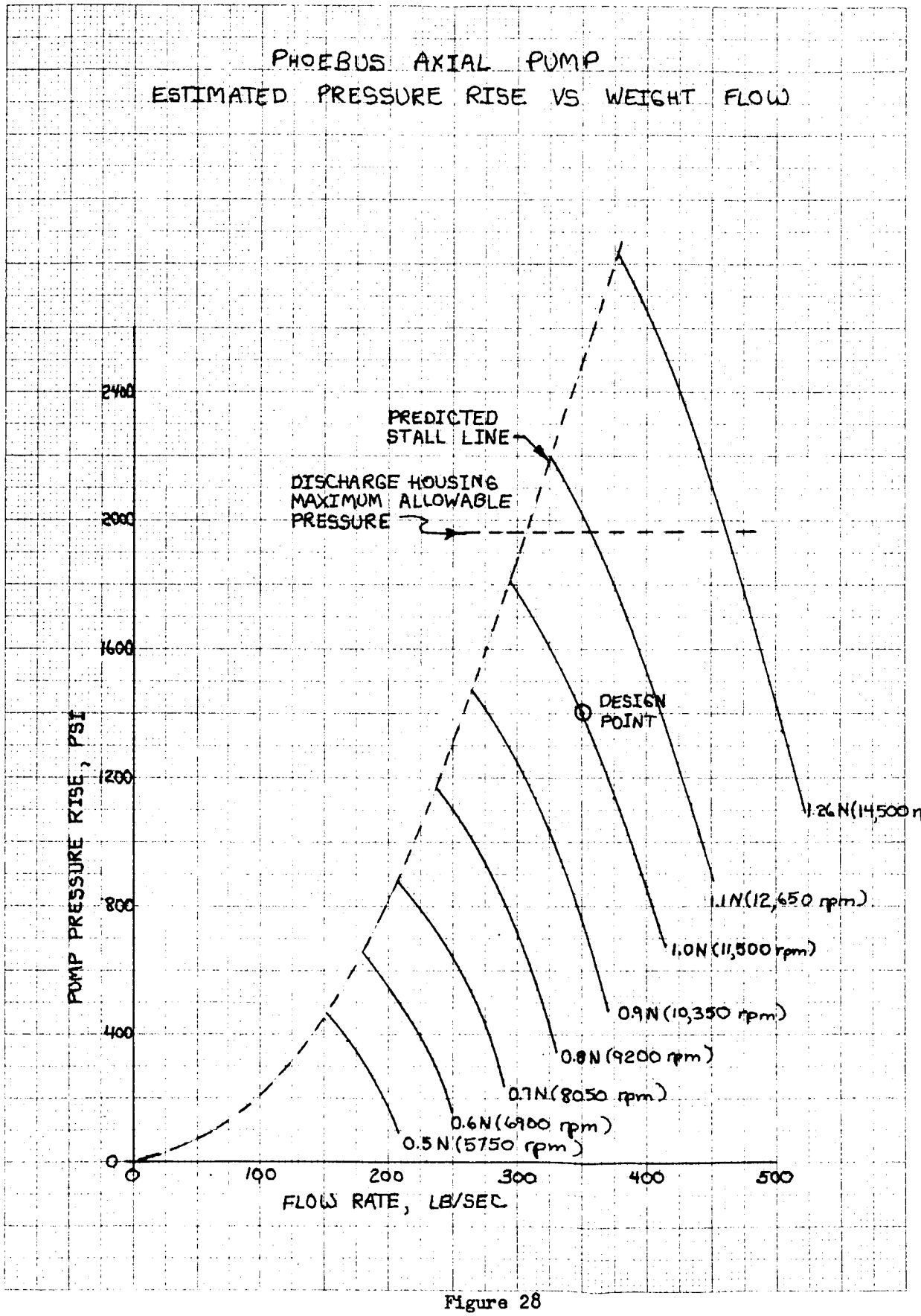

Figure 28
Page 46

The flat plate loading theory was used to ascertain pressure distributions for the inducer rotor stress analysis. This method, which was also used for the M-1 interim inducer, gives maximum expected pressure differentials across the blade.

Pressures and velocities for all blade elements were obtained from the axial flow program previously discussed.

7. Radial Load on Rotor

Stepanoff's method(3) was used to estimate the radial load on the rotor caused by a circumferential pressure gradient. The "worst case" of radial loading would be represented by assuming the condition at the guidevane discharge to be equivalent to a centrifugal impeller. The calculated load of 2500 lb was based upon equivalent head and flow coefficients, the discharge diameter, and the passage width.

D. PHOEBUS TURBINE DESIGN MODIFICATIONS AND PERFORMANCE

An essentially unmodified version of the Model II M-1 fuel turbine will supply the pump power requirements for the PHOEBUS application. Operating with hydrogen at ambient temperature, this turbine will readily produce 37,200 horsepower at a rotational speed of 11,500 rpm. Under these conditions, a weight flow of approximately 55 lb/sec at a turbine inlet pressure of 440 psia is required. This turbine is capable of producing a peak power output of 72,400 horsepower at a rotational speed of 14,500 rpm, using hydrogen gas at ambient temperature.

The Model II version of the M-1 fuel turbine is a two-stage Curtis-type turbine, originally designed to produce 88,150 horsepower at a speed of 13,225 rpm using the combustion products of hydrogen and oxygen.

M-1 and PHOEBUS design and nominal/operating conditions are as follows:

	M-1	PHOEBUS
Power BHP	88,150	37,200
Rotational Speed RPM	13,225	11,500
Total Inlet Pressure PSIA	1,000	440
Total Inlet Temperature °F	1,460	520
Pressure Ratio	4,673	7.35

(3) Stepanoff, A. J., Centrifugal and Axial Flow Pump, 2nd Edition, 1957, John Wiley and Son, New York

During the nominal PHOEBUS operating condition, liquid hydrogen will be diverted from the pump discharge at a pressure of approximately 1400 psia for use in the turbine. The hydrogen will pass through a water-to-liquid hydrogen heat exchanger where it will be converted to gas and its temperature raised to near-ambient. It is estimated that the hydrogen will experience a pressure loss of approximately 400 psi through the heat exchanger resulting in a maximum pressure of approximately 1000 psia available to the turbine. A turbine speed control valve will orifice the flow to reduce the pressure from 1000 psia to 440 psia at the inlet for nominal turbine conditions.

The Model II turbine was originally designed with a small reaction occurring in the reversing vanes and second rotor. The first stage was designed with a converging-diverging nozzle and slight after-expansion occurring under design conditions.

Although turbine efficiencies can generally be improved in impulse turbines by providing a small amount of reaction in the rotors, the original design for this turbine omitted any reaction in the first rotor to reduce axial thrust. Because the theoretical Mach number at the nozzle discharge was approximately 1.575 for the design gas with a specific heat ratio (γ) of 1.37, the first stage was designed with a converging-diverging nozzle to avoid excessive after-expansion.

The original conditions for the M-1 engine fuel turbine required that the turbine accommodate an isentropic enthalpy drop of 999/Btu/lbm. Centrifugal and thermal stresses in the blades and disc limited the pitch line velocity of the blading to 1300 ft/sec. Under these conditions, the blade/jet velocity ratio (u/co) was approximately 0.1878. To obtain maximum efficiency with this velocity ratio, a multi-stage turbine would have been required. However, weight and size limitations dictated some compromise in turbine efficiency resulting in the current two-stage M-1 fuel turbine design. Also, further study indicated that relatively large negative thrusts might occur which would increase the problems in the M-1 fuel turbopump thrust balancer system. To overcome this potential difficulty, the first stage rotor blades were closed down slightly.

1. Performance Predictions

Figures 29 and 30 show the predicted power and torque parameters, respectively, for this turbine as functions of pressure ratio using gaseous hydrogen. These curves peak at certain maximum pressure ratios and further increase of the pressure ratio does not increase the power output. However, until the maximum pressure ratio is reached, power output does increase substantially.

Figure 31 shows a composite of the power parameter, inlet pressure, exhaust pressure, and weight flow parameter as functions of pressure ratio. These curves show that the turbine is choked at pressure ratios greater than approximately 1.5. From Figure 31, it can

PHOEBUS TURBINE PERFORMANCE
POWER PARAMETER VS PRESSURE RATIO
MOD II M-1 FUEL TURBINE — $6H_2$

T = Turbine Inlet Temperature, °R
PTI = Turbine Inlet Pressure, psia
PSE = Turbine Exit Pressure, psia
N = Rotational Speed, rpm
HP = Power, hp

⊙ Operating Point
T = 578.7°R
C_p = 3.475 BTU/lb °R
γ = 1.399
R = 771.5 lbf-ft/lbm°R
$\frac{\omega\sqrt{T}}{P_{TI}}$ = 2.824
Nozzle choked for PTI/PSE > 1.47

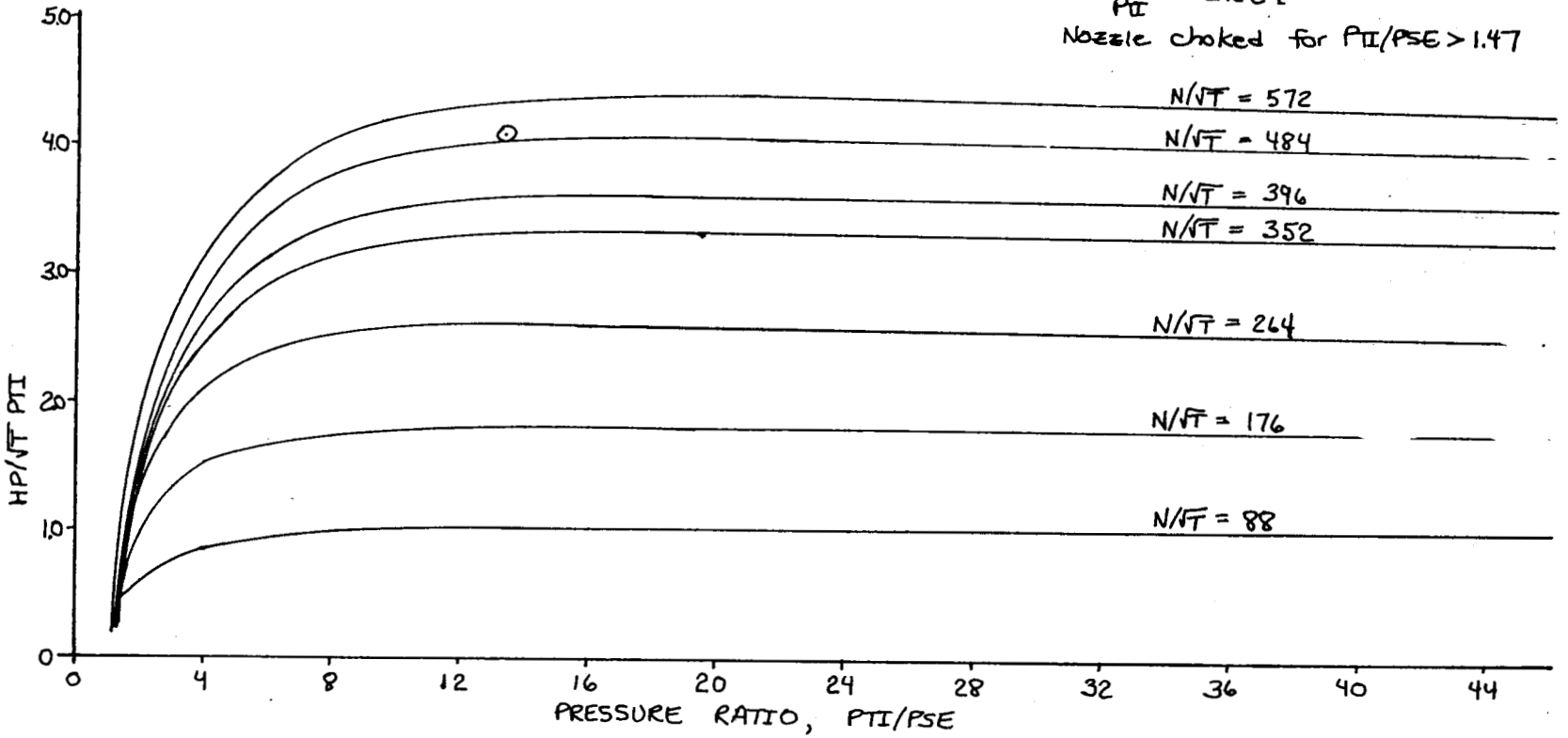

Figure 29
Page 19

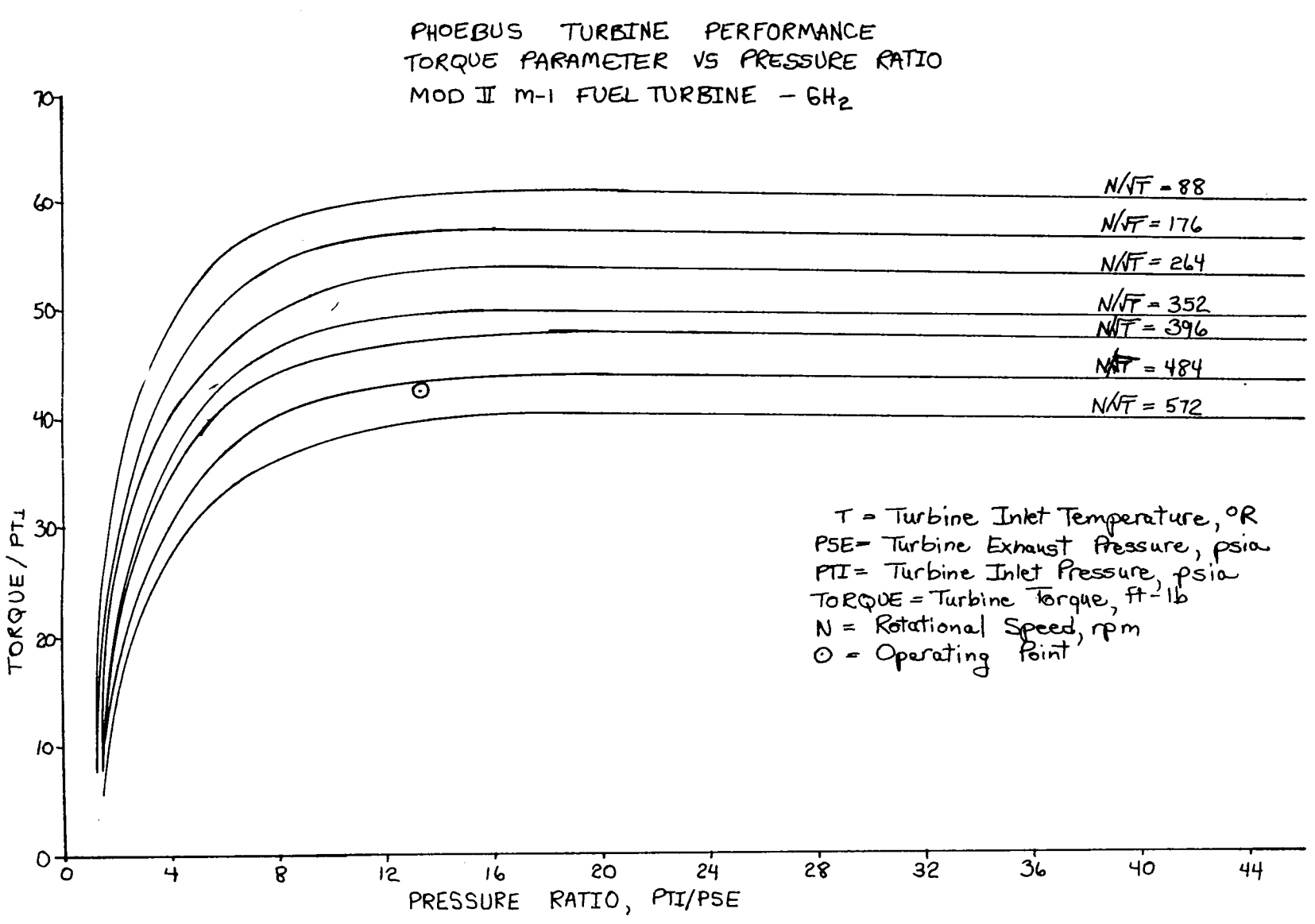
PHOEBUS TURBINE PERFORMANCE
TORQUE PARAMETER VS PRESSURE RATIO
MOD II M-1 FUEL TURBINE – $6H_2$
N/√T = 88
N/√T = 176
N/√T = 264
N/√T = 352
N/√T = 396
N/√T = 484
N/√T = 572
T = Turbine Inlet Temperature, °R
PSE = Turbine Exhaust Pressure, psia
PTI = Turbine Inlet Pressure, psia
TORQUE = Turbine Torque, ft-lb
N = Rotational Speed, rpm
⊙ = Operating Point
TORQUE / PT1
PRESSURE RATIO, PTI/PSE
0
10
20
30
40
50
60
70
0
4
8
12
16
20
24
28
32
36
40
44

Figure 30

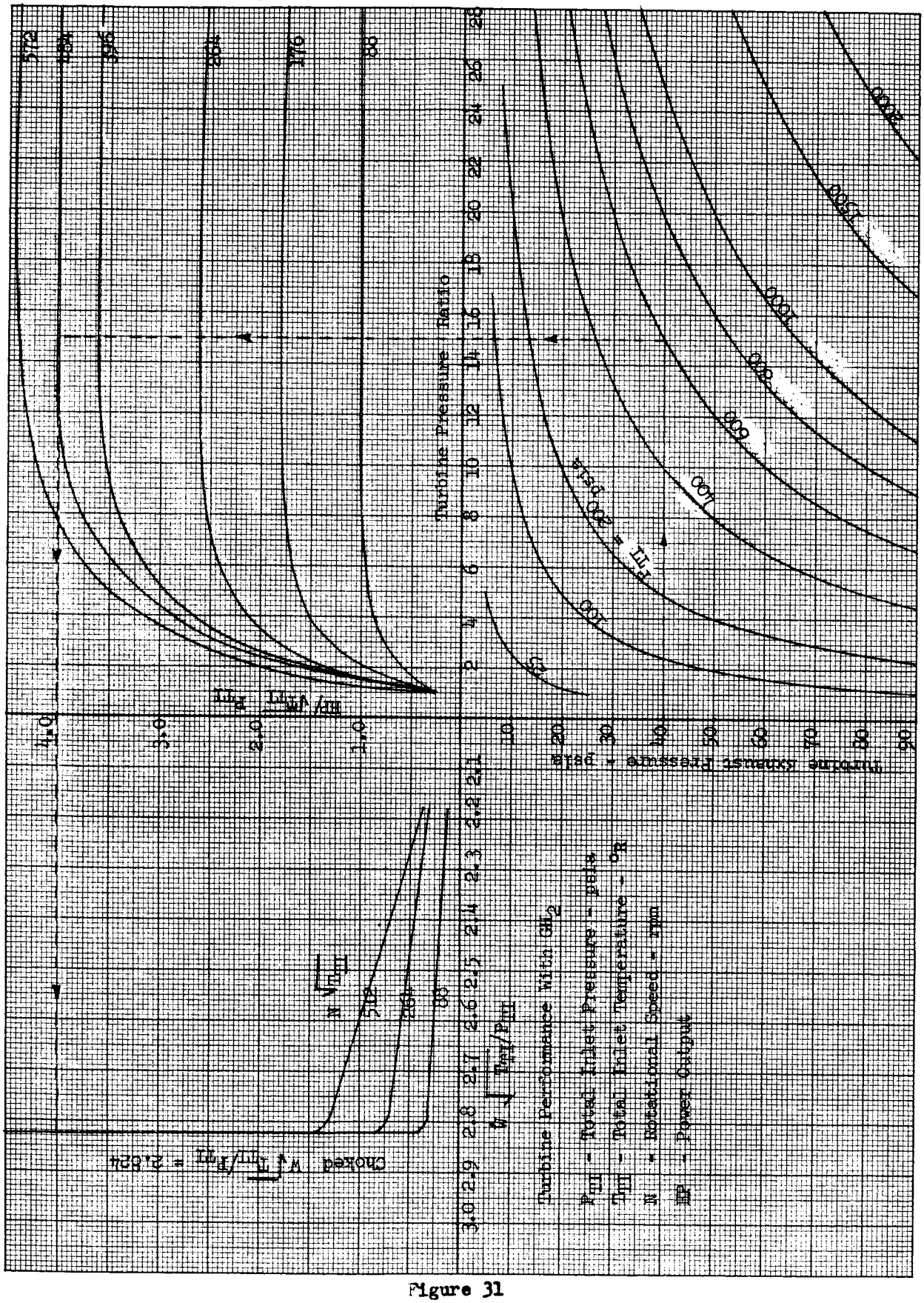
PREDICTED TURBINE PERFORMANCE
Turbine Performance with GH2
Turbine Pressure Ratio
Turbine Exhaust Pressure - psia
Choked
Power Output
Total Inlet Temperature - °R
Rotational Speed - rpm
Total Inlet Pressure - psia
Power Output
Rotational Speed - rpm
Total Inlet Temperature - °R
Total Inlet Pressure - psia

Figure 31

be calculated that for the nominal operating point ($N/\sqrt{RT} = 535$), the minimum turbine weight flow occurs at a pressure ratio of 18. This requires an inlet pressure of approximately 387 psia and a resulting back-pressure of 21.5 psia. However, calculation for pressure losses through the NRDS exhaust duct to the flare stack indicate that this is a lower exhaust pressure that can be obtained. These calculations show that as the pressure ratio across the turbine is increased, the Mach number in the exhaust duct increases, thereby increasing the pressure losses. This effect is illustrated in Figure 32, which shows the Mach numbers in the inlet and exhaust duct as a function of exhaust pressure.

Figure 33 shows the weight flow and turbine efficiency as a function of exhaust pressure for the nominal operating point. Because the pressure ratio increases as the exhaust pressure decreases, this curve shows that as the pressure ratio increases, both the efficiency and weight flow decrease.

Figure 34 shows the static exhaust pressure over the entire range of operation as a function of power output with rotational speed and pressure ratio as variables. Statis inlet-to-exhaust temperature ratio is shown in Figure 35 as a function of the power parameter. These curves provide exhaust conditions covering the entire range of the PHOEBUS application.

2. Blade Forces

The following is a tabulation of turbine blade forces for the maximum power output for the PHOEBUS application. These blading loads were used for the turbine stress analysis.

BLADE FORCES PER UNIT LENGTH AND STATIC EXIT PRESSURES

NOZZLE 1, NUMBER BLADES = 37

Location	Radius in.	Axial lb/in.	Tangential lb/in.	Ps psia
Tip	12.05	880	226	382
Mean	11.50	890	249	344
Hub	10.95	925	257	300
	ROTOR 1, NUMBER BLADES = 80			
Tip	12.10	170	151	200
Mean	11.50	140	161	186
Hub	10.90	108	173	171

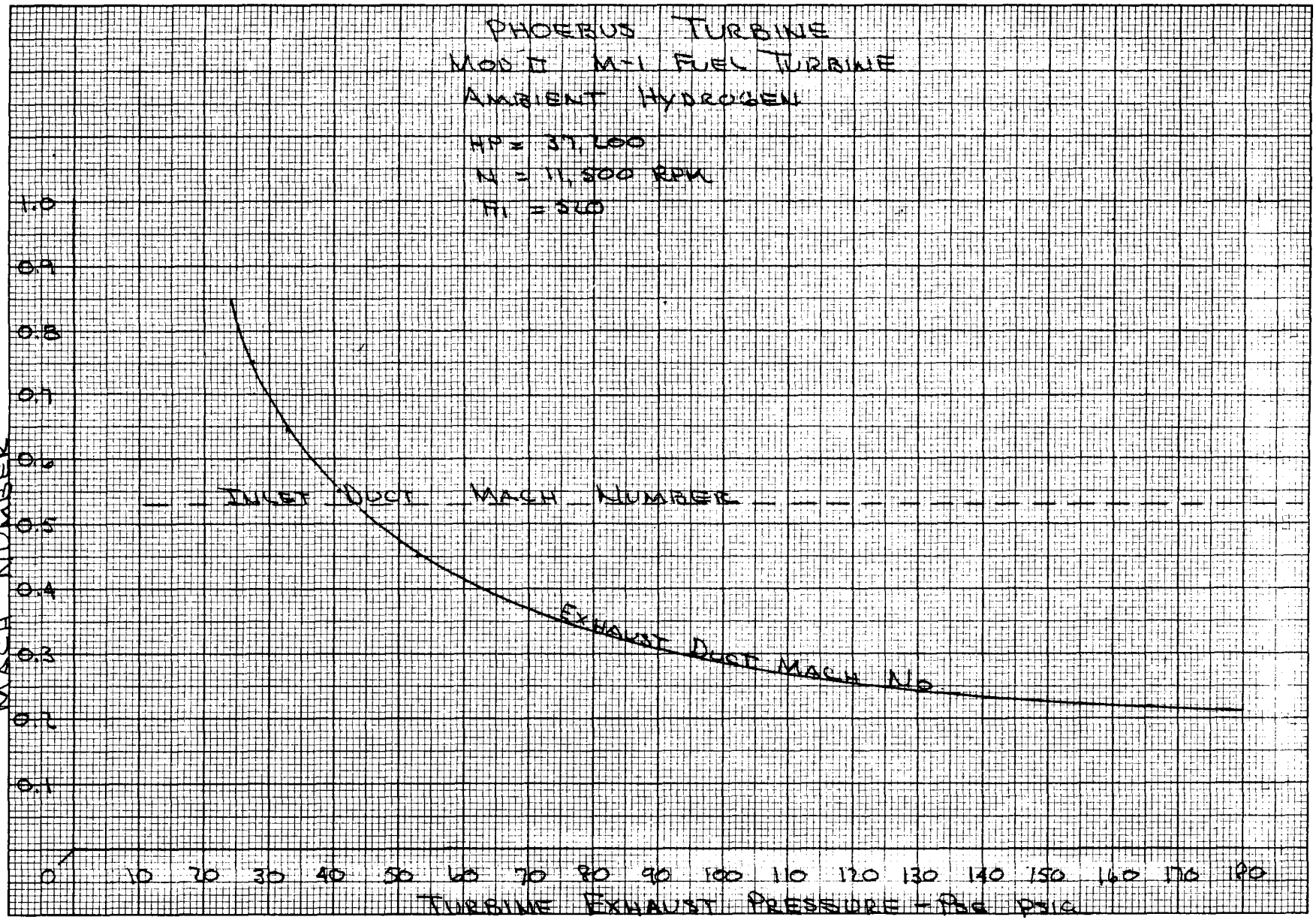

Figure 32
Page 53

Figure 33
Page 54

Figure 34
Page 55

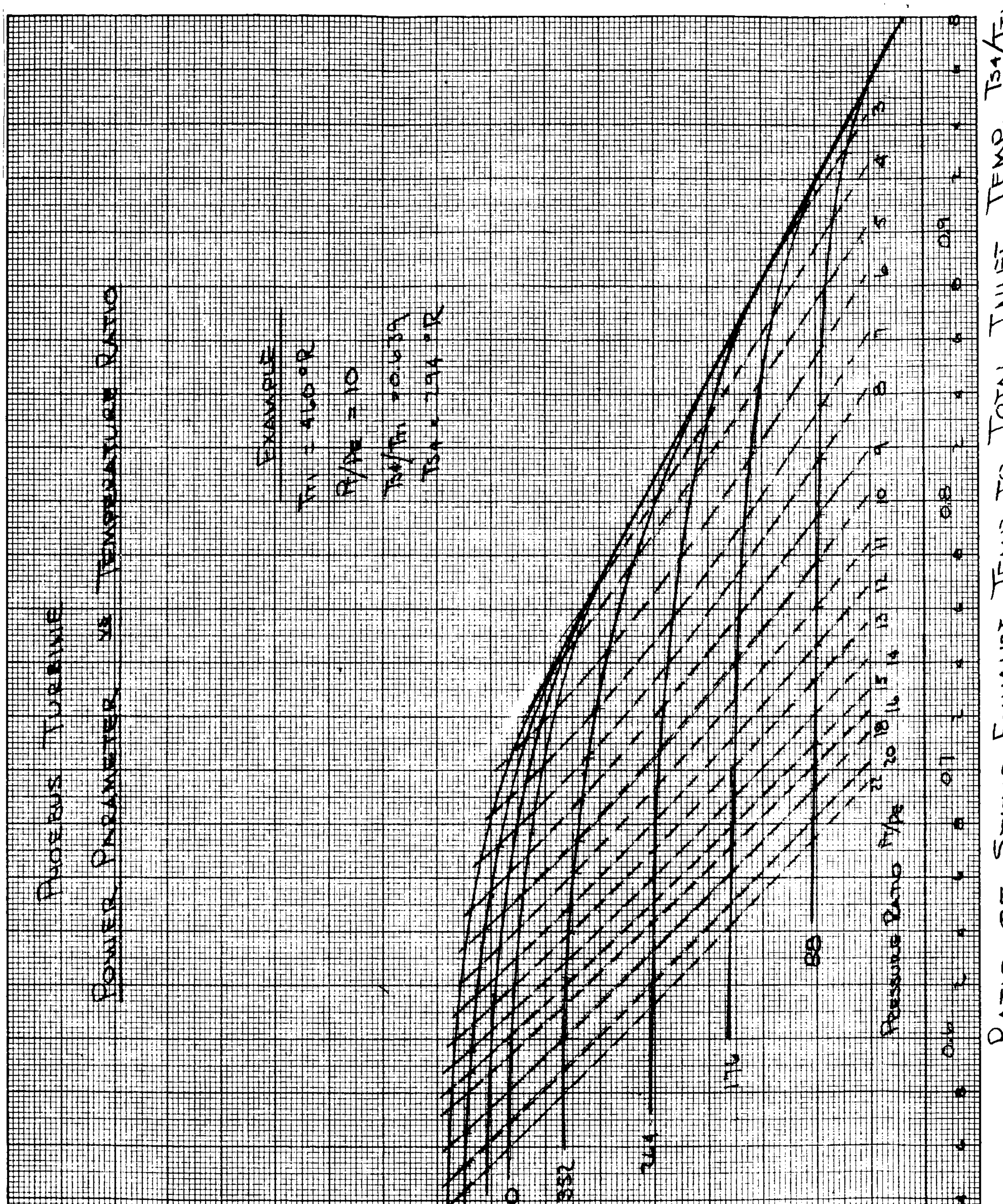

PHOEBUS TURBINE
POWER PARAMETER VS TEMPERATURE RATIO
EXAMPLE
T_{T1} = 460 °R
P_1/P_2 = 10
T_{S4}/T_{T1} = 0.639
T_{S4} = 294 °R
$N/\sqrt{T_{T1}}$
572
528
484
440
352
264
176
88
PRESSURE RATIO P_1/P_2
RATIO OF STATIC EXHAUST TEMP. TO TOTAL INLET TEMP. T_{S4}/T_{T1}
$HP/P_1\sqrt{T_{T1}}$
0.5
0.6
0.7
0.8
0.9
1.0
2.0
3.0
4.0
5.0
J.R.
1-28-65

Figure 35

REVERSING VANES, NUMBER BLADES = 67

Tip	12.37	3.45	120	152
Mean	11.5	15.65	131	132
Hub	10.63	30.2	144	109

ROTOR 2, NUMBER BLADES = 78

Tip	12.40	82.6	73.9	14.7
Mean	11.50	50.4	81.6	14.7
Hub	11.60	28.4	91.0	14.7

3. Design Modifications

The only design modifications made to the M-1 turbine are the addition of honeycomb shrouds over both rotors and an increase in size of the outlet ducts from 10-in. to 15-in.

The M-1 fuel turbine was designed as a velocity staged impulse turbine. However, at the PHOEBUS "design point" condition, both stages run with considerable reaction. These increased reactions result in significant pressure drops across the rotor blade rows and higher tip leakages. This additional loss caused by the higher reaction is estimated at 5.5 efficiency points. This extra loss, which corresponds to an 11% additional weight flow requirement, is eliminated by providing smaller tip clearances through the use of the stationary honeycomb shrouds.

The increased outlet duct size allows the turbine to run with 30-psia back pressure at the PHOEBUS "design condition". This change also provides a significant uprating capability.

4. Performance Analysis

The turbine off-design program was used to estimate the performance of the M-1 Model II fuel turbine over a range of speeds and pressure ratios. Computations were performed for both hydrogen and nitrogen gas at ambient temperature. The program follows, in principle, the usual procedure for pump off-design calculations.

For a given rotational speed, a total-to-static-pressure ratio over the first nozzle is assumed and the corresponding weight flow through this nozzle is computed, using an appropriate loss coefficient and flow coefficient. This weight flow stays constant throughout the turbine (except for leakage and coolant flows). Application of the continuity equation, using the given blade and annulus dimensions in addition to the assumed blade losses and flow coefficients, produces the flow parameters (velocities, pressures, temperatures, gas angles, etc.) at inlet and outlet of each blade row.

In the next step, the pressure ratio over the first nozzle is increased and the calculations are repeated. This procedure is continued until one of the following blade rows cannot pass the weight flow calculated for the first nozzle. The nozzle pressure ratio that corresponds with the choking of one of the following blade rows (e.g. first rotor) is determined and kept constant from thereon. Subsequently, the pressure ratio over the choking blade row (other than first nozzle) is increased by predetermined amounts until one of the blade rows further downstream chokes. Finally, the pressure ratio over the last rotor is increased in steps until one of the following established limits is reached:

a. Maximum over-all turbine pressure ratio (given as computer input).

b. Limiting loading of last stage.

c. Maximum elapsed computer time (specified on submittal card).

This completes the computations for the selected speed. The complete procedure is then repeated for other speeds, at which data is desired.

The program takes into account jet deflection with its associated losses and blade incidence losses. Primarily, the program computes the parameters at mean blade height. However, using simplified assumptions, parameters at hub and tip are also calculated.

Figure 36 shows the calculated turbine weight flow parameter as a function of pressure ratio and speed.

Figure 37 presents the shaft horsepower versus turbine inlet pressure and speed for this system.

The following is a tabulation showing a comparison between the PHOEBUS and M-1 nominal point operating parameters:

	PHOEBUS	Approximate M-1
Gas	Gaseous Hydrogen	LO_2-LH_2
Shaft Power	37,200 hp	90,000 hp
Gas Weightflow	49.5 lb/sec	100 lb/sec
Gas inlet total temperature	60°F	1000°F
Pressure Ratio	13.3	4.67

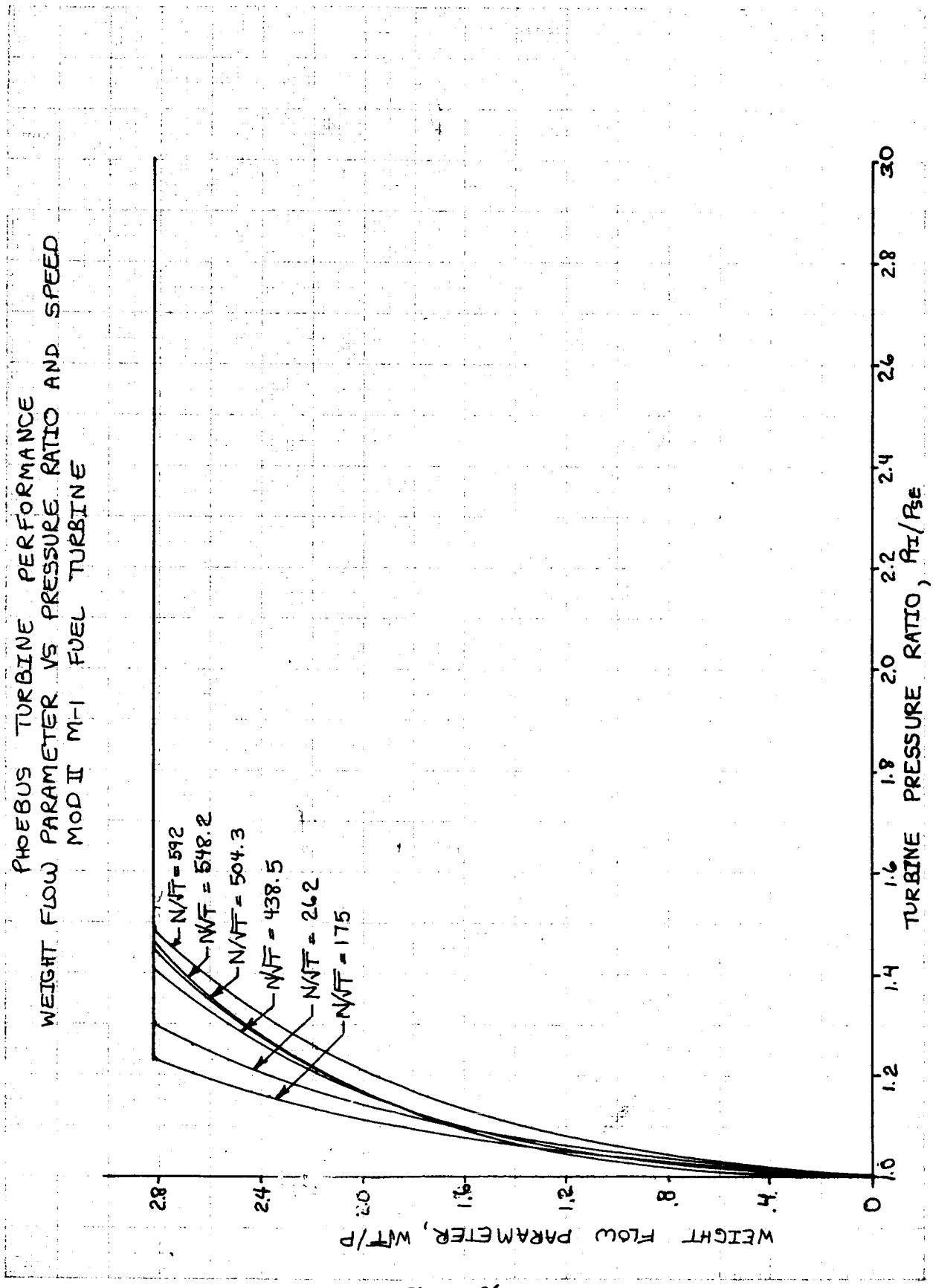
PHOEBUS TURBINE PERFORMANCE
WEIGHT FLOW PARAMETER VS PRESSURE RATIO AND SPEED
MOD II M-1 FUEL TURBINE
N/√T = 592
N/√T = 548.2
N/√T = 504.3
N/√T = 438.5
N/√T = 262
N/√T = 175
WEIGHT FLOW PARAMETER, WT/P
TURBINE PRESSURE RATIO, PTI/PSE
0
.4
.8
1.2
1.6
2.0
2.4
2.8
1.0
1.2
1.4
1.6
1.8
2.0
2.2
2.4
2.6
2.8
3.0

Figure 36

PHOEBUS TURBINE PERFORMANCE
SHAFT POWER VS TURBINE INLET PRESSURE
AND SPEED

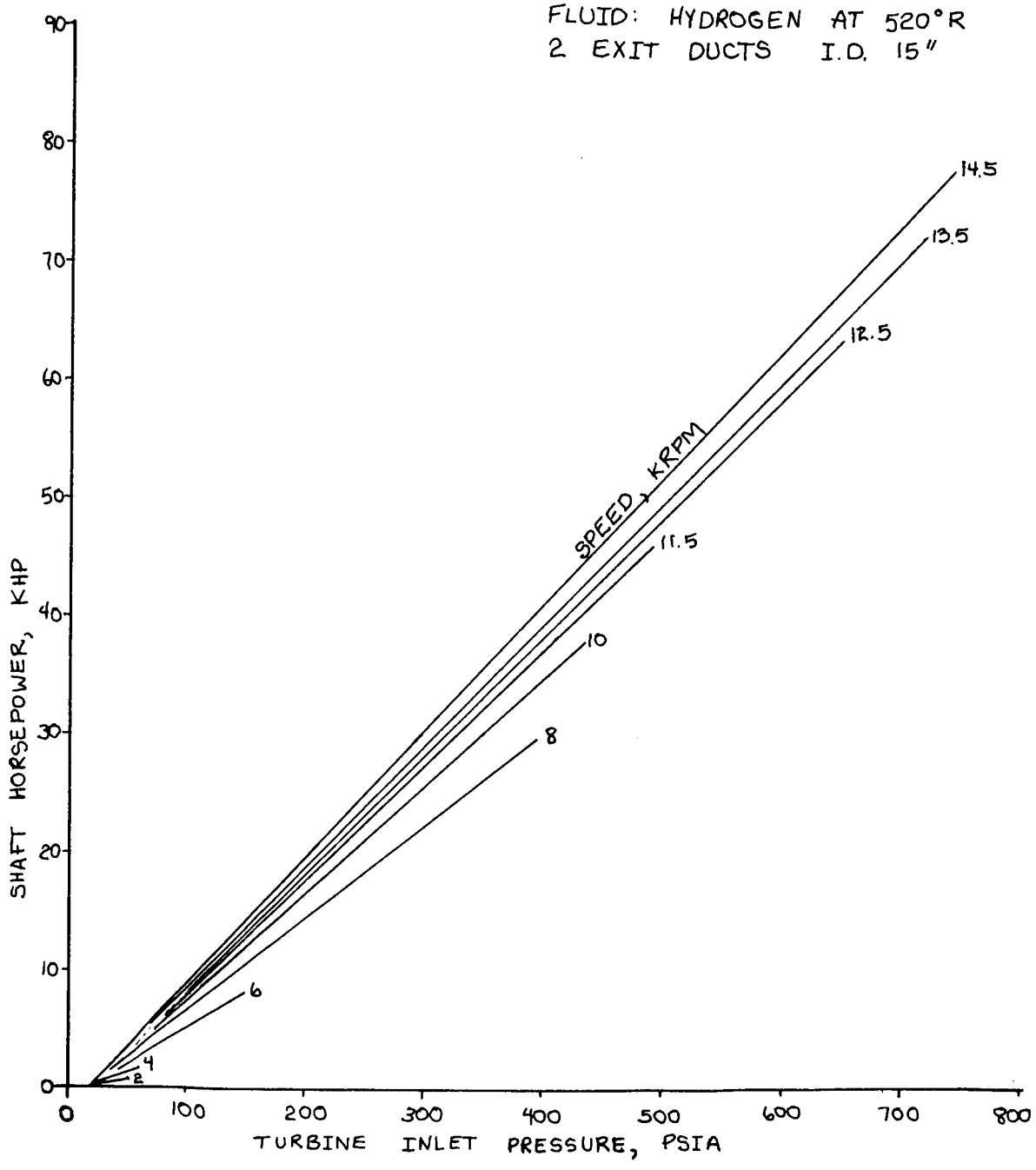

Figure 37
Page 60

	PHOEBUS	Approximate M-1
Inlet total pressure	400 psia	1000 psia
Outlet static pressure	30 psia	-
Efficiency (total to static)	0.562	0.63
Shaft speed	11,500 rpm	13,200 rpm
First turbine stator throat area (effective)	20.25 $in.^2$	20.25 $in.^2$
Specific heat at constant pressure	3.475 Btu/lb°R	2.01 Btu/lb°R
Specific heat ratio	1.399	1.37
Gas constant	771.5 ft/°R	421.5 ft/°R

NOTE: The PHOEBUS turbine performance data is based upon a turbine exhaust pressure of 30 psia; therefore, gas weight flow and efficiency do not agree numerically with values shown elsewhere in this report.

5. Turbine Axial Thrust

The axial turbine rotor thrust was computed for a range of speeds and turbine inlet pressures, using the results of the off-design program. The thrust as a function of turbine inlet pressure and turbine shaft power is presented in Figures 38 and 39, respectively, for gaseous hydrogen at 60°F.

6. Turbine Exhaust Duct Flow Conditions

Figure 40 presents the turbine exit static pressure versus weight flow and turbine outlet total temperature (two 15-in. ducts are assumed) for hydrogen gas at 60°F at the turbine inlet. This supporting analysis was performed when it became apparent that the reactor facility turbine exhaust ducting was smaller than optimum for the M-1 Model II turbine.

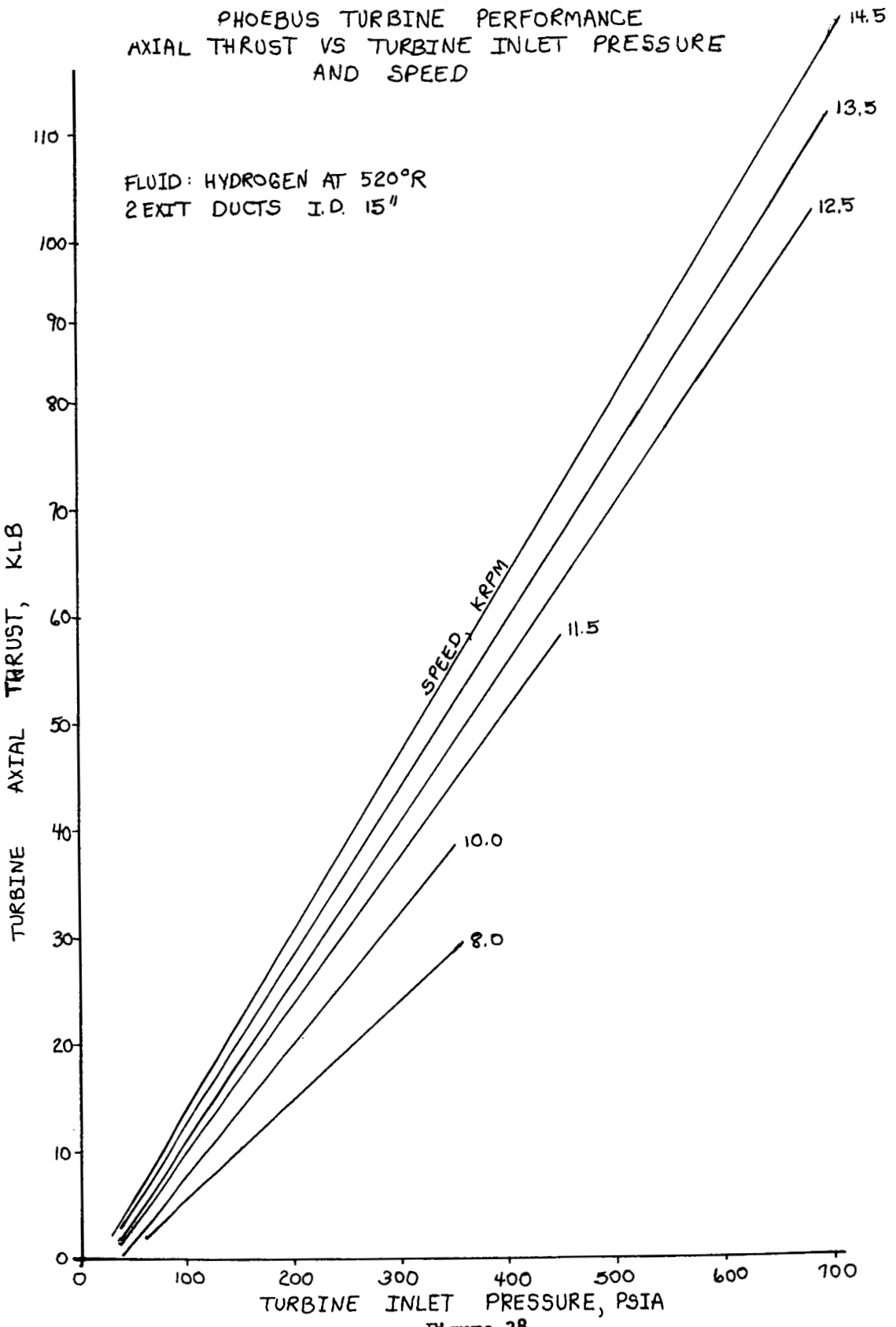

Figure 38
Page 62

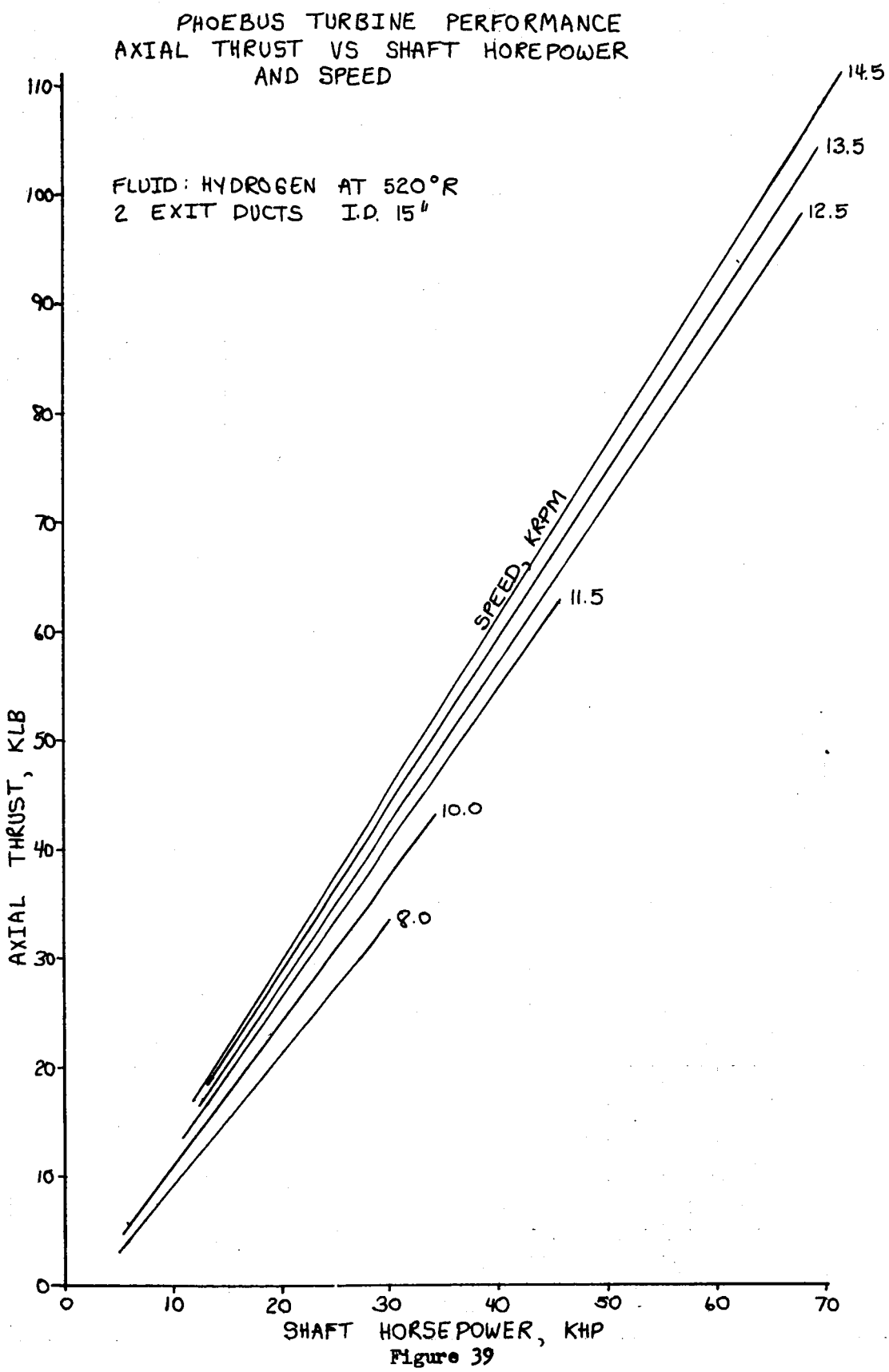
PHOEBUS TURBINE PERFORMANCE
AXIAL THRUST VS SHAFT HORSEPOWER
AND SPEED
FLUID: HYDROGEN AT 520°R
2 EXIT DUCTS I.D. 15"
SPEED, KRPM
14.5
13.5
12.5
11.5
10.0
8.0
AXIAL THRUST, KLB
SHAFT HORSEPOWER, KHP
0
10
20
30
40
50
60
70
80
90
100
110

Figure 39

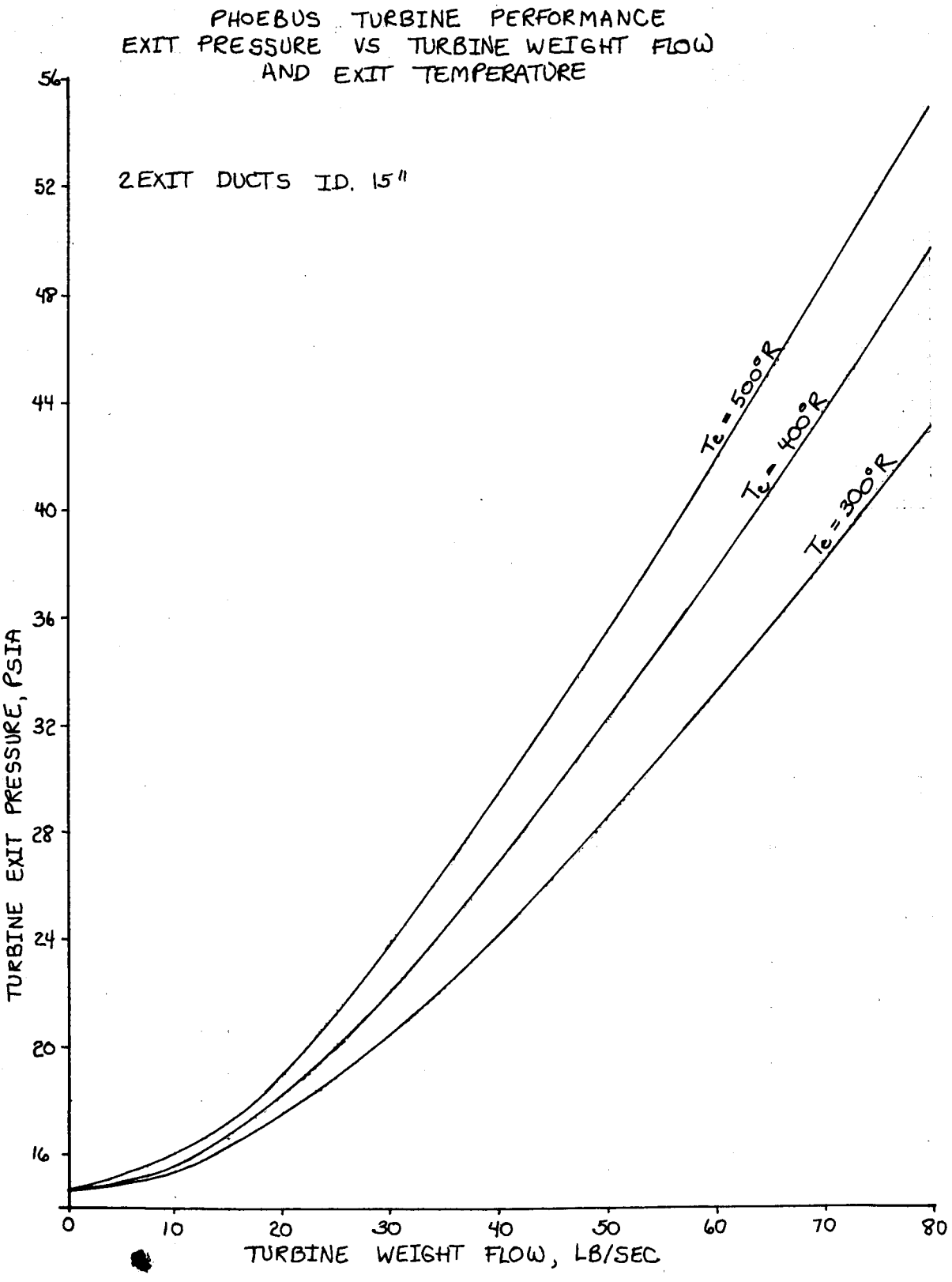

Figure 40
Page 64

E. STRUCTURAL ENGINEERING

1. Stress

Results of stress analyses shown in the appropriate summary tables are extracted from the stress analyses reports subsequently referenced as source analyses in this report, which also detailed the stress analysis methods used.

a. Pump

Table 3 is a summary of stress analysis results for the PHOEBUS pump components. The pump conditions selected for stress analysis were: an operating speed of 14,500 rpm; a flow rate of 360 lb/sec; and a pressure rise of 1965 psi. This operating point corresponds to the maximum allowable working stress of the pump discharge housing when the pump is operating at maximum speed. At this operating point, the hydraulic and centrifugal forces on the pump components are approximately 59% higher than at the PHOEBUS nominal operating point. The conservative stress analysis operating point was selected because the M-1 hardware is capable of operating at this condition with no additional modifications. This point is greater than required to obtain the highest desired hydraulic performance for the PHOEBUS application. Thus, it defines conditions at the full uprated capability of the PHOEBUS turbopump assembly.

Adequate positive margins of safety exist for all components at the stress analysis point. Also shown in Table 3 are estimated yield speeds for the rotating pump components.

Stress analysis results indicate that the pump is structurally sound for the PHOEBUS application as well as for the increased power level reactor applications.

b. Turbine

Table 4 contains a summary of stress analysis results for the PHOEBUS turbine components. The turbine operating point selected for stress analysis was an operating speed of 14,500 rpm, turbine horsepower of 89,000 and a turbine exhaust pressure of 14.7 psia. The power level is even higher than that corresponding to the operating point used for pump stress analysis. It corresponds to operation of the pump at 80% of the design flow coefficient. At this condition, the allowable working pressure of the pump discharge housing is exceeded; however, as shown in Table 4, the turbine is capable of operation with adequate positive margins of safety for all components. The turbine exhaust pressure of 14.7 psia was selected because this gives the most conservative values (highest disc and vane aerodynamic loading) for stress calculations. Also shown in Table 4 are estimated yield and burst speeds for the rotating turbine components.

The stress analysis results indicate that the turbine is structurally sound for the entire range of pump operation shown in Figure 1 and also for power levels corresponding to operating the pump down to stall at 14,500 rpm (a condition requiring a pump housing with higher pressure capabilities than the existing design).

TABLE 3

PHOEBUS PUMP STRESS ANALYSIS SUMMARY

Component	Min. Static Stress Margin of Safety Yield	Min. Static Stress Margin of Safety Rupture	Min. Fatigue Margin of Safety	Zero Hyd. Load Yield Speed (rpm)	Source*
Guide Vane Housing	+1.75	---	---	---	PH-TPA-SA-19
Inducer Spinner Lock Ring	+ .26	+ .57	---	16,300	PH-TPA-SA-10**
Inducer Spinner	+ .33	+ .94	---	19,500	PH-TPA-SA-13
Inducer Rotor Blade, Hub and Spline	+ .48	---	+0.36	19,600	PH-TPA-SA-5, PH-TPA-SA-15
Transition Rotor Blade and Ring	---	+1.02	+0.86	19,600	PH-TPA-SA-8A
Transition Stator Blade	---	+1.62	+ .40	---	PH-TPA-SA-7A
Main Stage Rotor Blade and Dovetail	---	+ 1.36	+0.54	28,800	PH-TPA-SA-1
Main Stage Stator Blade	---	+1.10	+0.23	---	PH-TPA-SA-2
Balance Piston	---	+ .45	---	18,600	FTPA-106

NOTE: For the Guide Vane Housing, the Minimum Margin of Safety to Yield During Thermal Transient is +1.84.

---

* Source Analysis; numbers indicate Aerojet-General Structures Department file identification.

** The source analysis lists negative margins of safety; however, design modifications have been made to give the margins of safety shown.

TABLE 4

PHOEBUS TURBINE STRESS ANALYSIS SUMMARY

Component	Min. Static Stress Margin of Safety		Min. Fatigue Margin of Safety	Zero Zerodynamic Load Overspeed		Source*
	Yield	Rupture		Yield Speed (rpm)	Burst Speed (rpm)	
First Stage Rotor Vanes	+1.49	+1.25	+ .44	---	---	PH-TPA-SA-12
First Stage Rotor Disc	---	+ .73	---	17,400	23,500	SA-PH-TPA-4
Reversing Row	+1.49	+4.7	+2.96	---	---	PH-TPA-SA-12
Second Stage Rotor Vanes	+1.14	+ .92	+ .23	---	---	PH-TPA-SA-12
Second Stage Rotor Disc	---	+ .77	---	18,800	23,800	SA-PH-TPA-4

* Source Analysis; numbers indicate Aerojet-General Structures Department file identification.

2. Vibration

Tables 5 and 6 summarize the results of pump blading and turbine blading vibration analyses, respectively. Predicted resonant speeds, modes of vibration, and sources of excitation are tabulated together with an estimate of the fatigue margins of safety for the individual blade resonant speeds of the turbopump.

Figure 41 summarizes the predicted turbopump blade resonance speeds for first and second flexural and torsional vibration modes. The excitation assumed is the upstream vane passing frequency and its second harmonic. Third vibration modes and third harmonic excitation frequencies are included for those cases, in which relatively high energy levels are predicted.

Several resonance speeds are predicted to occur within the PHOEBUS operating range. Further study, design, and test effort is required to define which of the predicted frequencies are of concern as well as those that can be alleviated or eliminated by minor design change or ignored because of inherent damping (as verified by M-1 vibration tests). Ultimately, turbopump speeds at which prolonged operation should be avoided will be defined.

In compressor experience and practice, it is frequently found that predicted vibration modes do not develop and unexpected modes do occur. Strain gage measurement of blade vibration during operation of rotating-type machines provides the most direct and effective means for defining blade vibration problems as well as demonstrating successful redesign. The slip-ring assembly described in the forthcoming alternative torquemeter discussion can be used for this purpose.

Strain gage bonding techniques have been evolved in the M-1 Program for liquid hydrogen applications and have been successfully used with the M-1 axial thrust sleeve.

The vibration analysis has predicted possible vibration modes which could occur, and includes an estimate of possible severity; however, it is not expected that all predicted modes will occur and it is possible that not all modes have been defined. In addition, the amount of damping assumed to be present by virtue of such conditions as blade dovetail friction, contact with adjacent blade segments, and coulomb damping, has not as yet been empirically verified in most cases. Therefore, the resonant frequency map of Figure 41 establishes areas which may require empirical investigation rather than defining speeds at which rapid blade fatigue would occur. Further effort in this area is an important aspect of the PHOEBUS Phase II Program. Considerable pertinent data will be obtained from the M-1 Program.

3. Running Clearance and Spline Fit

All PHOEBUS static spline fits and clearances are identical to M-1. The operating clearances along the rotor assembly vary because of PHOEBUS design philosophy and requirements. The mainstage and transition rotor are the same as used for M-1 except that the growth resulting from centrifugal force will be slightly less as a result of the reduced over-all blade tip radius.

TABLE 5 (Sheet 1 of 2)

PHOEBUS PUMP VIBRATION ANALYSIS SUMMARY

COMPONENT	MODE	EXCITATION**	RESONANT SPEED (rpm)	% MARGIN TO NOMINAL SPEED	REMARKS	SOURCE*
Transition Rotor Blade	1st Flexural (Span)	Inducer Stator, 3rd Harmonic	12,700	+10	Prolonged Operation should be avoided.	SA-PH-TPA-14
	1st Torsional	Inducer Stator, 3rd Harmonic	13,300	+14		
Transition Stator Blade	1st Torsional	Transition Rotor, 3rd Harmonic	9,800	-15		
	1st Torsional	Transition Rotor, 2nd Harmonic	14,700	+28		
Main Stage Rotor Blade	1st Torsional	Main Stage Stator, 3rd Harmonic	[illegible],300	-71	Prolonged operation permissible, low dynamic stresses.	
	1st Flexural (span)	Transition Stator, 3rd Harmonic	3,400	-70		
	1st Flexural (span)	Main Stage Stator, 2nd Harmonic	4,100	-64		
	1st Torsional	Transition Stator, 3rd Harmonic	4,200	-63		
	1st Torsional	Main Stage Stator, 2nd Harmonic	5,000	-57		
	1st Flexural (span)	Transition Stator, 2nd Harmonic	5,150	-55	Prolonged operation should be avoided.	
	1st Torsional	Transition Stator, 2nd Harmonic	5,400	-44	Prolonged operation permissible, low dynamic stresses.	
	2nd Torsional	Main Stage Stator, 3rd Harmonic	8,200	-29		
	1st Flexural (span)	Main Stage Stator, 1st Harmonic	8,200	-29	Prolonged operation should be avoided.	
	1st Torsional	Main Stage Stator, 1st Harmonic	10,050	-13		
	1st Flexural (span)	Transition Stator, 1st Harmonic	10,300	-10		
	2nd Torsional	Transition Stator, 3rd Harmonic	10,350	-10	Prolonged operation permissible, low dynamic stresses.	
	1st Flexural (chord)	Main Stage Stator, 3rd Harmonic	11,250	- 2		
	2nd Torsional	Main Stage Stator, 2nd Harmonic	12,300	+ 7		
	1st Torsional	Transition Stator, 1st Harmonic	12,650	+10	Prolonged operation should be avoided.	
	2nd Flexural (span)	Main Stage Stator, 3rd Harmonic	14,200	+23	Prolonged operation permissible, low dynamic stresses.	
	1st Flexural (chord)	Transition Stator, 3rd Harmonic	14,250	+24		

* Source Analysis; numbers indicate Aerojet-General Structures Department file identification.

** NOTE: Possible stimuli are 1st, 2nd, and 3rd harmonics of immediate upstream vane passing frequency exciting 1st or 2nd span wise or chordwise flexural modes or 1st or 2nd torsional mode.

(CONTINUED)

TABLE 5 (Sheet 2 of 2)

PHOEBUS PUMP VIBRATION ANALYSIS SUMMARY

COMPONENT	MODE	EXCITATION**	RESONANT SPEED (rpm)	% MARGIN TO NOMINAL SPEED	REMARKS	SOURCE*
Main Stage Stator Blade	2nd Flexural (span)	Main Stage Rotor, 2nd Harmonic	3,690	-68	Prolonged operation permissible, low dynamic stresses.	
	2nd Torsional	Main Stage Rotor, 3rd Harmonic	6,600	-43	↓	
	2nd Flexural (span)	Main Stage Rotor, 1st Harmonic	7,480	-35	Prolonged operation should be avoided.	
	2nd Torsional	Main Stage Rotor, 2nd Harmonic	9,950	-14	↓	
	3rd Torsional	Main Stage Rotor, 3rd Harmonic	12,800	+11	Prolonged operation permissible, low dynamic stresses.	
	3rd Flexural (span)	Main Stage Rotor, 3rd Harmonic	13,400	+16	Prolonged operation should be avoided.	

* Source Analysis; numbers indicate Aerojet-General Structures Department file identification.

** NOTE: Possible stimuli are 1st, 2nd, and 3rd harmonics of immediate upstream vane passing frequency exciting 1st or 2nd span wise or chordwise flexural modes or 1st or 2nd torsional mode.

TABLE 6 (Sheet 1 of 2)

PHOEBUS TURBINE VIBRATION ANALYSIS SUMMARY

COMPONENT	MODE	EXCITATION** SOURCE	RESONANT SPEED (rpm)	% MARGIN TO NOMINAL SPEED	REMARKS	SOURCE*
1st Stage Rotor Disk	Two Nodal Diameters	Mechanical Unbalance	18,000	+56	Above Maximum Design Speed	SA-PH-TPA-4
1st Stage Rotor Vanes	1st Tangential	Nozzle, 3rd Harmonic	3,600	-69	Prolonged Operation Permissible, Low Dynamic Stresses	PH-TPA-SA-18
	1st Axial	Nozzle, 3rd Harmonic	4,200	-63		
	1st Tangential	Nozzle, 2nd Harmonic	5,400	-53		
	1st Axial	Nozzle, 2nd Harmonic	6,300	-45		
	2nd Axial	Nozzle, 3rd Harmonic	6,300	-45		
	2nd Axial	Nozzle, 2nd Harmonic	9,500	-17		
	1st Tangential	Nozzle, 1st Harmonic	10,700	- 7		
	2nd Tangential	Nozzle, 3rd Harmonic	11,300	- 2		
	1st Axial	Nozzle, 1st Harmonic	12,400	+ 8		
	3rd Tangential	Nozzle, 3rd Harmonic	12,500	+ 9		
	3rd Axial	Nozzle, 3rd Harmonic	13,000	+13		
Reversing Vanes	1st Axial	1st Rotor, 3rd Harmonic	800	-93	Prolonged Operation Permissible, Low Dynamic Stresses	PH-TPA-SA-18
	1st Tangential	1st Rotor, 3rd Harmonic	1,000	-91		
	2nd Axial	1st Rotor, 3rd Harmonic	1,000	-91		
	1st Axial	1st Rotor, 2nd Harmonic	1,100	-90		
	1st Tangential	1st Rotor, 2nd Harmonic	1,500	-87		
	2nd Axial	1st Rotor, 2nd Harmonic	1,500	-87		
	3rd Axial	1st Rotor, 3rd Harmonic	1,500	-87		
	1st Axial	1st Rotor, 1st Harmonic	2,200	-81		
	3rd Axial	1st Rotor, 2nd Harmonic	2,400	-79		
	1st Tangential	1st Rotor, 1st Harmonic	2,900	-75		
	2nd Axial	1st Rotor, 1st Harmonic	2,900	-75		
	2nd Tangential	1st Rotor, 3rd Harmonic	3,100	-73		
	4th Axial	1st Rotor, 3rd Harmonic	3,200	-72		
	3rd Tangential	1st Rotor, 3rd Harmonic	3,500	-70		
	3rd Axial	1st Rotor, 1st Harmonic	4,700	-59		
	2nd Tangential	1st Rotor, 2nd Harmonic	4,700	-59		
	4th Axial	1st Rotor, 2nd Harmonic	4,800	-58		
	3rd Tangential	1st Rotor, 2nd Harmonic	5,300	-54		

* Source Analysis; numbers indicate Aerojet-General Structures Department file identification.

** NOTE: Possible stimuli are 1st, 2nd and 3rd harmonics of immediate upstream vane passing frequency exciting 1st or 2nd, 3rd, or 4th tangential or axial flexural modes or 1st, 2nd, or 3rd torsional mode. Stimulus for disk vibration is mechanical unbalance of rotating assembly.

TABLE 6 (Sheet 2 of 2)

PHOEBUS TURBINE VIBRATION ANALYSIS SUMMARY

COMPONENT	MODE	EXCITATION** SOURCE	RESONANT SPEED (rpm)	% MARGIN TO NOMINAL SPEED	REMARKS	SOURCE*
Reversing Vanes (Continued)	2nd Tangential	1st Rotor, 1st Harmonic	9,400	-18	Prolonged operation Permissible, Low Dynamic Stresses	
	4th Axial	1st Rotor, 1st Harmonic	9,700	-16	↓	
	3rd Tangential	1st Rotor, 1st Harmonic	10,600	- 8		
2nd Stage Rotor Disk	Two Nodal Diameters	Mechanical Unbalance	17,640	+53	Above Maximum Design Speed	SA-PH-TPA-4
2nd Stage Rotor Vanes	1st Tangential	Reversing Vanes, 3rd Harmonic	800	-93	Prolonged Operation Permissible, Low Dynamic Stresses	PH-TPA-SA-18
	1st Tangential	Reversing Vanes, 2nd Harmonic	1,100	-90	↓	
	1st Axial	Reversing Vanes, 3rd Harmonic	1,500	-87		
	1st Torsional	Reversing Vanes, 3rd Harmonic	1,600	-86		
	1st Axial	Reversing Vanes, 2nd Harmonic	1,200	-81		
	1st Tangential	Reversing Vanes, 1st Harmonic	2,300	-80		
	1st Torsional	Reversing Vanes, 2nd Harmonic	2,400	-79		
	2nd Tangential	Reversing Vanes, 3rd Harmonic	3,700	-68		
	2nd Torsional	Reversing Vanes, 3rd Harmonic	4,200	-63		
	1st Axial	Reversing Vanes, 1st Harmonic	4,400	-62		
	1st Torsional	Reversing Vanes, 1st Harmonic	4,800	-58		
	3rd Tangential	Reversing Vanes, 3rd Harmonic	5,400	-53		
	2nd Axial	Reversing Vanes, 3rd Harmonic	5,400	-53		
	2nd Tangential	Reversing Vanes, 2nd Harmonic	5,600	-51		
	2nd Torsional	Reversing Vanes, 2nd Harmonic	6,300	-45		
	3rd Torsional	Reversing Vanes, 3rd Harmonic	8,000	-30		
	3rd Tangential	Reversing Vanes, 2nd Harmonic	8,100	-29		
	2nd Axial	Reversing Vanes, 2nd Harmonic	8,100	-29		
	3rd Axial	Reversing Vanes, 3rd Harmonic	11,100	- 3		
	2nd Tangential	Reversing Vanes, 1st Harmonic	11,200	- 2		
	3rd Torsional	Reversing Vanes, 2nd Harmonic	11,900	+ 3		
	2nd Torsional	Reversing Vanes, 1st Harmonic	12,600	+10		

* Source Analysis; numbers indicate Aerojet-General Structures Department file identification.

** NOTE: Possible stimuli are 1st, 2nd, and 3rd harmonics of immediate upstream vane passing frequency exciting 1st or 2nd, 3rd, or 4th tangential or axial flexural modes or 1st, 2nd, or 3rd torsional mode. Stimulus for disk vibration is mechanical unbalance of rotating assembly.

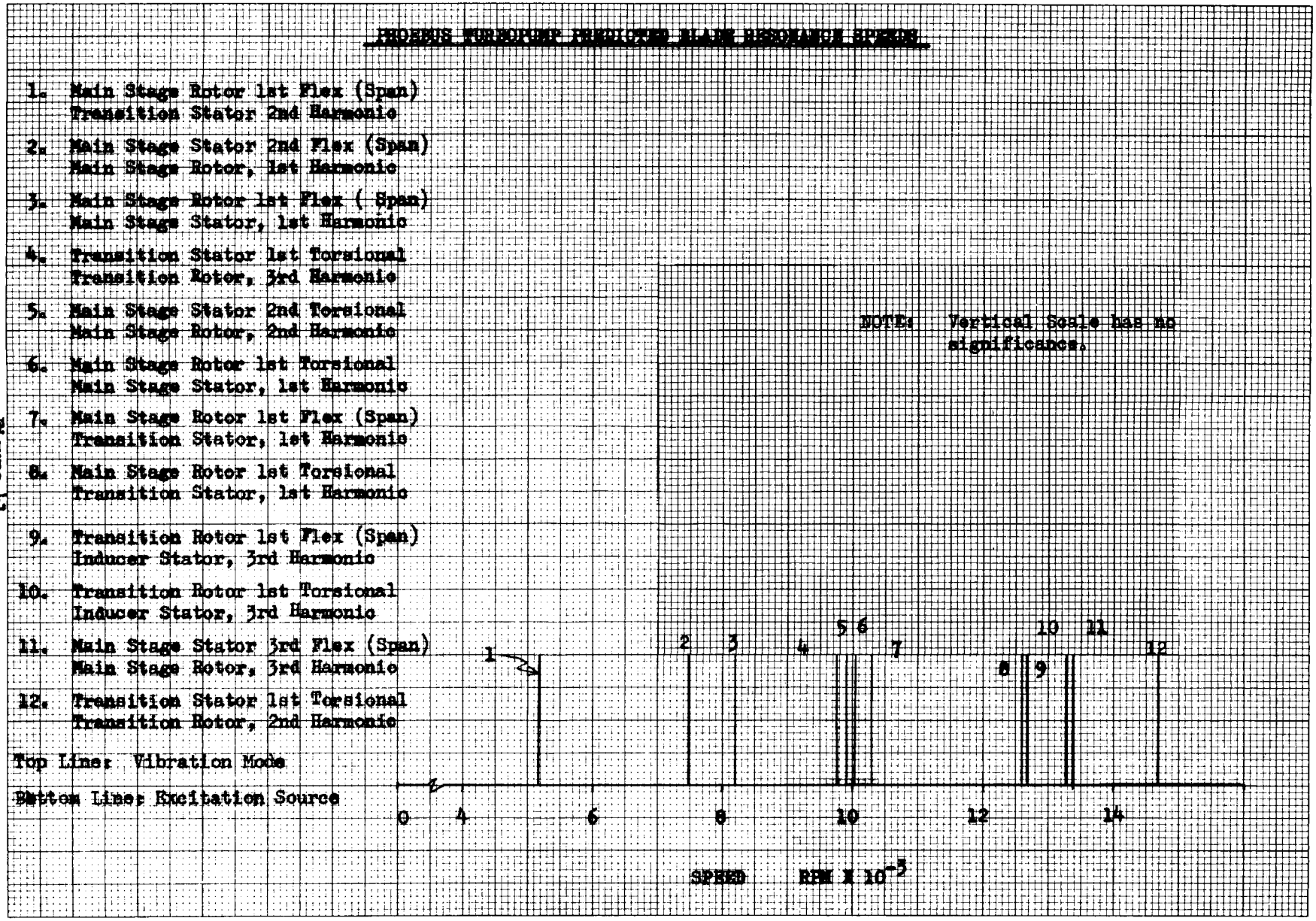

Figure 11
Page 73

The clearance of the inducer-to-housing has been changed from 0.150-in. M-1 nominal to a varying nominal clearance of 0.090-in. at the suction end to 0.050-in. at the exit end. This change was made because the M-1 clearance would allow excessive tip leakage when applied to the PHOEBUS design.

The balance piston and its housing, along with the labyrinth shaft riding seals and roller bearings, are identical to those used for M-1 and no changes in clearance were made.

The turbine in the PHOEBUS application will have honeycomb material added over the blade tips. This will permit operation at a very small clearance inasmuch as the turbine rotors can be "run-in" during the first test sequence resulting in a more efficient turbine.

F. POWER TRANSMISSION DESIGN MODIFICATIONS

1. Ball Bearings (Thrust)

The M-1 thrust bearing assembly requires some modification for use in the PHOEBUS turbopump assembly. Although the basic size and configuration of the M-1 bearing is acceptable, a change in internal geometry is necessary to meet the special operational requirements of PHOEBUS.

a. The M-1 design was predicated on the following requirements:

(1) Nominal operating speed of 13,235 rpm and 14,550 rpm overspeed for 10 sec.

(2) Maximum thrust load of 35,000 lb with a reverse loading capability of 6400 lb.

(3) Pump rotor axial movement of 0.014-in. to 0.020-in.

The limited allowable rotor axial movement dictated the use of a bearing with a "Gothic Arch."

b. The PHOEBUS thrust bearing requirements encompass a much wider range of steady state operating conditions than M-1.

(1) Nominal operating speed of 11,500 rpm with an operational capability for extended periods at any speed from 0 to 11,500 rpm and 14,500 rpm overspeed for 30 sec.

(2) Two-hour duration at any combination of speed and load within the pump operating map.

(3) Maximum thrust load of 20,000 lb with a reverse loading capability of 6400 lb.

(4) Pump rotor axial movement of ± 0.025-in.

2. Preload Grinding

Based upon data derived from oil-lubricated bearings, it is estimated that for a two-hour life at the nominal operating speed of 11,500 rpm, a maximum continuous thrust load on the triple stack should not exceed 20,000 lb. This assumes a load sharing capability of 50%, 25%, 25% respectively, for the three bearings in the stack. For a design load of 35,000 lb on the M-1 bearings, it was necessary to preload grind the bearings at 12,000 lb per bearing to obtain proper load sharing. The load for the PHOEBUS application is reduced to 20,000 lb and because of the wide speed and load range, it is advantagous to preload grind these bearings at a value closer to the center of the operating load range. Therefore, the PHOEBUS bearings will be ground at 6000 lb per bearing.

3. "Gothic Arch" Outer Race

The internal bearing configuration of the M-1 bearing is a "Gothic Arch" on both inner and outer races. This bearing design is appropriate for the M-1 application where operation takes place under relatively constant speed and load conditions. However, in the PHOEBUS application, the bearings must be capable of reliable operation under widely variable load and speed conditions. Use of "Gothic Arch" outer races imposes operational limitations in the PHOEBUS low load and high speed regions. Under low load and high speed, high centrifugal force results in two-point ball contact on the outer race (attributable to the "Gothic Arch") and a one-point contact on the inner race, thus establishing three-point contact in the bearing.

Three-point contact in the bearing during operation shortens the bearing life because of ball skidding. To alleviate this condition and because axial movement of the rotor shaft is no longer tightly restricted, the PHOEBUS bearings will have a conventional single radius outer race curvature.

4. Bearing Life-Load Characteristics and Cooling Requirements

a. Bearing Fatigue Life (General)

The bearing fatigue life curves presented in Figures 42 and 43 are based upon the existing theory from a statistical principle of crack propagation for oil-lubricated bearings manufactured from air-melted 52100 steel. The calculations are based upon a 90% probability of survival.

The material used in PHOEBUS bearings is consumable-electrode-vacuum-melted AISI 440C stainless steel. This steel has been selected over 52100 steel because of its resistance to corrosion and its demonstrated superior fatigue life characteristics. It is expected (with some bearing test verification) that the good fatigue life characteristics of CEVM 440C steel, combined with the excellent cooling properties of liquid hydrogen, will compensate for the deficiencies in the lubricating qualities of liquid hydrogen.

The method for bearing fatigue life prediction provides a means for estimating the probability of surviving any given load-speed-time condition. However, life is also dependent upon the major factors of material quality, installation cleanliness, operating temperature and pressure environment, lubrication and/or coolant, operating alignment, load balance, as well as shaft and housing fits.

PREDICTED BEARING LIFE

PHOEBUS THRUST BEARING

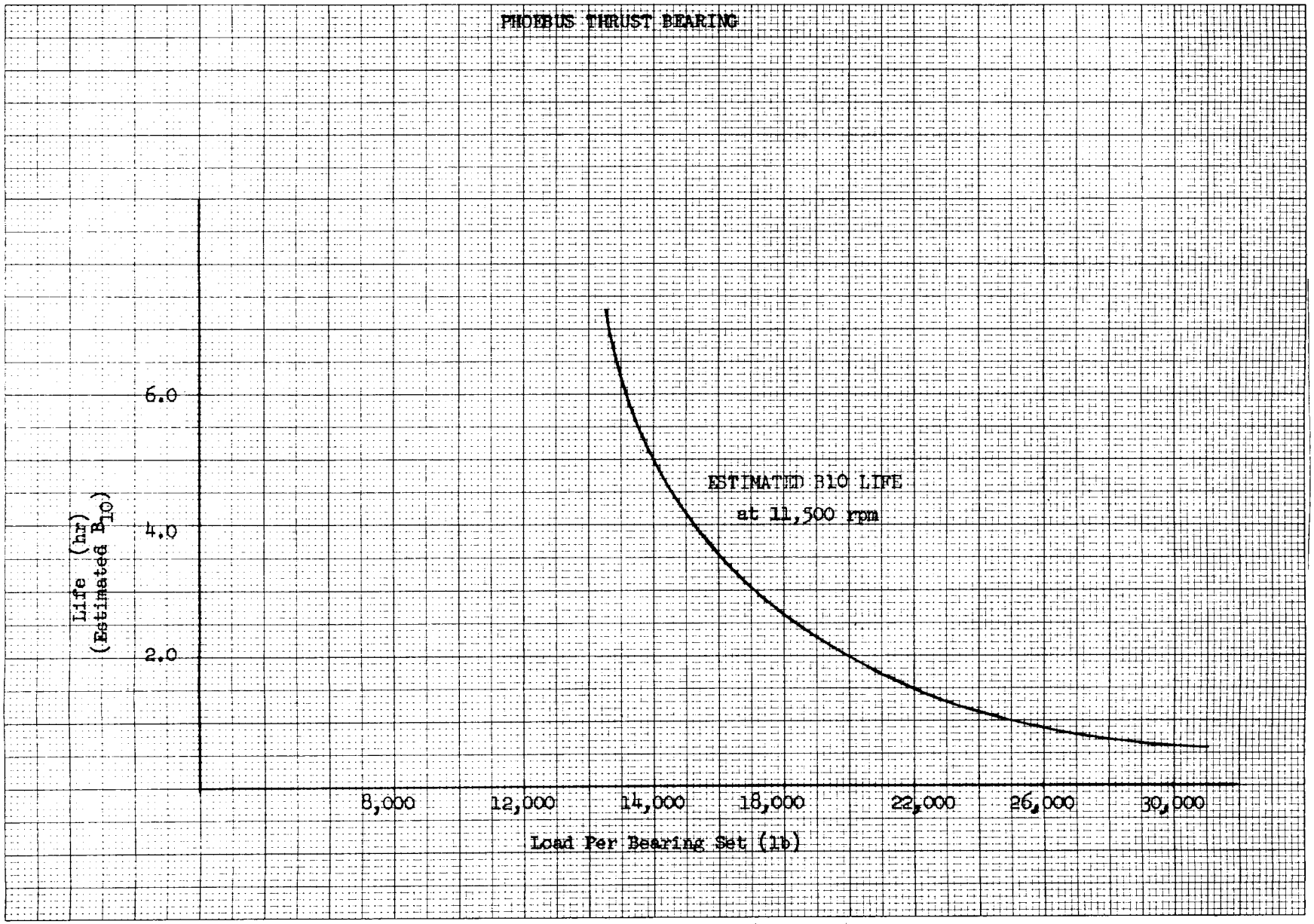

Figure 12

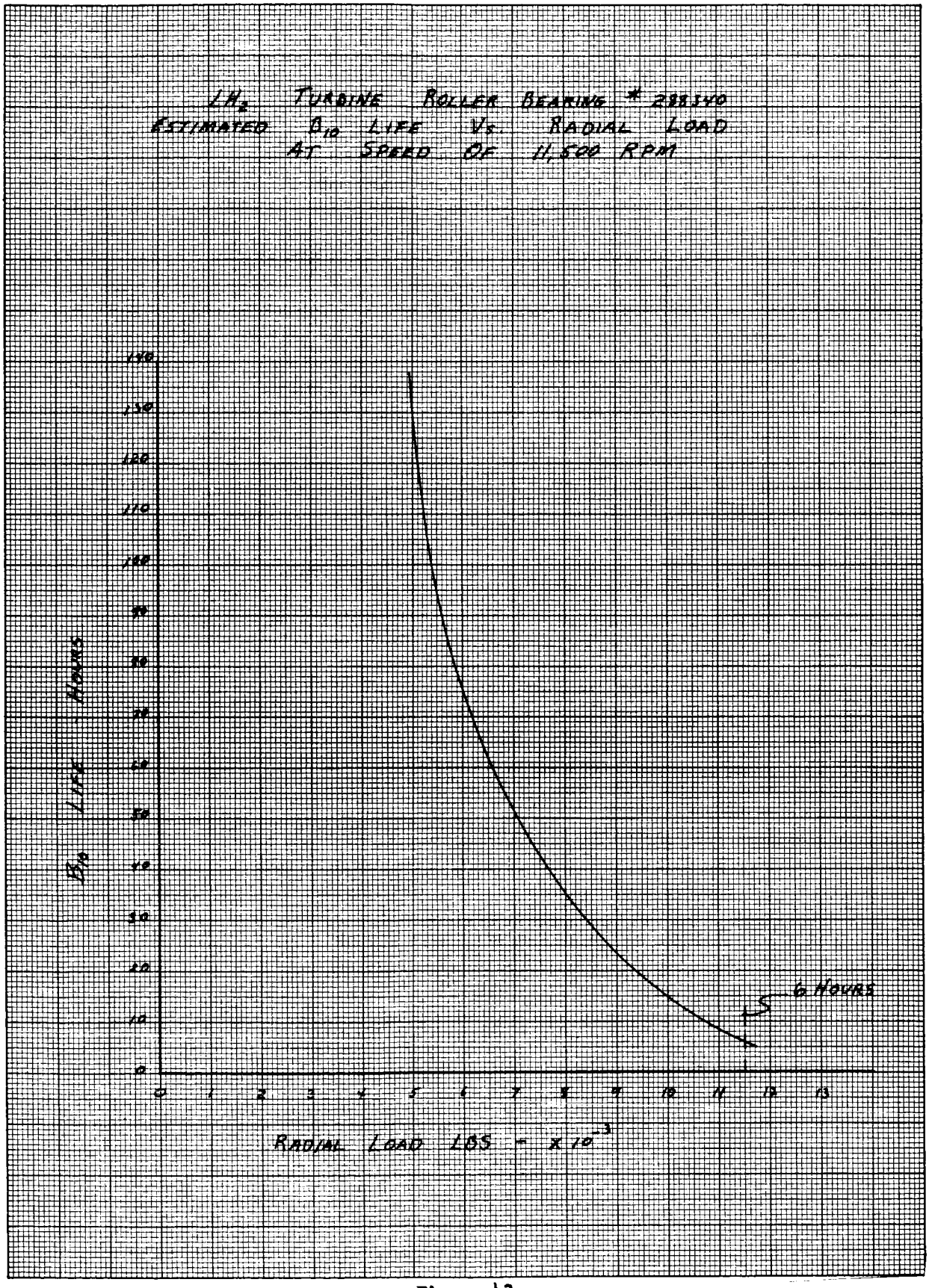
LH2 TURBINE ROLLER BEARING # 228140
ESTIMATED B10 LIFE VS. RADIAL LOAD
AT SPEED OF 11,500 RPM
B10 LIFE HOURS
150
120
110
100
90
80
70
60
50
40
30
20
10
0
0 1 2 3 4 5 6 7 8 9 10 11 12 13
6 HOURS
RADIAL LOAD LBS - X 10-3

Figure 43

b. Bearing Fit

The bearing mounting fits for the inner-race-to-shaft and outer-race-to-housing for the PHOEBUS application are identical to the thrust and roller bearing used in the M-1 Program and are duplicated in the bearing tester. Thus, M-1 bearing tests and M-1 turbopump experience will be applicable to PHOEBUS.

The calculated stresses and test data for both axial and radial bearings from the M-1 Program provide assurance that no problems will be encountered during the room temperature, chilldown, transients and operating conditions. PHOEBUS loads and speeds are lower and no problems are anticipated.

c. Thrust Bearing

It was estimated that two hours of B10 operating life for this triple bearing set can be obtained at a maximum thrust load of 20,000 lb and a speed of 11,500 rpm (see Figure 42). The corresponding maximum compressive (Hertz) stresses are calculated to be 340,000 psi. These compressive stresses are within the elastic limits of the bearing material where no permanent deformation of races will occur. The two-hour life estimate was made under the assumption that because of the variation in deflection characteristics of each bearing in this triplex set, the heaviest loaded bearing in the set will share 50% (10,000 lb) of total load and the remaining two bearings will share the remaining 10,000 lb.

The operating life curve shown on Figure 42 is an estimate requiring subsequent test verification. Tests may show that an improved method of bearing lubrication is desirable, such as utilizing an imoroved dry-film coating for balls and races. Moly-disulfide has proven very successful in NERVA bearing tests. However, M-1 bearings have not required such additional lubrication film.

Tests are necessary to establish the effect of low loads and high speed upon bearing life. During turbopump operation, it is possible that one, or even two bearings of the triple set may be unloaded and only the third one will carry the thrust load. Unloading of bearings at high speed may result in ball skidding; however, this condition will be minimized by utilizing the conventional outer race configuration.

d. Roller Bearings

An analysis was performed to determine the critical speed and roller bearing loads of the PHOEBUS fuel turbopump. As a result, the life of turbine end roller bearing and pump end roller bearing is estimated to be much longer than for the thrust bearing (see Figure 43). From the indicated analyses, Figure 44 was established which indicates that the turbine end and pump end roller bearings will be loaded to approximately 3200 lb and 1600 lb, respectively, at the nominal operating speed of 11,500 rpm. Predicted B10 life is in excess of 100 hours for these conditions.

For the PHOEBUS application, an allowable overspeed of 14,500 rpm for 30 sec duration is required. This imposes approximately 10,000 lb of radial load on the turbine end roller bearing and 5000 lb on the pump end roller bearing. The corresponding calculated maximum Hertz stresses are: 11,500 rpm, 213,000 psi for turbine end bearing and 205,000 psi for pump end bearing; for the overspeed conditions(14,500 rpm)., stresses are 325,000 psi and 326,000 psi, respectively.

Figure 44

PHOEBUS TURBOPUMP

ROLLER BEARING STRESS AND RADIAL LOAD VS SHAFT SPEED

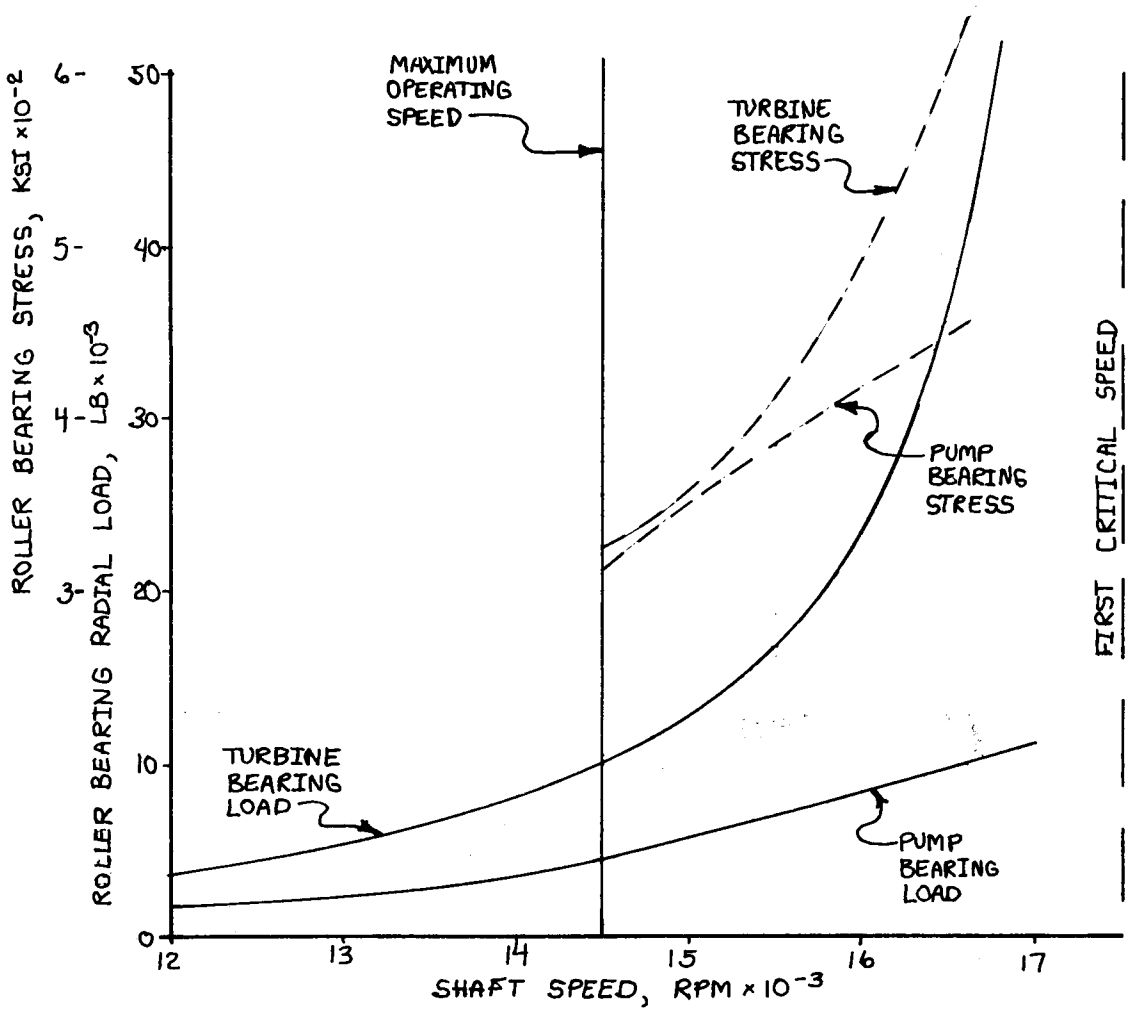

The Hertz stresses for both roller bearings are lower than those calculated for the thrust bearings. This increases the operational life expectancy for the roller bearings. Both of these roller bearings were successfully tested in the M-1 Program; therefore, only demonstration tests are now needed to obtain positive life data for these roller bearings at the PHOEBUS conditions.

e. Bearing Coolant System

Liquid hydrogen coolant for the pump end roller and thrust bearings is bled from the third main stage of the pump. It follows an external route to the pump housing to provide easy access to the filters and flow control orifices. Venturi flow meters are used in two of the four supply lines to measure coolant flow rate. Passages through the vanes of the guide vane housing carry the coolant to the pump side power transmission assembly. Spherical-ended thimbles transfer the coolant from the stationary housing to the moveable inner bearing housing, where it is distributed by the coolant jet rings. Coolant flow varies directly with shaft speed, which is desirable because heat generation in the bearings also varies approximately directly with speed for a constant load.

The M-1 coolant system was not changed for the PHOEBUS application. Because PHOEBUS loads and speed are less than M-1, a reduction in coolant flow should be possible. Selection of orifice sizes to provide an optimum flow will be made, based upon M-1 and PHOEBUS developmental tests. As currently designed, each bearing in the pump end power transmission will receive a coolant flow of approximately 0.75 lb/sec at the nominal operating point. Coolant flow required by the thrust bearings as a function of speed and load is shown by Figure 45 for a temperature rise of 22°F. Assuming a maximum thrust load of 20,000 lb at 11,500 rpm, 0.9 lb/sec of coolant is required. Approximately 2.2 lb/sec is available, which gives a margin of safety in the event of such occurrences as abnormal loads and plugging of filters.

High thrust loads are possible even at low speed; however, sufficient coolant is available at all points on the PHOEBUS operating map for thrust loads up to 20,000 lb.

Coolant for the turbine side roller bearing is taken from leakage through the labyrinths at the discharge end of the rotor. After passing through the bearing, the coolant discharges to the turbine. Coolant flow is affected by turbine pressures; however, a pressure differential and sufficient flow occurs at all operating conditions because turbine drive fluid is bled from pump discharge.

Coolant delivered to all bearings is in excess of that required, based upon M-1 bearing test results.

f. Coolant Flow Requirement Analysis

(1) Thrust Bearings

The mathematical model used in this analysis considers the heat generated within the bearing from ball spin on the inner race, the ball retainer friction, and the ball race hysteresis. This mode was derived theoretically and correlated with the M-1 bearing test data.

The liquid hydrogen cooling requirements were calculated upon the basis of a 100% "cooling effectiveness" because the highly-turbulent flow within the bearing promotes very high heat transfer. This approach for establishing coolant flow requirements has been successfully used in the M-1 Program (see Figure 45).

(2) Roller Bearings

The requirements for the heavier-loaded turbine end bearing were considered at the overspeed conditions of 14,500 rpm. The mathematical model used in this analysis considers the heat generated within the bearing attributable to cage friction and as the result of hysteresis. The same approach and conditions were used for the heat generation and flow requirements as were used for the thrust bearing.

The total heat generated in the bearing is shown on Figure 46 and the coolant flow requirements are shown on Figure 47.

5. Rotor Axial Thrust Control

The thrust balance system for the PHOEBUS application, schematically shown as Figure 48, utilizes a balance piston for maintaining the rotor net thrust within the load capability of the thrust bearings.

The pump side of the piston receives fluid at pump rotor discharge pressure. As originally designed, this fluid flowed through a variable axial gap and around the balance piston through a fixed radial clearance to the turbine side. The radial clearance varies somewhat with speed and pressure; however, this is a secondary effect. Fluid from the balance piston is returned to the transition stage of the pump by four 1-in. diameter tubes equipped with orifices for flow control and measurement.

In the M-1 application, at a fixed operating speed, orificing to obtain the desired thrust bearing load at the nominal operating point is a satisfactory method of thrust control. Because of the relatively large axial control gap required (0.030-in. nominal) on the balance piston to eliminate the possibility of rub, compensation for changes in thrust is not great.

For the PHOEBUS application, where long duration operation at all speeds up to 11,500 rpm is required, use of fixed orifices in the balance piston fluid return lines would result in thrust reversal at low speed and excessive thrust bearing load at high speed. To obtain the required two-hour thrust bearing life, the maximum thrust load will be limited to 20,000 lb toward the turbine, and thrust reversal will be permitted only at very low speed. This is accomplished by placing pneumatically-operated (open or closed) valves in three of the four return lines. The balance piston flow rate and hence, the pressure acting on the piston is controlled by the opening or closing of these valves as required to maintain the bearing load below 20,000 lb. Operation of the control system is illustrated by Figuer 49, which indicates how the valves are sequenced or positioned for operation at any point on the operating map. The thrust values shown are based upon 30 psia turbine exhaust pressure at nominal operation. At low speed, all valves are open and the flow coefficient is $C_{DE} = 0.43$. As speed is increased, the bearing load approaches 20,000 lb at approximately 7500 rpm. At this point, one valve is closed

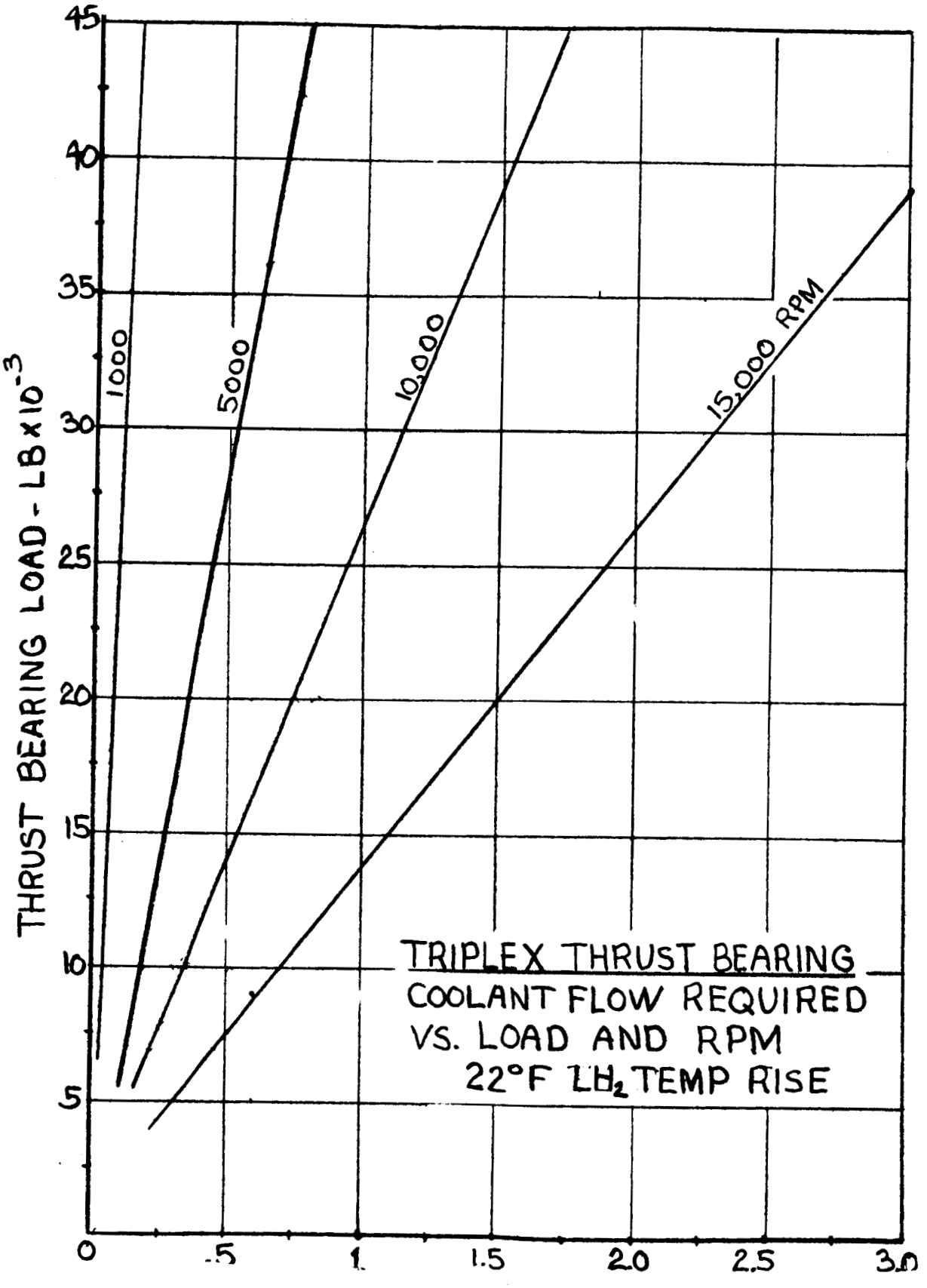

Figure 45

PHOEBUS Thrust Bearing Coolant Flow Requirements

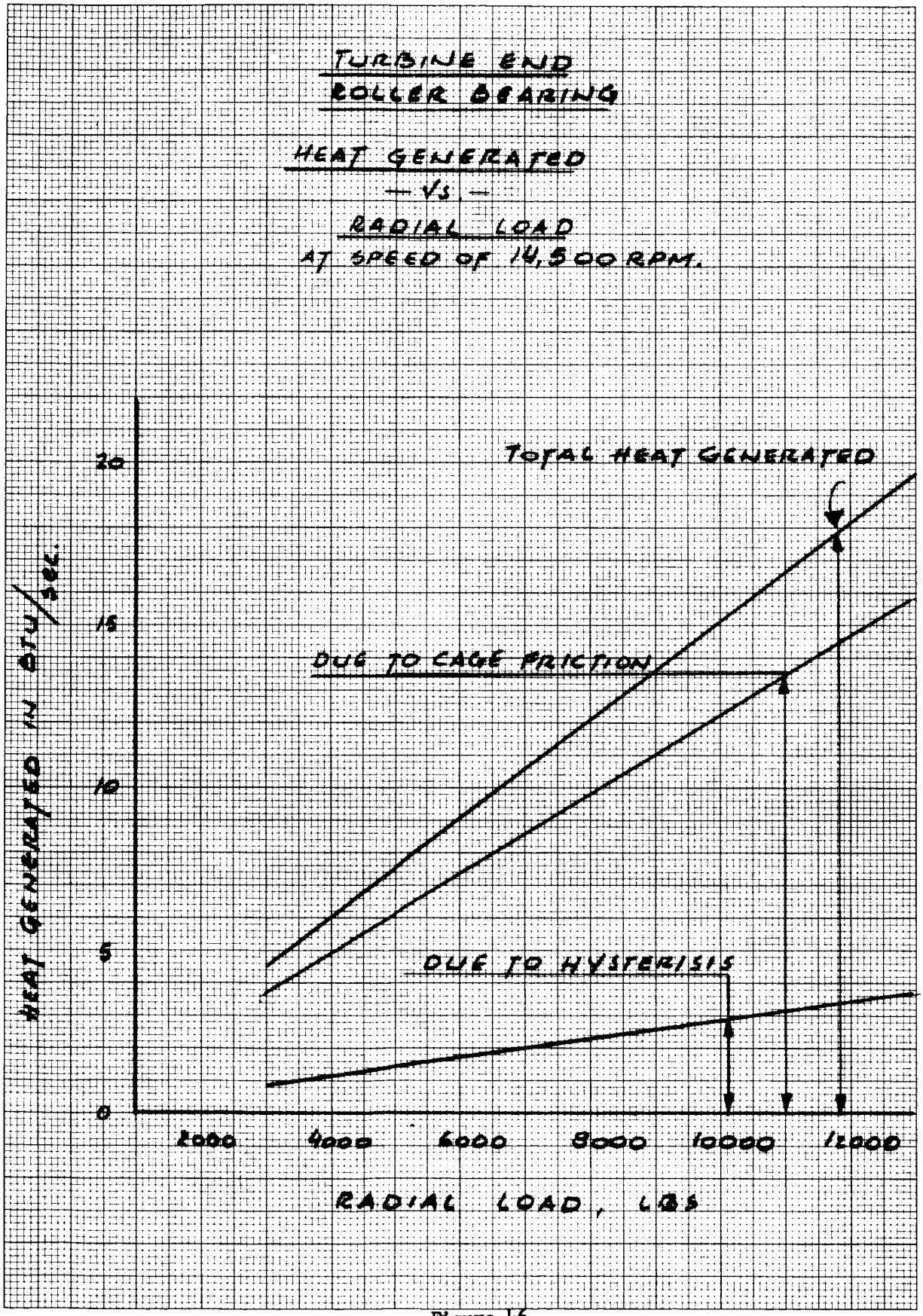
TURBINE END
ROLLER BEARING
HEAT GENERATED
— VS. —
RADIAL LOAD
AT SPEED OF 14,500 RPM.
TOTAL HEAT GENERATED
DUE TO CAGE FRICTION
DUE TO HYSTERISIS
HEAT GENERATED IN BTU/SEC.
20
15
10
5
0
2000
4000
6000
8000
10000
12000
RADIAL LOAD, LBS

Figure 46

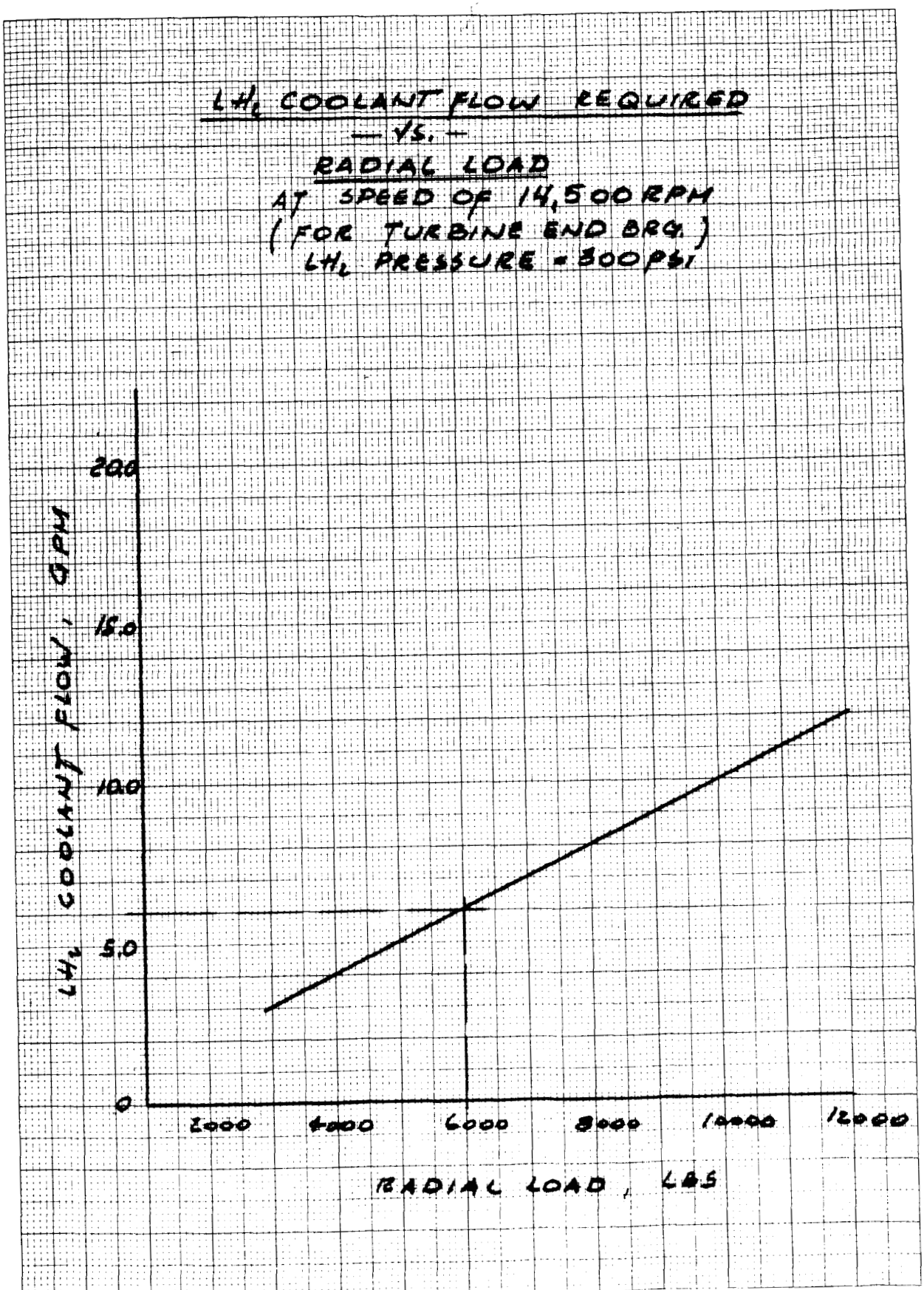
LH2 COOLANT FLOW REQUIRED
— VS. —
RADIAL LOAD
AT SPEED OF 14,500 RPM
(FOR TURBINE END BRG.)
LH2 PRESSURE = 300 PSI
LH2 COOLANT FLOW, GPM
20.0
15.0
10.0
5.0
0
2000
4000
6000
8000
10000
12000
RADIAL LOAD, LBS

Figure 47

THRUST BALANCE SYSTEM SCHEMATICS

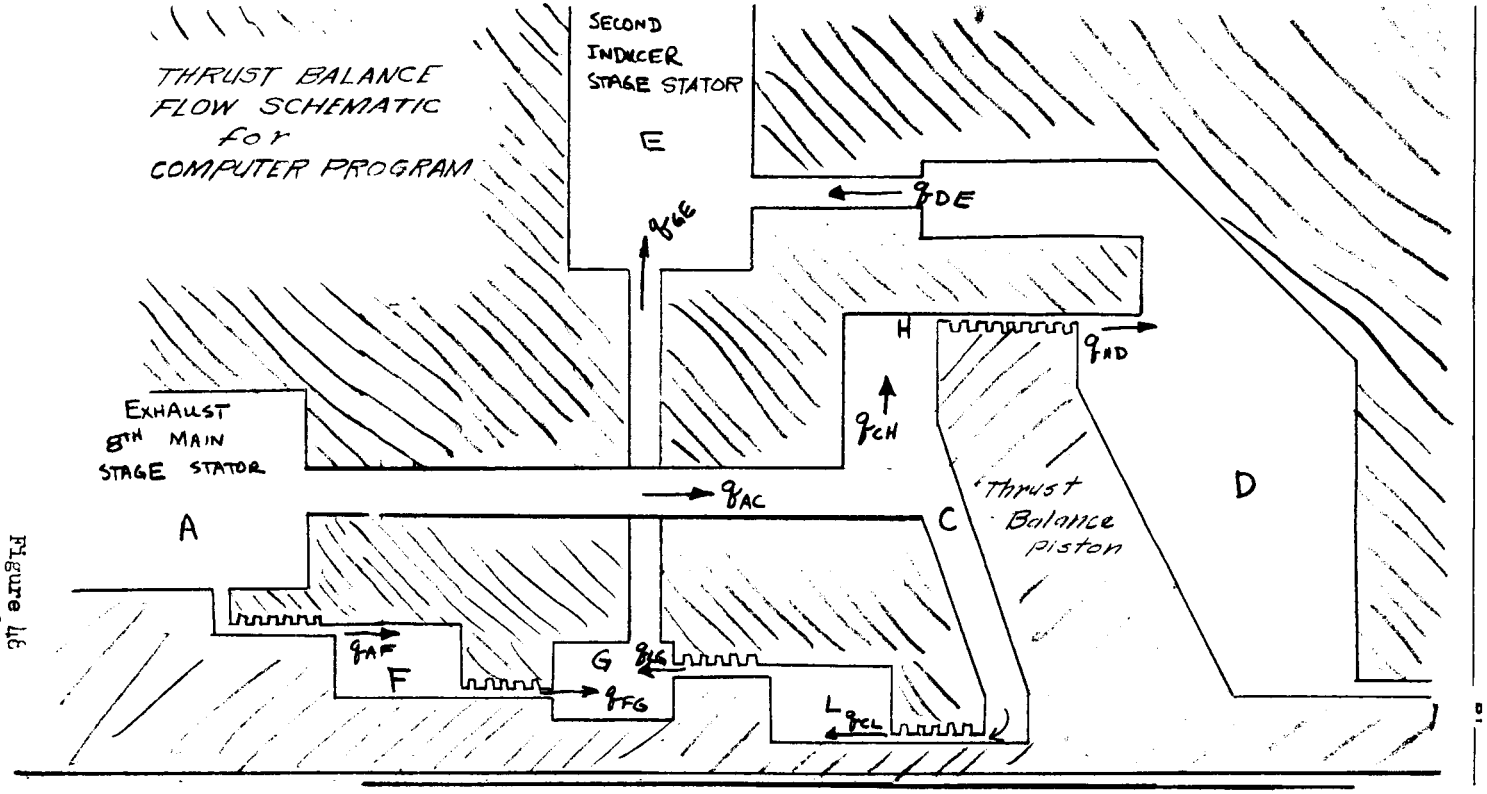

Figure 16
Page 85

THRUST BALANCE
MECHANICAL SCHEMATIC

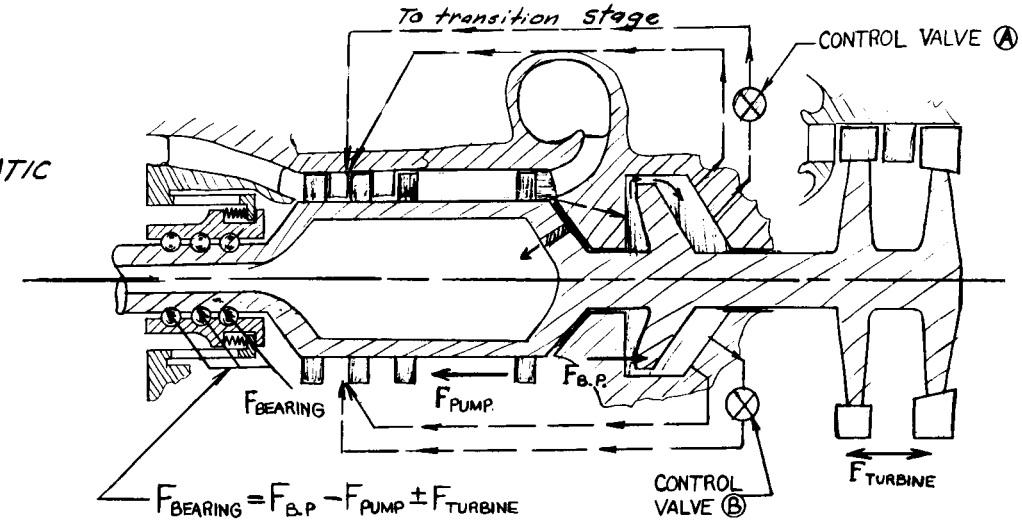

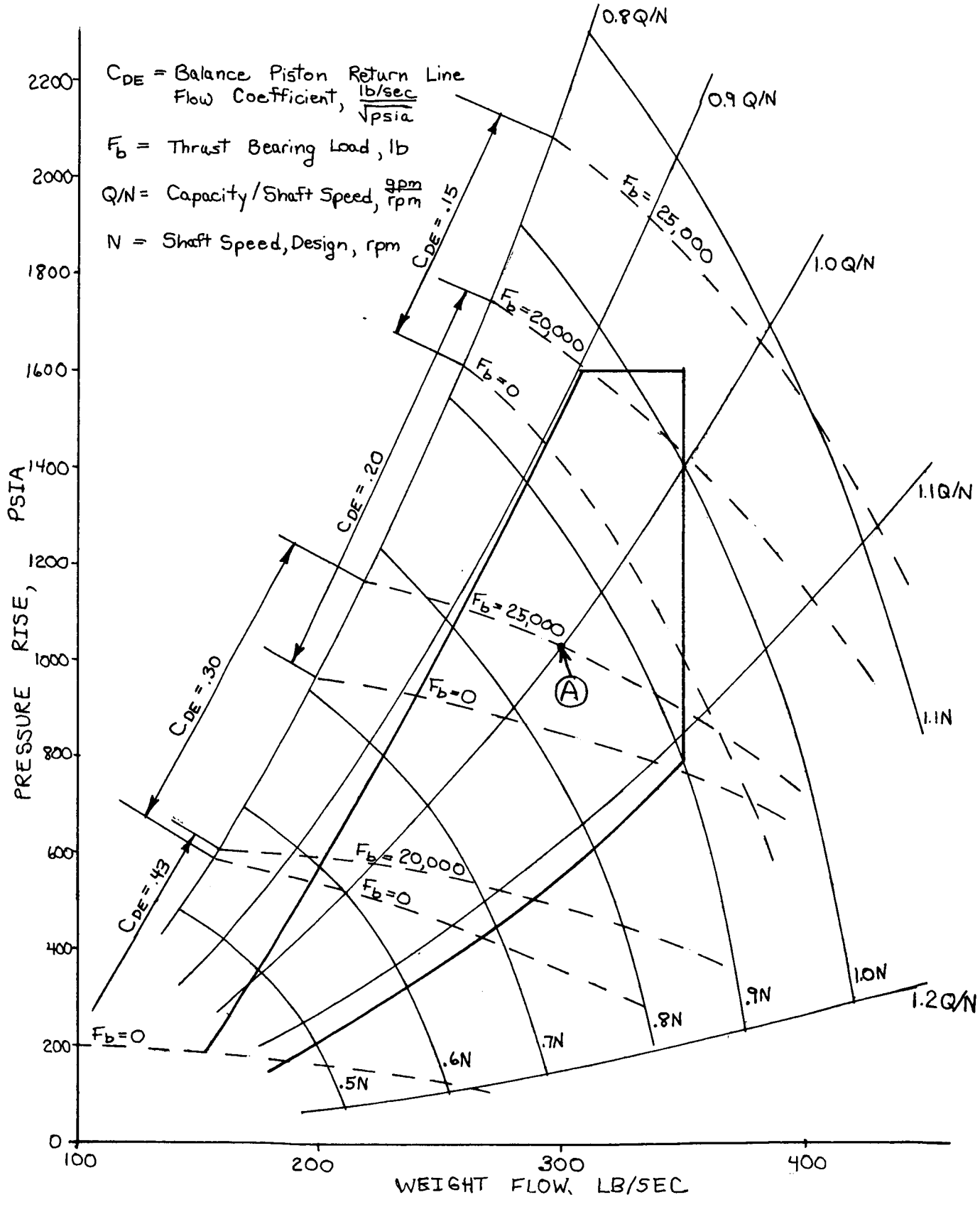

Figure 49
Page 86

and the thrust load drops to approximately 5000 lb. A further speed increase to 10,000 rpm again raises the load to 20,000 lb and the second valve is closed. The third valve is closed at approximately 11,000 rpm. The final orificing and speeds at which each valve is sequenced must be determined during development testing. However, Figure 49 does illustrate the practicality of this method for thrust control and is the result of extensive system analysis utilizing computer programs developed for the M-1 program. Automatic sequencing of the thrust control valves by the speed transducer is planned with direct readout of bearing load and manual control of the valves serving as a backup. Use of a signal from the pump discharge pressure transducer either along or in combination with a speed signal, may prove more reliable for automatic sequencing of the valves at low speed. Analysis of M-1 turbopump test data will permit an early selection of the best method for control. Interlocking of the speed and thrust transducers with the turbine control valve to provide additional safety against overloading the bearings can be easily accomplished. The 20,000 lb maximum bearing load permitted is far below the demonstrated short-term load capability of the bearings and accidentally exceeding this value by a factor of 2 or 3 will not result in failure but could shorten bearing life.

During operation at very low speeds, the balance piston is essentially ineffective and pump thrust may exceed turbine thrust resulting in bearing load reversal. The speed at which reversal occurs is difficult to predict at low speed but will be determined by test and "red-lined" as a speed to avoid for continuous operation because unloading and skidding of the balls could result.

Nitrogen gas will be used for turbine drive during some development tests. This results in much higher turbine thrust than that produced by hydrogen gas at the same turbopump speed and power. Because tests with gaseous nitrogen will be limited to approximately 6000 rpm, the thrust bearing load will not exceed 20,000 lb as shown by Figure 50. This is accomplished by the closing of all thrust control valves thereby reducing balance piston thrust.

6. Thrust Bearing Flexible Support

The pump rotor is supported radially by two roller bearings and axially by a triple set of ball thrust bearings. The thrust bearings and pump-end roller bearing are mounted in the pump-end power transmission assembly as shown on Figure 51. The thrust bearings, each provided with a coolant jet ring, are rigidly clamped in an inner bearing housing. The complete assembly is attached to the outer housing by a flexible support, which is shown disassembled in Figure 52. The support consists of 72 longitudinal bars which encircle the inner bearing housing. These bars provide relatively rigid axial restraint ($K_A = 17.4 \times 10^6$ lb/in.) for the thrust bearings and are capable of supporting a thrust load in either direction in excess of 200,000 lb. An important function of these bars is to provide the thrust bearing housing with a low radial spring rate ($K_R = 5.2 \times 10^4$ lb/in.). This low radial spring rate is desirable for the following reasons:

The thrust bearings are subjected to axial load only which ensures maximum thrust capacity and life.

The possibility of unloading and skidding of the roller bearing is minimized because it must carry all radial load.

Prediction of critical speed is more exact because the points of rotor radial support are clearly defined.

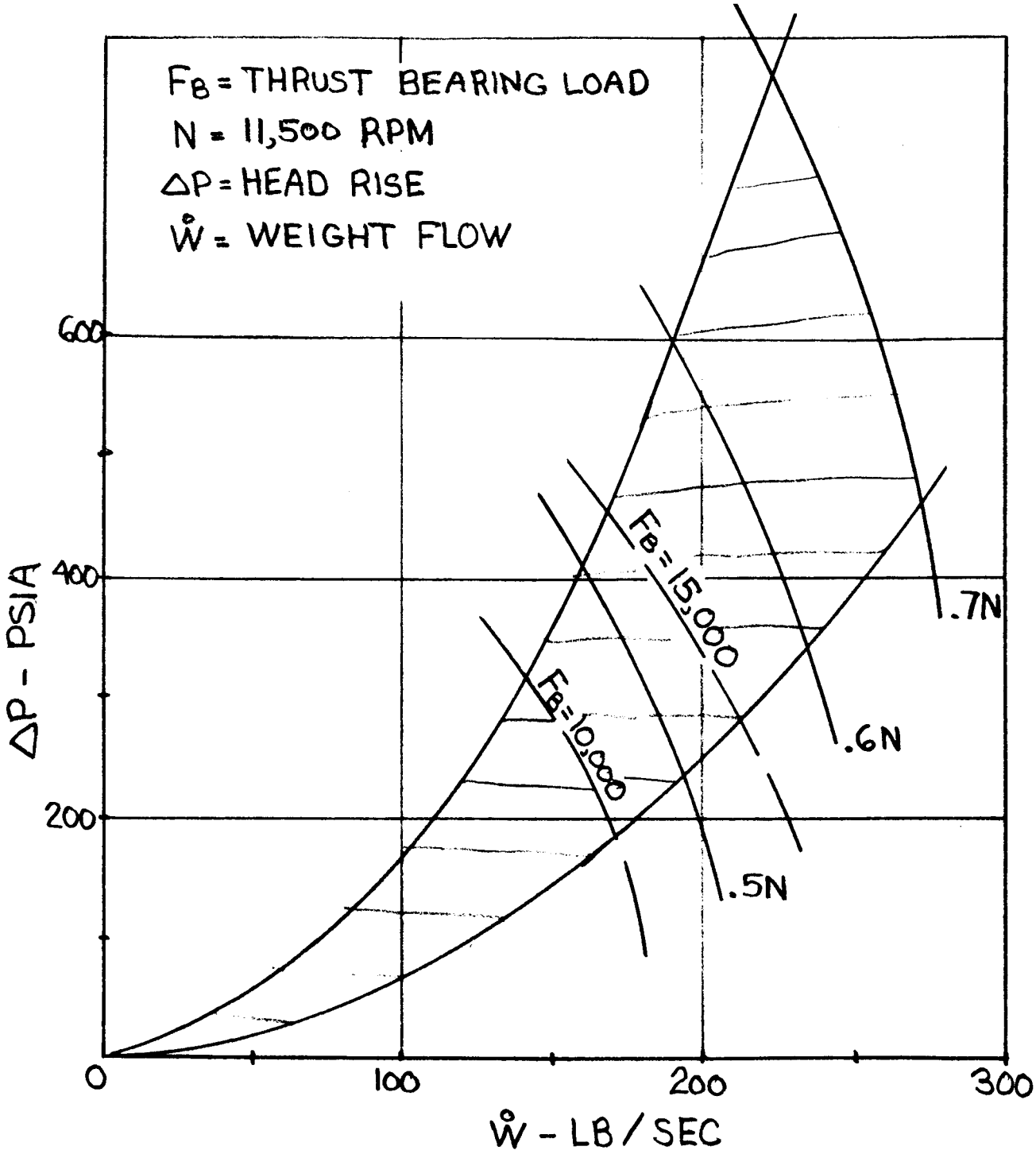

Figure 50

THRUST BEARING LOAD WITH GN_2 TURBINE DRIVE

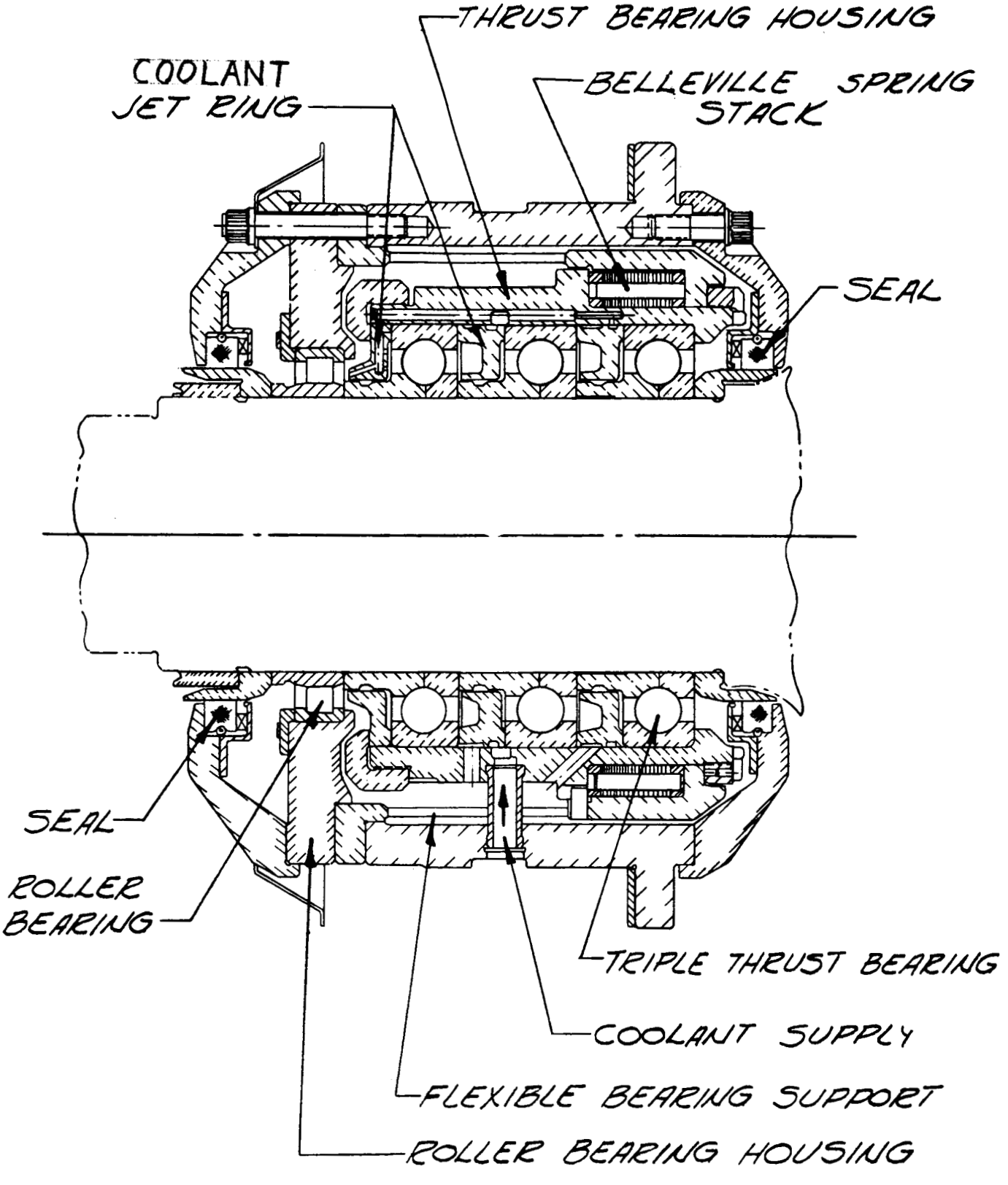

Figure 51

Pump End Power Transmission Assembly

Flexible Support Components

Figure 52

In addition to the above advantages, the longitudinal bars are equipped with strain gages and used as a load cell for measurement of thrust bearing load and the coefficient of friction. This instrumentation as well as the bearing temperature and acceleration transducers can be seen in Figure 52.

Rotor thrust is transmitted from the thrust bearing housing to the flexible support through 16 stacks of Belleville washer springs. These stacks each containing 40 washers are shown in Figure 51 in the assembly at the right. The M-1 turbopump uses 32 stacks of Belleville washers rather than 16 because of higher nominal thrust loads. Because of life requirements, PHOEBUS thrust bearing loads will be limited to 20,000 lb. Use of 16 stacks in PHOEBUS improves axial stability and balance piston effectiveness. The non-linear position of the spring deflection curve is eliminated by preloading the assembly to 2500 lb and total spring deflection is limited to 0.033-in. by a mechanical stop. The primary purpose of the springs is to reduce the rotor axial spring rate and thus, obtain increased feedback (deflection) for balance piston thrust compensation. In addition, dry friction in the washer stacks provides damping for improved rotor system axial stability. The springs offer little restraint to rotation of the thrust bearing assembly about any axis perpendicular to the rotor center line; hence, application of moment loads to the thrust bearings as a result of housing or rotor distortion and misalignment is not possible. This feature minimizes the possibility of bearing damage during chilldown and permits the bearings to maintain alignment with the shaft under all conditions.

Rotor axial deflection as a function of applied bearing load is shown by Figure 53. The springs provide a relatively low spring rate of 6.8×10^5 lb/in. over the expected load range of zero to 27,500 lb. At loads above or below this range, only the bearings and flexible bars deflect and the spring rate is 7.1×10^6, which limits total rotor movement. Rotor deflection in relationship to bearing load during decreasing load differs considerably from that for increasing load. This results from the dissipation of energy (damping) in the spring which makes the system somewhat insensitive to thrust changes.

7. Rotor Dynamics

a. Axial Stability

Rotor axial thrust is transmitted to the pump housing through the triple set of thrust bearings, the 72 longitudinal bars, and the Belleville washer stacks. These three components are in series and each as a spring. They produce the load versus deflection curve shown on Figure 53. Over the expected load range of zero to 20,000 lb, the deflection curve is essentially linear for increasing load. During decreasing load, deflection is non-linear with respect to load because of non-linear damping in the Belleville washers. The washer stacks are assembled in a manner which provides high coulomb friction and 50% dissipation of energy per cycle. The equivalent viscous damping attributable to this dry friction is approximately 500 lb-sec/in., based upon static tests of the system for increasing and decreasing loads. In addition to the damping in the washers, the balance piston provides the system with an additional 500 lb-sec/in. viscous damping which gives a total damping constant of C = 1000 lb-sec/in. over the expected thrust load range.

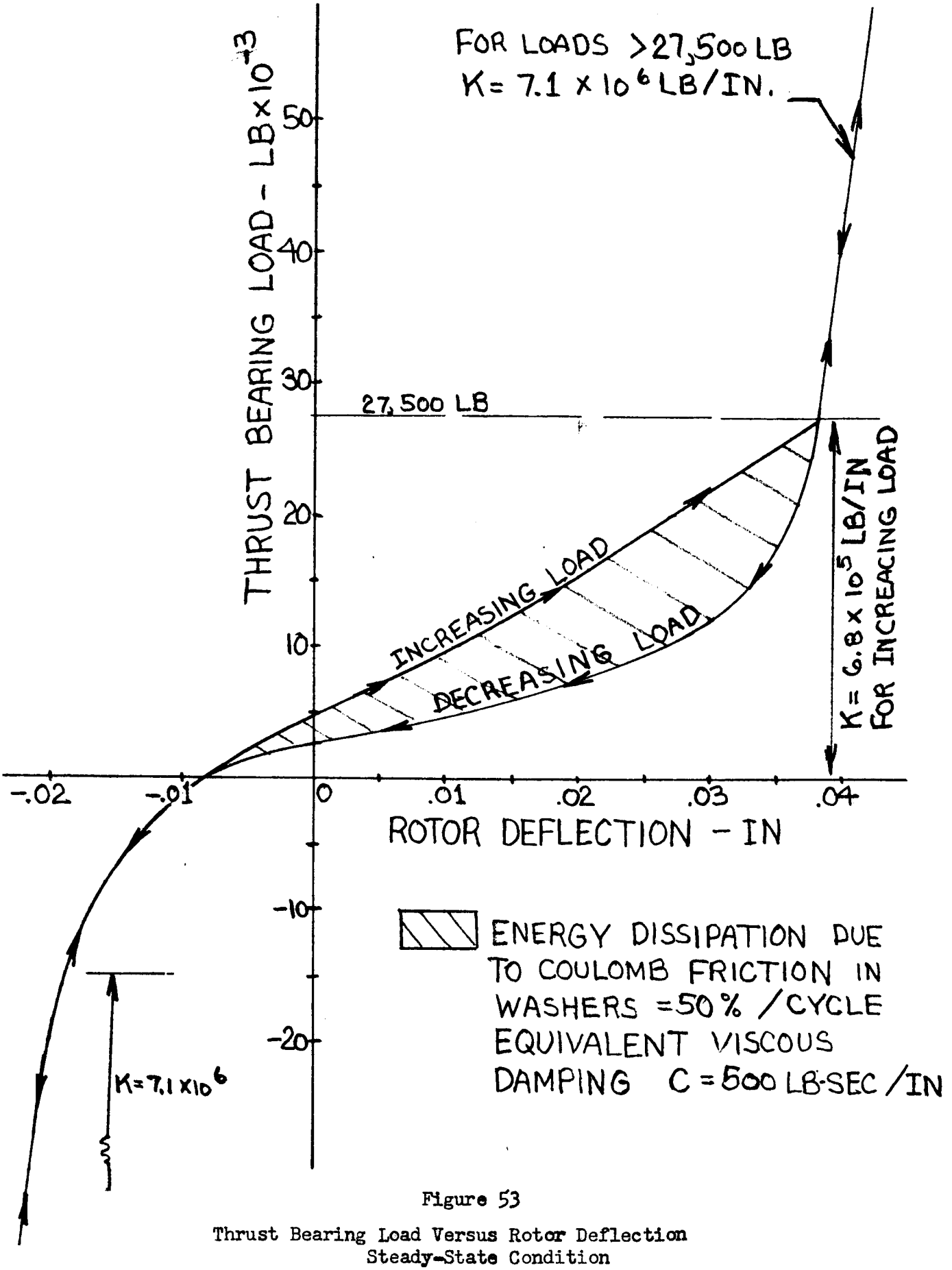

Figure 53

Thrust Bearing Load Versus Rotor Deflection
Steady-State Condition

The response of the system to a suddenly-applied step increase in thrust has been analyzed using both the equivalent viscous damping constant and by the use of a computer program which considers the non-linear spring rates and damping of the system. Both methods of analysis yielded the same response characteristic. The response of the system to a step change in thrust while operating at a steady state load in the 0 to 27,500 lb range is shown by Figure 54. The system is extremely stable and the transient oscillation produced damps out in approximately one cycle (0.0128 sec). Because of the non-linear nature of the damping and the Belleville washer spring rate for decreasing loads, the bearing load and rotor deflection are slightly out of phase and the amplification of load is greater than that of deflection. A step change in thrust of 1000 lb would result in a transient increase in bearing load of approximately 1350 lb (amplification factor of 1.35). The corresponding amplification of the static rotor deflection would be 1.2 Note that for small damping, amplification of load and deflection would approach 2 and oscillation of the system would continue for many cycles.

The damped natural frequency of axial vibration of the PHOEBUS rotor system is 78 cps, 4680 rpm. It is lower than M-1 because only 16 spring stacks are used instead of the 32 used in M-1. Stable operation of the PHOEBUS turbopump at or near this frequency is required. Response of the system to a force varying sinusoidally at the speed of rotation is shown by Figure 55. As the speed increases from 0 to 4680 rpm, the amplification factor increases.

b. Torsional Vibration

A torsional vibration analysis of the PHOEBUS turbopump rotor was completed. The lowest torsional critical speed occurs at approximately 20,000 rpm, well above the PHOEBUS overspeed point of 14,500 rpm. This lowest natural frequency occurs with the mode of vibration where the pump and turbine rotors rotate in opposite directions and with the turbine shaft acting as the torsional spring. Torsional vibration imposes no operational limitations.

c. Critical Speed

During development of the M-1 fuel turbopump, extensive analysis of critical speed and refinement of computer programs for this purpose were accomplished. With the exception of changes in pump blade height and modification of the inducer, the PHOEBUS turbopump is identical to the M-1 as regards critical speed. Analysis of the PHOEBUS turbopump, considering the above modifications, has been completed. For this analysis, the rotor and housing were considered as two beams connected by non-linear springs representing the roller bearings. The beams representing the rotor and housing were divided in 37 and 34 stations, respectively, with the mass of each station concentrated at the center of the station. Conical whirl of the rotor, resulting from eccentricity at -420°F was considered by placing forces at the inducer and turbine rotors which vary with shaft speed. The non-linear spring rates of the bearings were expressed as a function of load P as follows:

$$K_{pump} = 1.35\ (10)^6$$

$$K_{turbine} = 1.09\ (10)^6\ p\ 0.224$$

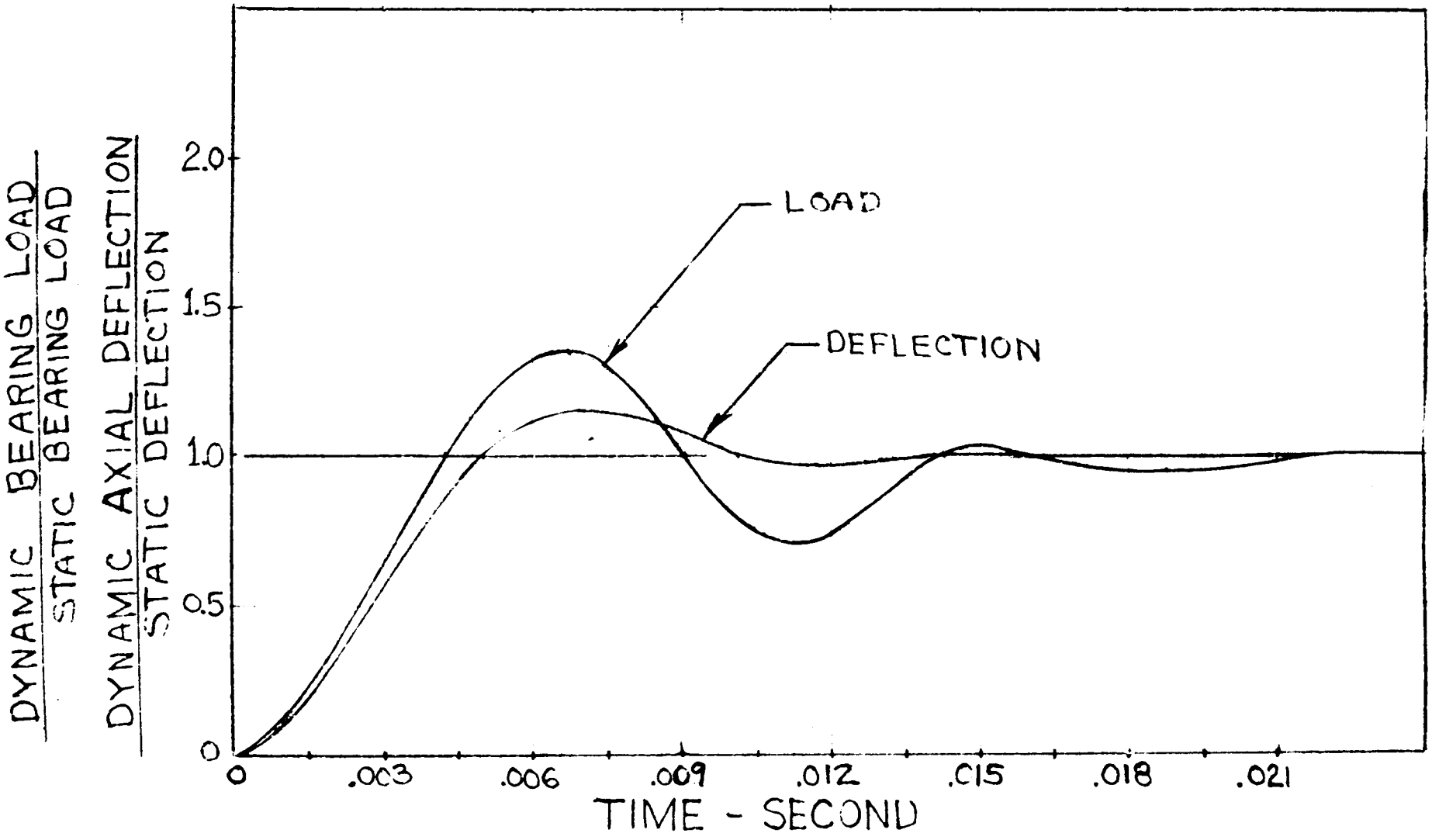

Figure 54

ROTOR AXIAL RESPONSE TO A STEP CHANGE IN AXIAL THRUST

ω = SHAFT SPEED - CPS

ω_N = SYSTEM DAMPED NATURAL FREQUENCY = 78 CPS

X = ROTOR AXIAL DEFLECTION

X_s = ROTOR STATIC AXIAL DEFLECTION DUE TO LOAD F

F = AMPLITUDE OF FORCING FUNCTION, $F \sin \omega t$

C = DAMPING CONSTANT, 1000 LB-SEC/IN

C_c = CRITICAL DAMPING

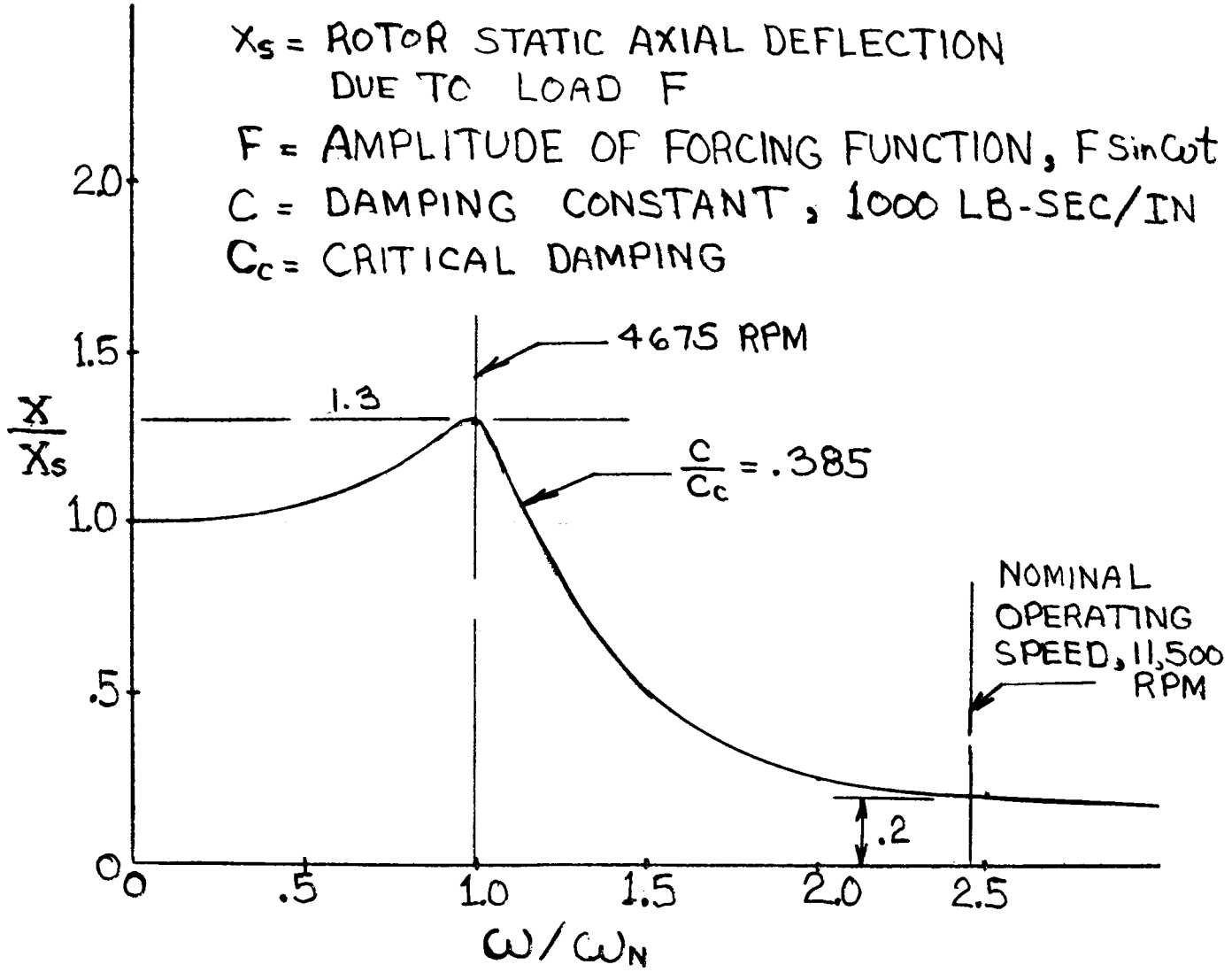

Figure 55
Rotor Response To Axial Vibration

The results of the analysis are presented in Figure 56 which shows the pump and turbine end roller bearing reactions as a function of shaft speed and the first apparent critical speed at 17,500 rpm. The bearing reactions at the overspeed condition of 14,500 rpm are 4,400 lb and 10,000 lb, both slightly below the bearing design loads. At the nominal operating speed of 11,500 rpm, loads are approximately 3,200 lb and, 600 lb for the turbine and pump bearings, respectively. These loads do not include radial loads caused by hydraulic unbalance in the pump and turbine; however, these should be quite small because both units are axial flow. No critical speed problem is envisioned even for continued operation at an overspeed condition of 14,500 rpm. Based upon M-1 roller bearing testing, overspeeding for short periods, even above 14,500 rpm, should not distress the more heavily-loaded turbine bearing.

An additional critical speed analysis considering the effects of the proposed PHOEBUS mounting stand was conducted. Stiffness of the mounting structure in each direction is represented by springs. It was found that the frame is sufficiently flexible such that the coupling of the rigid body and rotor dynamics is important only in the local vicinity of the rigid body natural frequencies of 47 and 64 cps. The power level is quite low at 2820 rpm and 3850 rpm, which correspond to these frequencies. Because the turbopump assembly will normally only be passing through these speeds to some higher speeds, no significant problem is expected. Should continued operation at these frequencies be required, introduction of damping or vibration isolators can easily be accomplished.

G. SPECIAL FEATURES

1. Torque Measuring Device

The M-1 turbopump is equipped with a unique device to measure shaft torque. A Permanickel Alloy 300 sleeve is keyed at both ends to the shaft between the turbine and pump rotor. A stationary coil is mounted concentric with the sleeve. Strain in the sleeve is proportional to the torque being transmitted. Because of the magnostrictive properties of Permanickel, the inductance of the coil varies with the strain of the sleeve and is used as a measure of shaft torque. Laboratory tests have shown that the torque versus inductance curves are linear, except for high and low strains. The sleeve is preloaded to eliminate the non-linear portion of the curve at low torque. This torque measuring concept has not as yet been demonstrated by test with the M-1 fuel turbopump. Maximum shaft torque for PHOEBUS is approximately one-half that for which the device was designed, thus its suitability for torque measurement in the PHOEBUS application with its lower speed and power is questionable although if it proves successful for M-1, it will be supplied in the PHOEBUS turbopump.

An alternative torque measurement system for PHOEBUS has been designed and is recommended for use if accurate measurement of torque is important with the PHOEBUS facility pump, or if unexpected problems arise with the M-1 device. This system utilizes a commercially-available slip-ring assembly produced by Lelow Associates, Inc. The assembly mounts at the end of the PHOEBUS turbine shaft inside of the rotor locking device. Electrical leads are carried through the hollow turbine shaft to an electrical resistance strain gage bridge located on the turbine shaft adjacent to the spline. Four gages (two tension and two compression) are oriented at 45-degrees to the shaft centerline and provide high signal output with

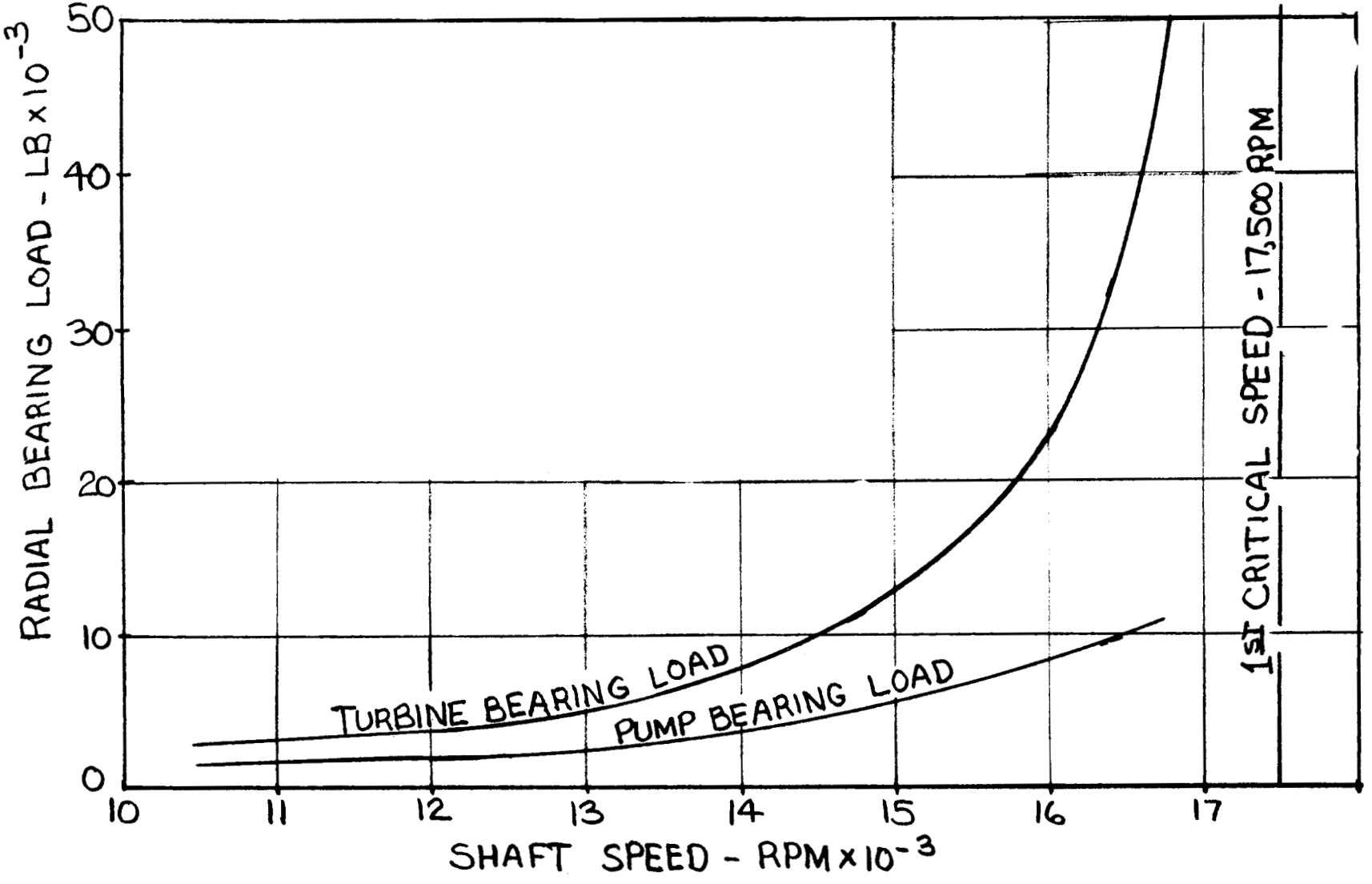

RADIAL BEARING LOADS AND CRITICAL SPEED

temperature compensation. Sensitivity is such that accurate measurement of torque is possible even at low shaft horsepower. Installation of this alternative torque measuring system requires only minor rework of the turbine shaft (i.e., drilling of holes for electrical leads). The turbine exhaust housing and rotor lock device have been designed to permit installation of the slip ring assembly.

The alternative torque measuring system offers the additional advantage of providing electrical circuits from the rotor which can also be used for transmitting signals other than torque. Measurement of rotor and stator vane strain, vane vibration, and temperatures can be easily accomplished by routing electrical leads from the slip-ring assembly, through the hollow rotor to the desired locations. This capability would be most useful during development testing. The torque measurement device requires only four channels and slip-ring units with up to 22 channels are available.

2. Rotor Lock Device

During the chilldown and purge cycle, it is advantageous to either control pump rotation or to stop it altogether. Inasmuch as the chill and purge cycles could be of long duration, it appears advantageous to hold the rotor stationary until it is desirable to allow rotation.

The locking device is located downstream from the second stage turbine wheel. Other locations within the pump were evaluated, but they were discarded because of complexity and servicing difficulty. In the selected location, the complete assembly is easily accessible without disturbing the turbo-pump assembly or test setup.

The parameters governing the locking of the rotor are:

a. Positive mechanical lock in either direction.

b. Positive lock engagement in any rotational position in which the rotor stops.

c. Mechanical integrity to resist 210 ft-lb of torque.

d. Positive indication as to engagement and disengagement of the locking device.

The design of the rotor locking device is shown in Figure 57. The hub of the second stage turbine wheel is used as the anchoring point for the torque-resisting adapter ring.

The use of the second stage wheel hub gives a positive attachment point with a minimum amount of rework to the existing configuration. This rework consists of adding four equally-spaced key slots, matching four slots in an adapter ring that fits around the hub and provides the means by which the locking device is attached to the rotor assembly. To provide for engagement and disengagement between the pump rotor and the locking device assembly, a bevel gear is bolted to the adapter ring on the turbine wheel hub. These two parts with their keys become a permanent part of the second stage turbine wheel.

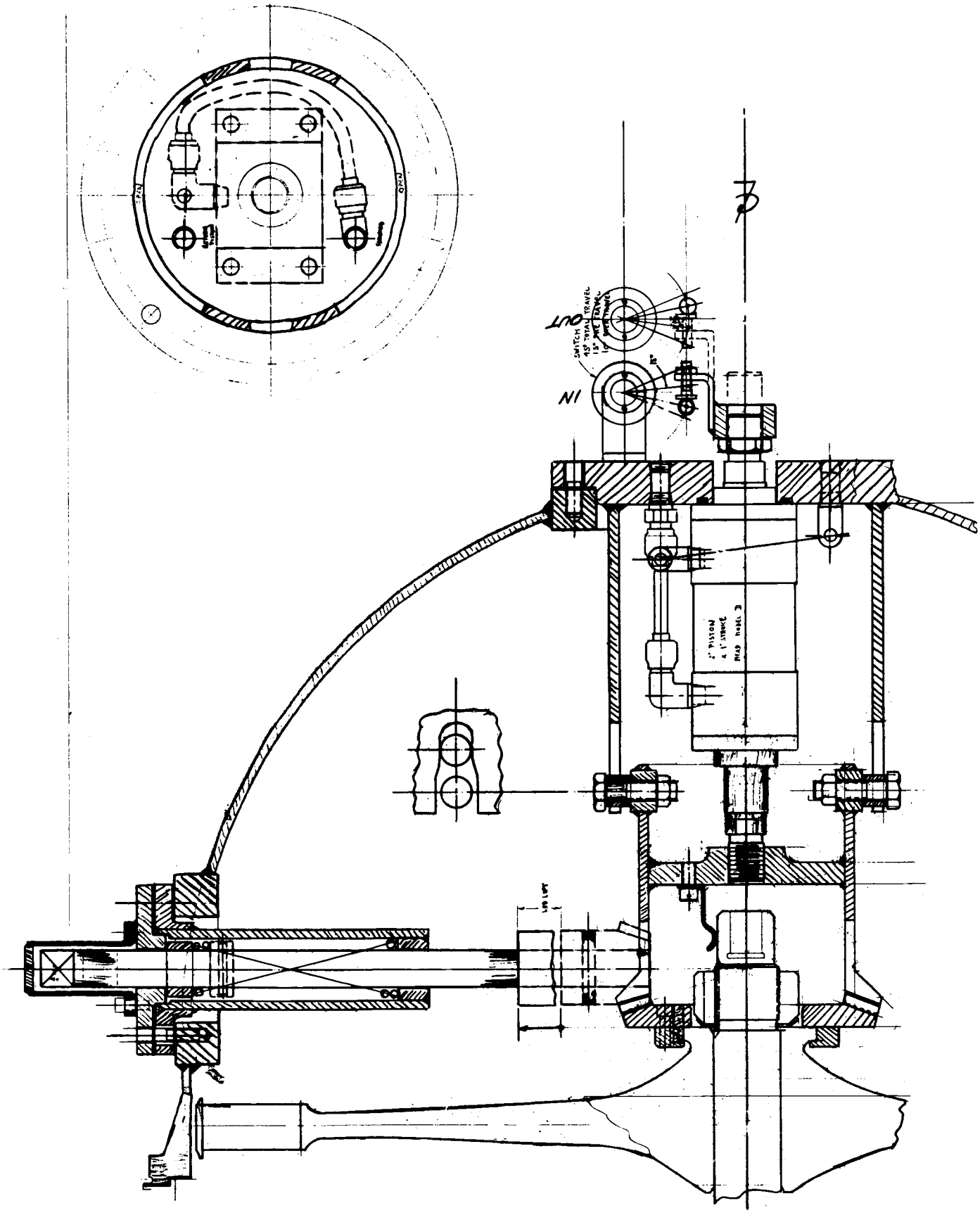

Figure 57
Rotor Locking Device

The rotor locking device assembly consists of a pneumatic piston carrying a reverse bevel gear. This gear moves axially in a torque resisting tube (bolted to the turbine exhaust manifold) and engages the mating gear attached to the turbine wheel. The complete unit can be assembled separately and installed in the pump as a kit.

The rotor is locked by engaging the two bevel gears. The actuating piston is cushioned on both ends to allow smooth engagement of the gear teeth and gentle actuation of the position micro switches. The gear driven by the piston has three 1-in. diameter bosses welded to the outside diameter of the gear tube. These bosses extend through slots in the torque-resisting tube, which is mounted to the pad on the bottom of the turbine exhaust manifold. As torque is applied from the turbopump rotor assembly, it is transmitted through the gear teeth to the three bosses which are engaged in slots in the torque resisting tube. The tube then transmits the torque into the turbine exhaust manifold.

The position of the locking gear is indicated by a set of limit switches. They are actuated by an adjustable arm mounted on the piston rod. For reliable position indication, there are two switches to signal the locked position and two switches to signal the unlocked position.

The piston and switches could be installed inside the turbine exhaust manifold, however, it appears more advantageous to mount them externally, which simplifies the plumbing and wiring requirements. Also, it allows space between the end of the turbopump rotor shaft and the piston rod, into which a slip-ring-type torque measuring device could be installed should it become necessary to replace the existing M-1 torquemeter for low speed operation.

3. Rotor Breakaway and Running Torque Measurement

Although it is not a specific requirement to provide a means for determining the pump breakaway torque, it is recommended that this be included in the modifications.

The rotor lock device provides a simple inexpensive means for measuring pump breakaway torque (see Figure 57).

The bevel gear, which is attached to the turbine wheel and used for the rotor lock, is the driven member. When the rotor lock piston disengages, a bevel pinion gear can be pushed into position and turned with a torque wrench to determine the turbopump assembly breadaway and running torque.

The assembly consists of a rod extending through the side of the exhaust manifold. This rod has a bevel gear pinion on the inner end and a socket for a torque wrench on the outer end. It is supported by two bushings mounted in a housing bolted to a pad on the outside of the exhaust manifold. To ensure the pinion is clear of the rotor lock, a spring is provided in the housing around the shaft so that as pressure is released, the pinion and rod pull out of the way of the rotor lock. A sealed cover is provided for the torqued end of the rod when the turbopump assembly is in operation.

4. Rotor Position Metering System

For measuring the axial and radial displacement of the rotor, four "Bentley" distance detector probes are used. Two probes are mounted 90 degrees apart in the guide vane housing facing the inducer hub for axial movement detection, and the other two probes are also placed 90 degrees apart and held in the sixth stage stator blade retainer ring to detect radial displacement (see Figure 58).

The distance detector consists of a control unit and a proximity sensor head. This head is mounted at the point where the measurement is to be made and connected by a shielded bi-axial cable through leak-proof connectors on the pump housing to the control unit.

The sensor element is a pancake-wound coil, excited from an outside source, and produces an eddy current field. Any conductive surface (in this case, the aluminum inducer or Inconel blading) placed near the coil will load it in proportion to the gap between the coil and conductive surface producing a change in the voltage output of the control unit.

The electrical circuit is essentially a tuned collector-emitter configuration with necessary rectifying and amplification stages to provide a desired output impedance.

To operate within the linear portion of the EMF slope, establishment of a scale factor will be necessary by calibration at operating temperatures. To accomplish this, a 0.003/0.005-in. deep radial slot is milled into the inducer back face and one of the sixth stage rotor blades is made shorter by 0.003/0.005-in. This known difference in the gap will result in deflections on the instrumentation record at different distances from which the slope and scale factor of the calibration curve is obtained.

5. Turbopump Response to 4 cps Speed Change Command

The energy required to accelerate the turbopump rotating assembly is relatively small as compared with the energy required to accelerate the fluids in pump suction and discharge lines as well as to compress and accelerate the fluids in the turbine inlet and exhaust lines. The required response is comparable to an average speed ramp of approximately 10,000 rpm/sec^2. A detailed study of the dynamic response of the turbopump operating in the NRDS system is beyond the scope of this effort; however, alculations were performed to ensure that the mass moment of inertia of the rotor does have a relatively small effect upon the dynamic response of the reactor feed system.

The following are ratios of the energy required to accelerate and compress the fluids in one foot lengths of the pump and turbine lines, to the energy required to overcome the mass inertia of the pump rotating assembly:

PIPE	ASSUMED PIPE INSIDE DIAMETER (in.)	RATIO (ENERGY TO ACCELERATE AND COMPRESS FLUID IN ONE FOOT OF LINE TO ENERGY TO ACCELERATE ROTOR)
Pump Suction	10	1.98
Pump Discharge	8	2.89
Turbine Inlet	8	23.4
Turbine Discharge	15	18.3

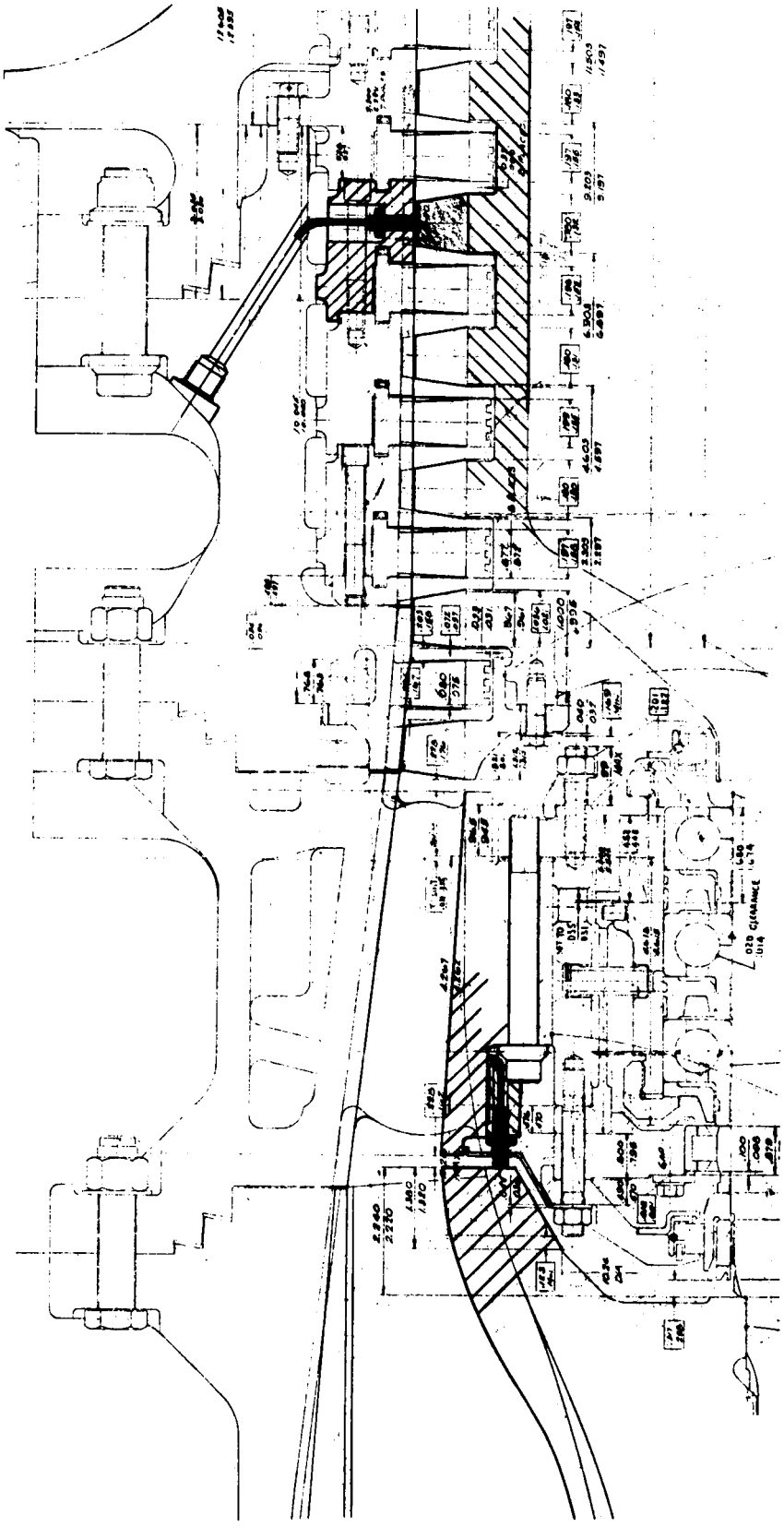

Figure 58
Rotor Position Detector

This tabulation indicates that the dynamic response of the system is predominately a function of the line lengths and the mass inertia of the pump rotor has only a minor influence. The turbine can produce more than sufficient torque to produce a 10,000 rpm/sec^2 average speed ramp at 11,500 rpm.

6. Control and Safety Requirements

a. Normal Operation

(1) Pre-Test Bleed-In and Chilldown

Currently, temperature and pressure measurements are to be used to determine the extent to which the M-1 fuel turbopump is chilled down. Particular attention is given to measurements in the regions of the bearings to ensure that the pressures are close to the vapor pressure of hydrogen. These measurements, which will be demonstrated with the M-1, will also be used for the PHOEBUS turbopump to determine the extent of chilldown.

(2) Turbopump Acceleration and Deceleration

No limits for turbopump shaft acceleration or deceleration have been specified for the M-1 fuel turbopump. It is anticipated that in an M-1 engine nominal start transient, a maximum instantaneous fuel turbopump acceleration of 12,500 rpm per second will be experienced. A 4 cps speed variation of ± 5% at nominal speed, which is a desired value, corresponds to a maximum instantaneous acceleration or deceleration of 14,500 rpm/sec if a sinusoidal speed variation is assumed. It is recommended that the larger of the above values, 14,500 rpm/sec, be used as a maximum limit for acceleration and deceleration of the PHOEBUS turbopump.

(3) Stall Detection and Control

Pump stall can be detected by a sudden drop in pump discharge pressure or flow rate, or an increase in speed. Both the M-1 and PHOEBUS pump designs have relatively lightly-loaded stages so that the stall excursion is not expected to be severe. Scale model pump test data (water) for the M-1 configuration is currently available. These data indicate that the stall point is at 78% to 80% of the design flow coefficient and stall recovery occurs at 83% to 86%. The stage tip static pressure drops approximately 13% below the unstalled value shen stall occurs. These values may differ from those obtained in hydrogen because of the large differences in Reynold's number between the water and hydrogen tests, the compressibility of hydrogen, and size effects. However, satisfactory stall recovery characteristics are expected for the M-1 and PHOEBUS designs pumping hydrogen.

No data are available to firmly establish upper limits in speed for pump operation in stall. It is recommended that, if the pump must be operated in stall, the speed of the pump be limited to as low a value as possible. If the pump should inadvertently be operated in stall at speeds approaching nominal speed or greater, it is recommended at this time that the pump be disassembled for inspection of all pump blading before further operation is attempted. This may not be required after additional experience is gained.

(4) Axial Thrust Balance-Control

Control of axial thrust and a discussion of the possible parameters that may be used to monitor pump axial thrust were provided in the discussion under Power Transmission Design Modifications.

(5) Pump Cavitation Detection and Control

No difficulty with pump cavitation is expected over the nominal range of pump flow rates, speeds, and suction pressures. If the pump should inadvertently be operated at lower than nominal suction pressures, or higher than nominal flow rates or speeds, a pump overspeed may result because of unloading of the pump, caused by cavitation. Experience may show that speed and pressure instability precede pump overspeed.

(6) Bearing Failure Detection

Experience gained from the M-1 bearing test program indicates that bearing temperature measurements may be used as a "kill" parameter to initiate a programed shutdown if a bearing failure is experienced. No instance of damage to the bearing tester because of bearing failure has been experienced in the M-1 bearing test program. In all cases of bearing failure, temperature indications permitted a shutdown in time to avoid damage to the tester.

Bearing accelerometers are provided on the PHOEBUS turbopump as well as temperature measurements; however, at this time, it is planned to use temperature measurements to monitor bearing performance, with accelerometers as an alternative. To date, the accelerometer data obtained from bearing tests have been difficult to evaluate. If such difficulties are resolved in the future, the accelerometer measurements may prove to be an even more reliable indicator of bearing performance.

To prevent bearing failures, it is recommended that the turbopump be disassembled at two-hour intervals for inspection of bearings and bearing replacement as required. Inspection of the bearings at more frequent intervals is recommended if the nominal speeds or nominal bearing loads are exceeded.

(7) Pump and Turbine Blade Failure Detection

To aid in the detection of pump and turbine blade failures, it is recommended that pump casing vibration be monitored by vibration or displacement pickups, mounted to measure vibration along three mutually-perpendicular axes. Any abnormal vibration observed during steady operation of the pump, combined with sudden shifts in turbopump speed, flow rate, or discharge pressure, would probably indicate structural failure in the pump or turbine blades. An abnormally high required turbine inlet pressure for a given pump operating condition should also be considered as indicative of blading distress.

As in the case of the bearings, the pump and turbine blading should be inspected at two hour intervals of operating life, or more frequently if the nominal operating range or turbopump suction pressures, speeds, and flow rates is exceeded, or the turbopump is operated at speeds close to blade resonance speeds.

(8) Turbopump Emergency Shutdown

In the event a malfunction in the turbopump is detected, turbopump operation should be terminated as rapidly as possible to minimize damage to the turbopump and other components of the test system. Bearing failures, in particular, progress very rapidly. For this reason, it may be necessary to provide an alternative means for supplying coolant to the test reactor system to be used in the event an emergency turbopump shutdown is required.

b. Overspeed

Figure 44 is a plot of the roller bearing radial loads and contact stress versus shaft speed. At the M-1 design overspeed of 14,500 rpm, the turbine end and pump end roller bearing stress values are 315 and 325 ksi, respectively. The estimated elastic limit contact stress of the bearing material is 350 ksi at the operating temperature. Because the turbine end roller bearing stress value is close to this limit, it is recommended that the overspeed control system be designed so that maximum shaft speed is limited to 14,500 rpm. If required, additional control of turbopump overspeed can be achieved by: incorporating blow-off hatches in the gas system close to, or in the turbine manifold; rapid closing turbine exhaust valves; a blow-off gas vent from the turbine inlet to the turbine exhaust; or independent pressure supply to rapidly pressurize the turbine exhaust.

It may be possible to operate the turbopump at speeds higher than 14,500 rpm for brief periods of time without damaging any of the components; however, because of limited available knowledge concerning high speed bearing operation, it is recommended that the turbopump bearings be inspected after operation above 14,500 rpm and before further operation of the turbopump.

A pair of electromagnetic speed transducers are provided as an integral part of the turbopump. A flight safety-certified overspeed detector would be supplied along with the turbopump. This detector uses the pulse signals generated by the speed transducer. The signal is conditioned as to amplitude and width, then continuously beat against a pre-set time interval. If an excessive number of pulses are received in any one time interval, a trip signal is generated. This system has demonstrated excellent accuracy and repeatability.

V. SUPPORTING EFFORT

In addition to the technical analysis and design effort directly concerned with modification and operation of the existing M-1 Fuel Turbopump (Figure 59), work was performed in several supporting areas, including Design Producibility, Three-Stage Turbine, Reactor Facility Installation Plumbing, and the Turbopump Mount.

A. DESIGN PRODUCIBILITY

1. Inducer

Under the cognizance of the M-1 Program, an advanced computerized method of translating inducer designs into machine tapes for the Omnimil was developed. This method was evolved to significantly reduce lead-time. In view of the short lead-time available in the PHOEBUS program, it appeared most expeditious to investigate the applicability of this technique for PHOEBUS and at the same time verify correctness of the new program. A prototype PHOEBUS inducer was designed and machined using this method. With the exception of a minor indexing error made by the machine operator during the machining of the last portion of the last blade, an excellent part was produced. As a result of this experience, appropriate changes in the computer program were made to preclude repetition of this human error. Figure 60 shows the part being inspected immediately after removal from the Omnimil.

The computer program was written in Fortran for the IBM7094 computer and consists of seven chains, which are delineated in Appendix B.

The prototype PHOEBUS inducer was machined in less than 50 Omnimil hours. Inspection of the vane track, trim, and hub dimensions showed that deviations limited to 0.005-in. to 0.015-in. from the drawing coordinates were achieved.

2. Guide Vane Housing

The guide vane housing (inducer stator) also carries the forward bearing assembly. It includes coolant and instrumentation passages through the vanes, thereby requiring a very complex casting. To adapt to the reduced flow rates for the PHOEBUS application, it was necessary to decrease the flow annulus area of the main channels. This had to be accomplished without increasing the over-all material content of the part because it was the same as the Inconel 718 pour capacity of the foundry. Several methods were considered, including cast-in-place inserts, welded inserts, complete redesign, and minimum redesign.

Complete redesign was discarded because of high cost, long schedule, and the uncertainty of results. Inserts, although proved feasible by plaster sections, were discarded because of the uncertainty of structural integrity during thermal transients. The minimum redesign approach selected consisted of reducing the exterior diameter of the outer shroud and increasing the interior diameter of the inner shroud to gain sufficient material to provide for the required fill-in of the flow annulus.

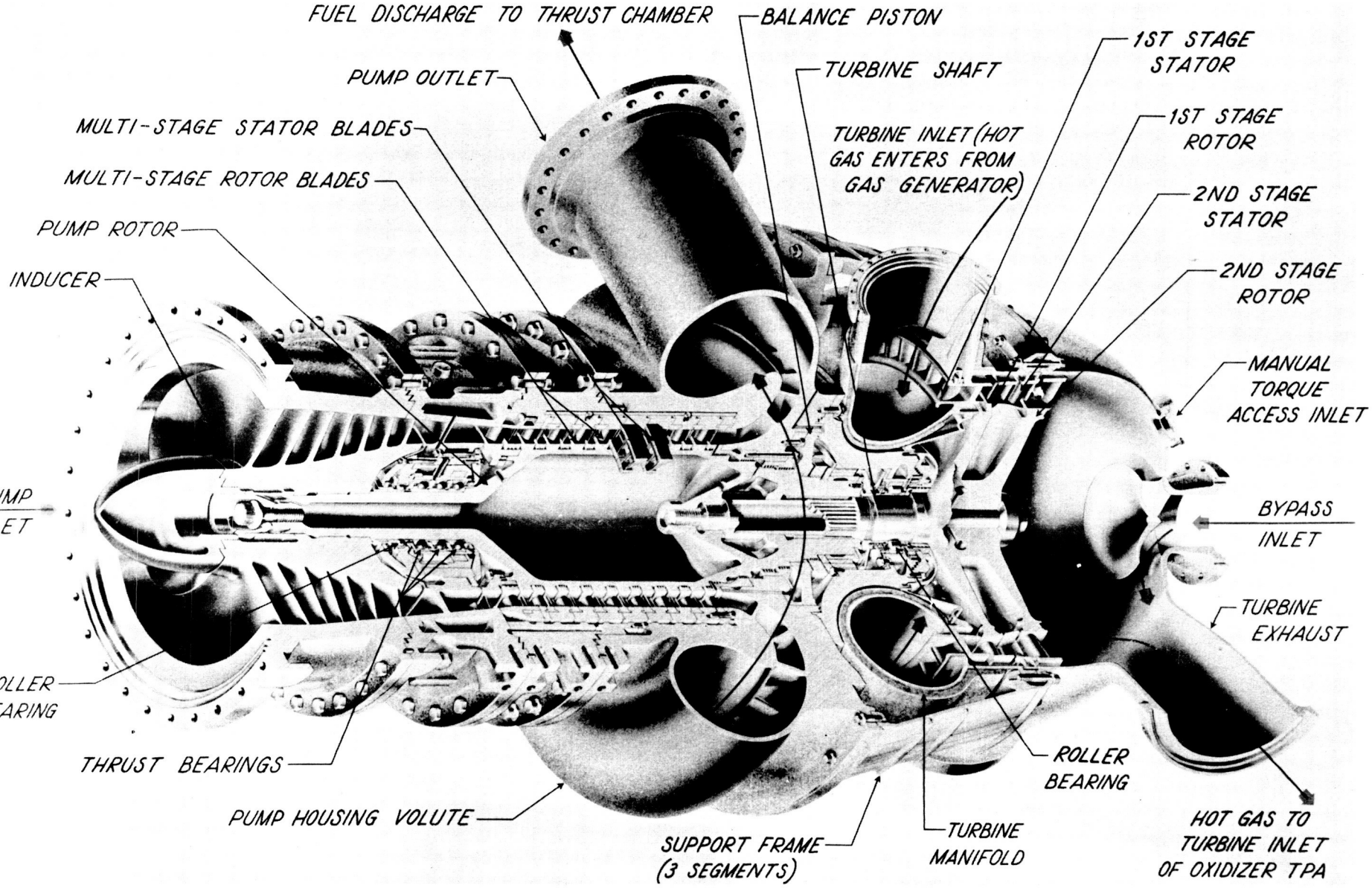

Figure 59
Page 107

EXISTING M-1 FUEL TURBOPUMP ASSEMBLY

Omnimil-Machined Inducer

Figure 60

To ensure that this design change did not render the casting extremely difficult to produce, casting patterns were prepared for the new configuration. The work was completed to the point where it is possible to immediately initiate casting of the modified guide vane housing. Based upon foundry experience in the M-1 Program, no major difficulties are anticipated in the production of this part.

Figures 61 and 62 show various aspects of the guide vane pattern work in progress.

B. THREE-STAGE TURBINE

The M-1 Model II turbine is not optimum for low-power high-pressure ratio operation (hydrogen gas at ambient temperature). The large flow area is its main deficiency. As a result, the turbine develops the required horsepower at too low an inlet pressure (approximately 440 psig) with the consequence that the gas is used at too low a level of available energy. A turbine requiring higher inlet pressures and thereby, using gas at a higher available energy per pound would make it possible to significantly reduce the required turbine weight flow.

The M-1 turbine remains the prime candidate for the PHOEBUS application because it is extremely rugged, can be extensively uprated, design has been completed, fabrication experience gained, and test data will soon be available. It is made from high-temperature materials; therefore, it could ultimately serve in a heated hydrogen reactor bleed cycle. Also, the low inlet pressure requirement increases the range of bootstrap capability and/or simplifies the heat exchanger requirements.

In support of the eventuality that minimum turbine gas flow is an over-riding aspect of feed system operation at the reactor facility, a preliminary design analysis was made of a three-stage turbine, specifically designed for ambient temperature, hydrogen gas operation at the PHOEBUS conditions. It was found that a relatively simple turbine could be evolved which would reduce the required turbine weight flow by approximately 20 to 25%. The three-stage turbine is of smaller diameter and would directly replace the existing Model II turbine without any increase in overhang or rotor mass. Thus, it would not decrease critical speed. For ambient temperature service, it could be made from more readily-fabricated materials. However, new tooling would be required.

Assuming that reduced turbine weight flow is the only consideration, the three-stage turbine appears to be a very practical alternative. One approach meriting consideration is to provide the three-stage turbine as a future replacement, which would be installed during overhaul. In this case, the assembly would be used for subsequent reactor tests for which higher powers and longer durations would be programed and provide a substantial total gas savings.

C. PLUMBING

1. Propellant Inlet Line

a. Design Requirements

(1) Interface facility plumbing with 16-in. schedule 30 standard pipe.

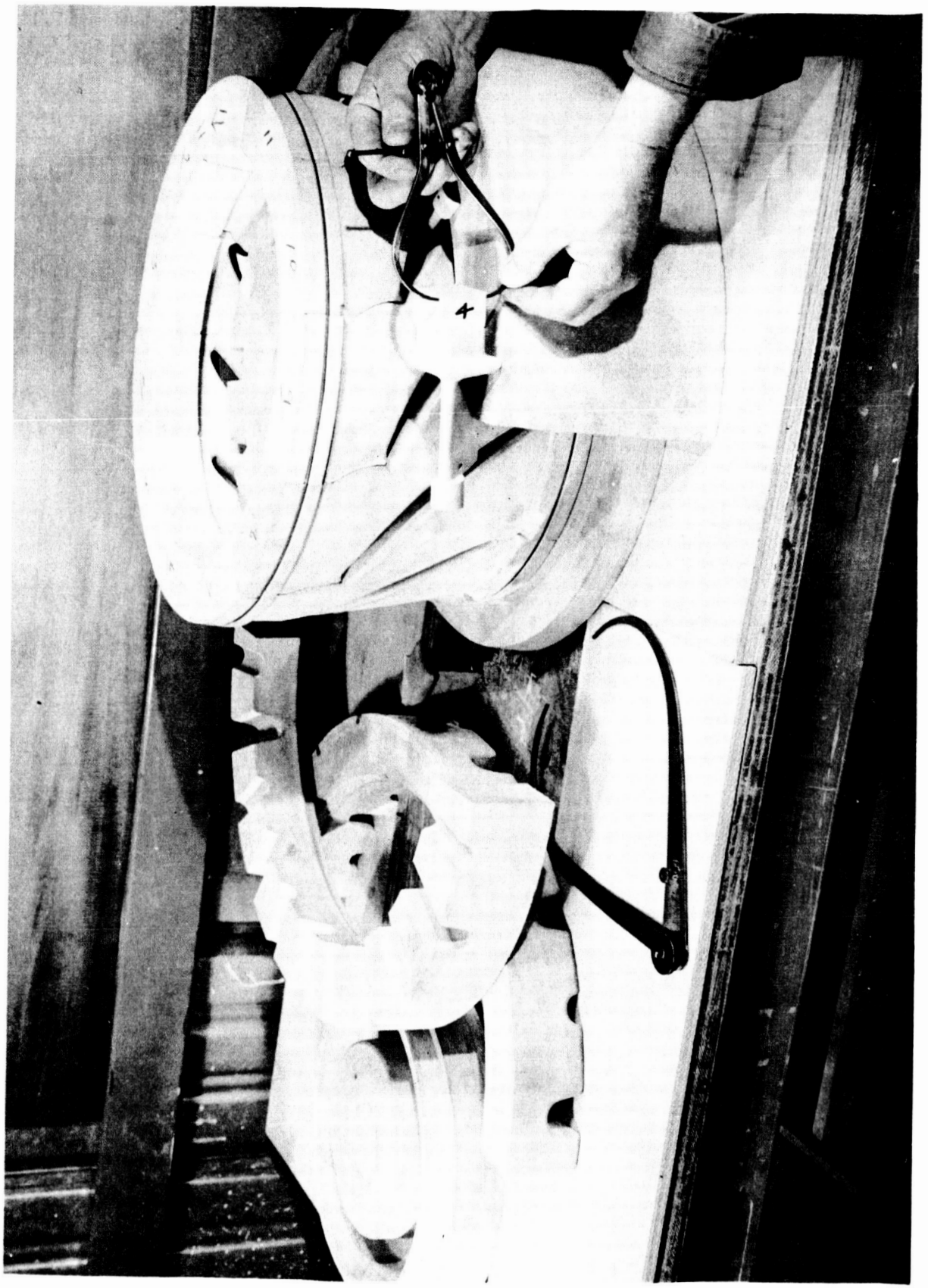

Plaster Cast Core Sections

Figure 61

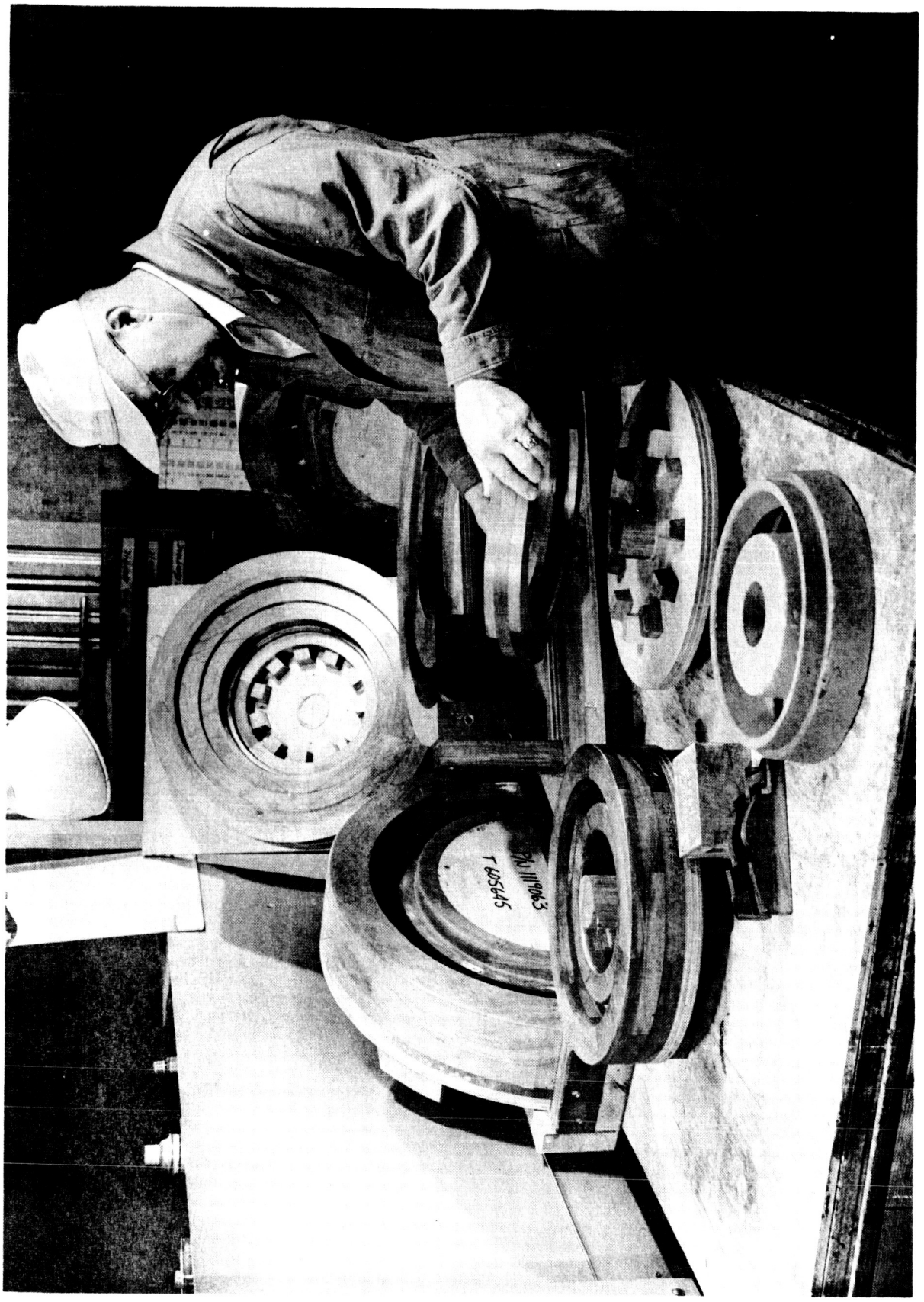

Completed Core Box Parts

Figure 62

(2) Interface pump with an appropriate flange.

(3) Support reactive forces and line weight with minimum loads induced into the pump.

(4) Flow conditions:

(a)	Pressure	75 psia total
(b)	Weight Flow	350 lbs/sec
(c)	Temperature	-421°F

b. Design Philosophy

(1) Interface to Facility Plumbing

Aerojet-General Corporation will supply an interfacing stub to be welded to the facility propellant inlet line. This stub will be fabricated from 16-in. schedule 30 pipe (0.250-in. wall) and an ASA 150-lb, 16-in. ring-type joint flange. The pressure rating for the stub assembly is 275 psig at -423°F.

(2) Suction Inlet Line to Inlet Line Bellows

This line has been designed using ASA 150-lb flanges and schedule 10 standard pipe rated at 275 psig at -423°F. A 16-in. ring-type joint flange mates to the facility stub and a 19.5-in. appropriate flange will mate to the inlet bellows.

(3) Inlet Line Bellows

An unrestrained bellows flexible coupling will be installed immediately upstream of the pump to permit flexibility for line shrinkage and tolerances. The bellows was designed for 0.100-in. nominal compression at a working pressure of 150 psig at -420°F. Line shrinkage from nominal will reduce the pre-set of the bellows by 0.16-in. The parallel off-set between the ends of the coupling has been estimated to be 0.12-in. maximum. Maximum operating capability of this bellows assembly is 1.5-in. extension, 2.3-in. compression, and 0.5-in. parallel off-set.

(4) Line Support

A line support has been designed to carry the vertical component load of the line and the reacting force exerted by the bellows. The line shrinkage expected in the horizontal run of the line will require a loose fit between the pipe and the support. The support cradle and strap have been designed for line clearance to permit the pipe to slide in the support.

(5) Materials

All ducting was designed using standard pipe and fittings, except for the mating flanges. The flange stub design has been fabricated and installed in the test area for M-1 turbopump testing. All parts have been designed

with 300 series stainless steel materials. The standard parts and material were selected to permit the usage of readily-available parts and materials.

2. Propellant Discharge Line

a. Design Requirements

Nominal Discharge Pressure	1425 psia
Design Discharge Pressure	1600 psia
Proof Pressure Discharge	1920 psia
Burst Pressure Discharge	2560 psia
Weight Flow Nominal	350 lbs/sec
Operating Temperature	-421°F
Gas Constant R	771.5
Specific Heat Ratio K	1.399

b. Design Philosophy

Economy in fabrication and maximum reliability in service were the basic objectives of this design. Elimination of gimbal joints provide a significant cost reduction. Utilization of high strength, thin wall Inconel 718 tubing provides the flexibility needed to remain within the allowable loads at the turbopump discharge flange. By using "cold springing", the loads induced by chilldown of the line will be reduced by approximately 50%. This is accomplished by producing the line too long in a given plane (one half the calculated shrinkage). The line is then installed under compression. When chilldown occurs, the line passes through a neutral condition to approximately half the tension value which would occur if this technique were not used.

3. Turbine Inlet Line

a. Design Requirements

(1) The turbine inlet line is the interconnect piping assembly between the outlet of the facility shut-off valve (No. ACV 150) and the turbine inlet flange. The design criteria for this system are:

Media - Gaseous Hydrogen

Pressure[4] - 410 psi (nominal) 650 psi (maximum design) 780 psi (proof) 1040 psi (burst)

Temperature (total) - 58.7°F (nominal) + 100°F (maximum) + 25°F (minimum)

(4) Proof Pressure = 1.2 x Maximum design; Burst Pressure = 1.6 x Maximum design; Leak Pressure = 0.75 x Proof Pressure

Weight Flow = 51 lb/sec (nominal) 60 lb/sec (maximum)

Specific Heat Ratio (K) = 1.399

Gas Constant (R) = 771.5

Velocity = Less than 0.5 Mach No. (nominal)

(2) In addition to satisfying the above requirements, this line assembly must be sufficiently flexible to assure that excessive flange loads are not imposed upon the turbine.

b. Design Philosophy

(1) Two basic concepts for the inlet line system are being investigated. One system is a semi-rigid line without flex-joints. This line would be fabricated from 6061 aluminum and because there would be generous use of bends (approximately 348°) along with the low material bulk modulus anticipated line deflections will not cause excessive flange loads. This line will be relatively economical to fabricate. The alternative system would be fabricated from 300 series stainless steel and would utilize bellows to accommodate anticipated deflections. Although this system would be heavier and possibly more costly than the semi-rigid system, it offers the advantage of less total line volume (1760 in^3 as compared to 3120 in^3 for the semi-rigid line).

D. REACTOR FACILITY TURBOPUMP STAND

A tripod arrangement and vertical mounting for the turbopump was selected in designing the test stand for the PHOEBUS turbopump in compliance with the Nevada Test Facility drawings.

Standard structural steel suitably treated for corrosion resistance, is used for the frame construction. ASME, ASTM, and AWS safety codes were adhered to.

Calculated stresses in all members and their connections occur within the elastic range of the material. The combined stresses do not exceed safe limits.

Basically, the design is a "rigid-frame" construction. End connections of all members in the frame have sufficient rigidity to maintain the angles between the connected members under all expected loading conditions.

The turbopump is supported by its trunions in self-aligning monoball bearings. Lateral arrest is provided by two adjustable sway braces, which are also anchored in other self-aligning monoball bearings. The sway braces are adjusted concurrently with the trunion centering screws during installation of the pump to achieve correct alignment.

Ease of installation or removal of the pump is provided by the utilization of split pillow block mounting of the trunion bearings, which are retained by two clamping caps.

The cross-braced front panel of the stand is removable to facilitate installation of the PHOEBUS turbopump. This panel will be facing the northerly unobstructed approach in the test bay, providing direct access for wheeling the turbopump to the trunion bearing supports.

Alignment and mating of the turbopump inlet and exit flanges with those of the test bay ducting is accomplished by the indicated adjustments. Additional adjustments can be made by the leveling jack screws, which are part of the tripod base plates.

APPENDICES

APPENDIX A

-

SYMBOLS LIST

SYMBOLS LIST

V, V_Z, V_T	Velocity: Absolute, Axial, Tangential (ft/sec)
i	Incidence Angle (degrees)
δ	Deviation Angle (degrees)
β	Blade Angle (degrees)
α	Fluid Angle (degrees)
$\bar{\omega}$	Loss Coefficient
D^*	Diffusion Factor
r	Radius (in.)
ΔH	Rotor Head Rise (ft)
ΔHa	Stage Actual Head Rise (ft)
ΔHi	Stage Ideal Head Rise (ft)
Ψ	Actual Head Coefficient
ϕ	Flow Coefficient
η	Efficiency (percent)

SUBSCRIPTS

1	In front of rotor
2	Between rotor and stator
3	Behind stator

APPENDIX B

INDUCER - IMPELLER DESIGN

AND FABRICATION COMPUTER PROGRAM

This computer program, written in Fortran for the IBM 7094 computer, consists of 7 chains which perform the following functions:

A1) Design with vane surface coordinates O, R, Z, specified for generation and inspection.

A2) Maximum cutter selection for fabrication.

A3) Cutter path coordinates for cam or numerical control (NC) machines.

A4) Most efficient cutting paths for metal removal between vanes.

A5) Feeds, cutter speeds, and depth of cuts.

A6) Punch tape for the Omnimil 5-axis NC machine.

These functions for design, roughing and finishing (vane and hub) are accomplished in less than 10 minutes on a 7094 computer as a single job.

The design phase requires the following input:

B1) Tip and hub contours in equation format or as data points.

B2) Blade angle distribution along the tip and hub streamtubes.

B3) Leading edge sweep in degrees of wrap.

B4) Blade cant angle in degrees which the pressure surface makes with the radial element (only required at the sweep angle indicated by B3).

B5) Leading edge thickness (constant over the trim area).

B6) Thickness distribution along tip and hub streamtubes.

B7) Inspection streamtubes are limited to surface of revolutions generated by straight lines, conics, circles and ellipses.

The pressure surface coordinates (R, Z, θ) are obtained by integrating

$$\theta = \frac{dm}{r \tan \beta} \qquad 1)$$

where

$$dm = dz^2 + dr^2 \qquad 2)$$

The beta distribution as prescribed in item B2 above is assumed to be those values which defined the lead of the pressure surface only (the vane centerline is not used in this program). The suction surface coordinates $(S(R,Z)_{On})$ are computed by the vector cross-product of two vectors lying in the pressure surface, i.e.

$$S(R, A)_{On} = t(\bar{V}_1 \times \bar{V}_2)_{On} \qquad 3)$$

where $\bar{V}_1$ is the vector from tip to hub, $\bar{V}_2$ is the vector parallel to the pressure surface lead, and t is the thickness normal to the plane established by the vectors V_1 and V_2. The pressure and suction surface coordinates are corrected to the required inspection streamlines by linear interpolation along the intersection of the vane surfaces with the meridional plane.

The numerical control (NC) fabrication phase of the computer program requires:

C1) Vane surface coordinates, tip and hub contour coordinates, and leading edge trim coordinates (stored on magnetic tape from design phase).

C2) Cutter table, i.e. cutter diameter, length, etc., for all cutters on hand or cataloged.

C3) Holder table consisting of all holders which adapt cutters to the Omnimil.

C4) Fixture requirements.

C5) Vane stock remaining per this machining sequence.

As an aid in cutter selection, the maximum cylinder between vanes per degree of wrap is computed and tabulated with the assumption that the cutter path is obtained when the cutter centerline projects through the impeller's centerline of rotation. A cutter is selected from the cutter table input based on the following criteria:

$$CD_{MAX} + \text{Stock} \leq CY_{MAX} \qquad 4)$$

where CD_{MAX} is the maximum cutter diameter available and CY_{MAX} is the maximum cylindrical diameter (minimum value from the tabulated cylinders) which may be used in machining the selected section or passage. The cutter path is computed and recorded on magnetic tape for NC machines (the cutter path as prescribed is compatible to both NC and cam control machines). Holder selection is made based on the requirement that the holder and tool spindle shall clear the impeller by a clearance band at all times during the machining process.

The actual machining process for vane generation requires numerous stages before vane completion. These stages are

D1) Passage metal removal using flat end cutters.

D2) Passage metal removal using ball end cutters (required near hub because of the fillet).

D3) Cutting TRIM.

D4) Finishing hub to drawing requirements.

D5) Finishing vane track to drawing requirements.

Feeds, speeds, depth of cuts, and number of cuts are computed based on the selected cutter diameter, length of cutter, type of material being machined, and the machining sequence listed above.

As a program verification and demonstration, a prototype PHOEBUS inducer was machined in less than 50 Omnimil hours. Inspection of the vane track, trim, and hub showed that deviations limited to approximately 0.005 to 0.015-in. from the drawing inspection coordinates were achieved.

REPORT NASA CR-54122 DISTRIBUTION LIST

W. F. Dankhoff/W. W. Wilcox (3 Copies)
NASA
Lewis Research Center
21000 Brookpark Road
Cleveland, Ohio 44135
Mail Stop 500-305

J. A. Durica (1 Copy)
Mail Stop 500-210

N. T. Musial (1 Copy)
Mail Stop 77-1

F. J. Dutee (1 Copy)
Mail Stop 23-1

W. J. Anderson (1 Copy)
Mail Stop 6-1

W. R. Britsch (1 Copy)
Mail Stop 500-209

Report Control Office (1 Copy)
Mail Stop 500-305

G. Hennings (1 Copy)
NASA
Lewis Research Center
Plum Brook Station
Building 1, Room 62
Sandusky, Ohio

Dr. K. Salisbury (1 Copy)
c/o Aerojet-General Corporation
Liquid Rocket Operations
Sacramento, California

Library (1 Copy)
NASA
Ames Research Center
Moffet Field, California

Library (1 Copy)
NASA
Flight Research Center
Edwards AFB, California

Library (1 Copy)
NASA
Goddard Space Flight Center
Greenbelt, Maryland

Library (1 Copy)
NASA
Langley Research Center
Langley Station
Hampton, Virginia

Library (1 Copy)
NASA Manned Spacecraft Center
Houston, Texas

Library (1 Copy)
NASA
George C. Marshall Space
Flight Center
Huntsville, Alabama

Library (1 Copy)
NASA
Western Operations
150 Pico Boulevard
Santa Monica, California

Library (2 Copies)
NASA
Lewis Research Center
21000 Brookpark Road
Cleveland, Ohio

Library (1 Copy)
Jet Propulsion Laboratory
4800 Oak Grove Drive
Pasadena, California

A. O. Tischler (1 Copy)
NASA Headquarters
Code RP
Washington, D.C.

H. Burlage, Jr. (1 Copy)
NASA Headquarters
Code RPL
Washington, D.C.

Dr. E. B. Konceei (1 Copy)
National Aeronautics and Space
Council
Executive Office of the President
Executive Office Building
Washington, D.C.

Technical Reports Library (3 Copies)
U.S. Atomic Energy Commission
Washington, D.C.

Technical Information (3 Copies)
Service Extension
U.S. Atomic Energy Commission
P.O. Box 62
Oak Ridge, Tennessee

H. F. Beduerftig (1 Copy)
NASA
Code R-[redacted]VE-PA
George C. Marshall Space Flight
Center
Huntsville, Alabama

Dr. Kurt Rothe (1 Copy)
Rocketdyne
A Division of North American
Aviation, Inc.
6633 Canoga Avenue
Canoga Park, California

NASA Representative (6 Copies)
NASA Scientific and Technical
Information Facility
Box 5700
Bethesda, Maryland

F. Edeskuty (1 Copy)
Los Alamos Scientific Laboratory
DMF-9
P.O. Box 1663
Los Alamos, New Mexico

A. Schmidt (1 Copy)
National Bureau of Standards
Cryogenic Division
Boulder, Colorado

Dr. George Wislicenus (1 Copy)
Penn State University
Naval Ordinance Laboratory
University Park, Pennsylvania

Dr. A. Acosta (1 Copy)
California Institute of
Technology
4800 Oak Grove Drive
Pasadena, California

Dr. Michael Vavra (1 Copy)
Naval Post Graduate School
Monterey, California